

STATUS OF THESIS

Title of thesis

EFFECT OF EPOXIDATION LEVEL ON THE PHYSICOCHEMICAL AND FIELD-DEPENDENT RHEOLOGICAL PROPERTIES OF EPOXIDIZED NATURAL RUBBER-BASED MAGNETORHEOLOGICAL ELASTOMERS

I MUHAMAD SHAKIR BIN YUSOFF

hereby allow my thesis to be placed at the Information Resource Center (IRC) of Universiti Teknologi PETRONAS (UTP) with the following conditions:

Chapter 2 The thesis becomes the property of UTP

Chapter 3 The IRC of UTP may make copies of the thesis for academic purposes only.

Chapter 4 This thesis is classified as

Confidential

Non-confidential

If this thesis is confidential, please state the reason:

The contents of the thesis will remain confidential for _____ years.

Remarks on disclosure:

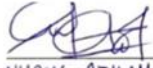


Signature of Author

Permanent address: UTP

Date : 8/9/2022 _____

Endorsed by


NURUL AZHANI YUNUS
378/NURULAZHANI YUNUS
Lecturer
Department of Mechanical Engineer
Universiti Teknologi PETRONAS
32610, Seri Iskandar
Terak Darul Ridzuan, Malaysia

Signature of Supervisor

Name of Supervisor

DR NURUL AZHANI BT YUNUS

Date : 8/9/2022 _____

UNIVERSITI TEKNOLOGI PETRONAS

EFFECT OF EPOXIDATION LEVEL ON PHYSICO-CHEMICAL AND FIELD-DEPENDENT RHEOLOGICAL PROPERTIES OF MAGNETORHEOLOGICAL ELASTOMERS FEATURING EPOXIDIZED NATURAL RUBBER

by

MUHAMAD SHAKIR BIN YUSOFF

The undersigned certify that they have read and recommend to the Postgraduate Studies Program for acceptance this thesis for the fulfillment of the requirements for the degree stated.



NURUL AZHANI YUNUS
DR NURUL AZHANI YUNUS
Lecturer
Department of Mechanical Engineering
Universiti Teknologi PETRONAS
32610, Seri Iskandar
Perak Darul Ridzuan, Malaysia

Signature:

Main Supervisor:

DR NURUL AZHANI BINTI YUNUS

Signature:

Co-Supervisor:



AP DR AHMAD MAJDI BIN A RANI

Signature:

Head of Department:



ASSOC. PROF. DR. MASDI BIN MUHAMMAD
Chair
Mechanical Engineering Department
Universiti Teknologi PETRONAS
32610 Seri Iskandar
Perak Darul Ridzuan, Malaysia

AP DR MASDI BIN MUHAMMAD

Date:

7/9/2022

EFFECT OF EPOXIDATION LEVEL ON THE PHYSICOCHEMICAL AND
FIELD- DEPENDENT RHEOLOGICAL PROPERTIES OF EPOXIDIZED
NATURAL RUBBER BASED MAGNETORHEOLOGICAL ELASTOMERS

by

MUHAMAD SHAKIR BIN YUSOFF

A Thesis

Submitted to the Postgraduate Studies Program

as a Requirement for the Degree of

MASTER OF SCIENCE

MECHANICAL DEPARTMENT

UNIVERSITI TEKNOLOGI PETRONAS

BANDAR SERI ISKANDAR,

PERAK

FEBRUARY 2022

DECLARATION OF THESIS

Title of thesis

EFFECT OF EPOXIDATION LEVEL ON PHYSICO-CHEMICAL AND FIELD-DEPENDENT RHEOLOGICAL PROPERTIES OF EPOXIDIZED NATURAL RUBBER BASED MAGNETORHEOLOGICAL ELASTOMERS

I MUHAMAD SHAKIR BIN YUSOFF

hereby declare that the thesis is based on my original work except for quotations and citations which have been duly acknowledged. I also declare that it has not been previously or concurrently submitted for any other degree at UTP or other institutions.

Witnessed by



NURUL AZHANI YUNUS
378/NURDZAHANI YUNUS
Lecturer
Department of Mechanical Engineering
Universiti Teknologi PETRONAS
32610, Seri Iskandar
Perak Darul Ridzuan, Malaysia

Signature of Author

Signature of Supervisor

Permanent address: _____

Name of Supervisor

DR NURUL AZHANI BT YUNUS

Date : 7/9/2022

Date : 7/9/2022

DEDICATION

To my beloved parent, siblings, supervisor, friends

ACKNOWLEDGEMENTS

This study is wholeheartedly dedicated to my beloved parent and sibling, who have been my source of inspiration and gave the strength to finish the MSc Mechanical Engineering. They also continually provided source of spiritual, emotional, and financial support.

To my understanding supervisor, Dr Nurul Azhani Binti Yunus, who have been help me through my study. Without her guidance, I would not to be able to understand about my experiment and study. Her advice always remembers in my mind regarding life matter and study. Furthermore, thank you for being the best supervisor ever.

To my the only one teammate that I have, Norizatie Binti Mohd Zaki, who have been help me since I am started up my study in MSc. She always made me understand the concept of the study and discuss together when I have problems regarding the project. And lastly, I would like to dedicate to department for helping me in completing my MSc program of Mechanical Engineering.

ABSTRACT

Two commercialized variants of epoxidized natural rubber (ENR), namely, ENR 25 and ENR 50, have been explored. ENR-based MREs has several advantages such as good mechanical properties, particularly damping property, which can be applied to vibration and control noise devices. ENR 25 and 50 is chosen as it is easy to fabricate and already commercialized. However, there is a dearth of concrete information on physicochemical characteristics and rheological properties in terms of different levels of epoxidation. Therefore, the main contribution of this study is to investigate the effect of epoxidation level of ENR 25- and ENR 50-based MREs on physicochemical characteristics and rheological properties. Both ENR-based MREs were fabricated by mixing with carbonyl iron particles (CIPs) and other additives. The mixture then was cured at 150°C for 30 minutes. Ten different samples with different weight percentages (wt%) of CIPs were produced. The t_{90} increased upon increasing weight of CIPs, while t_{s2} decreased for both ENRs. Randomly distributed CIPs particles within the matrix were observed, and isotropic type is identified. MRE/ENR 25 had the highest saturated magnetization with 42.54 emu/g compared to MRE/ENR 50 with 40.80 emu/g using 70 wt% CIPs. At 1245 cm^{-1} (C–O group), MRE/ENR 50 showed the highest peak compared to MRE/ENR 25. The glass transition temperature (T_g) of MRE/ENR 50 was slightly similar with range -24.5°C to -26.1°C compared with MRE/ENR 25 samples with temperature ranging from -53.2°C to -55.1°C . The addition of CIPs in both ENR samples delayed the thermal degradation process, where T_{onset} shifted toward higher temperature. MR effect for MRE/ENR 25 increased from 1.88% to 22.6%, while for MRE/ENR 50, it increased from 2.47% to 18.18%. Results and their analysis confirm that different levels of epoxidation of ENR slightly affect the physicochemical and rheological properties of ENR-based MRE. Overall, this research can be used by the researchers since both ENR-based MRE in this study resulted in different values in any aspect of analysis that had be done in this study when it is implemented in any MRE device such as potential vibration control devices.

ABSTRAK

Dua varian komersial getah asli terepoksida (ENR), iaitu, ENR 25 dan ENR 50, telah diterokai oleh penyelidik magnetorheological elastomer (MRE). MRE berasaskan ENR mempunyai beberapa kelebihan seperti sifat mekanikal yang baik, terutamanya sifat redaman, yang boleh digunakan untuk getaran dan mengawal peranti hingar. Walau bagaimanapun, terdapat kekurangan maklumat konkrit mengenai ciri fizikokimia dan sifat reologi dari segi tahap epoksidasi yang berbeza. Oleh itu, sumbangan utama kajian ini adalah untuk menyiasat kesan tahap epoksidasi MRE berasaskan ENR 25- dan ENR 50 terhadap ciri fizikokimia dan sifat reologi. Kedua-dua MRE berasaskan ENR telah dibuat dengan mencampurkan dengan zarah besi karbonil (CIP) dan bahan tambahan lain. Campuran kemudian diawetkan pada suhu 150°C selama 30 minit. Sepuluh sampel berbeza dengan peratusan berat berbeza (berat%) CIP telah dihasilkan. T_{90} meningkat apabila berat CIP meningkat, manakala t_{s2} menurun untuk kedua-dua ENR. Zarah CIP yang diedarkan secara rawak dalam matriks diperhatikan, dan jenis isotropik dikenal pasti. MRE/ENR 25 mempunyai kemagnetan tepu tertinggi dengan 42.54 emu/g berbanding MRE/ENR 50 dengan 40.80 emu/g menggunakan 70 wt% CIPs. Pada 1245 cm^{-1} (kumpulan C–O), MRE/ENR 50 menunjukkan puncak tertinggi berbanding MRE/ENR 25. Suhu peralihan kaca (T_g) MRE/ENR 50 adalah serupa sedikit dengan julat -24.5°C hingga -26.1°C berbanding dengan sampel MRE/ENR 25 dengan suhu antara -53.2°C hingga -55.1°C . Penambahan CIP dalam kedua-dua sampel ENR melambatkan proses degradasi haba, di mana Tonset beralih ke suhu yang lebih tinggi. Kesan MR untuk MRE/ENR 25 meningkat daripada 1.88% kepada 22.6%, manakala untuk MRE/ENR 50, ia meningkat daripada 2.47% kepada 18.18%. Keputusan dan analisisnya mengesahkan bahawa tahap pengoksidaan ENR yang berbeza sedikit mempengaruhi sifat fizikokimia dan reologi MRE berasaskan ENR. Secara keseluruhannya, penyelidikan ini boleh digunakan oleh penyelidik memandangkan kedua-dua MRE berasaskan ENR dalam kajian ini menghasilkan nilai yang berbeza dalam mana-mana aspek analisis yang telah dilakukan dalam kajian ini apabila ia dilaksanakan dalam mana-mana peranti MRE seperti peranti kawalan getaran yang berpotensi.

In compliance with the terms of the Copyright Act 1987 and the IP Policy of the university, the copyright of this thesis has been reassigned by the author to the legal entity of the university,

Institute of Technology PETRONAS Sdn Bhd.

Due acknowledgement shall always be made of the use of any material contained in, or derived from, this thesis.

© MUHAMAD SHAKIR BIN YUSOFF, 2022

Institute of Technology PETRONAS Sdn Bhd

All rights reserved.

TABLE OF CONTENT

ABSTRACT.....	vii
ABSTRAK.....	viii
LIST OF FIGURES	xiii
LIST OF TABLES	xv
CHAPTER 1 INTRODUCTION.....	16
1.1 Background of study.....	16
1.2 Problem Statement.....	3
1.3 Objectives	6
1.4 Scope of study.....	6
CHAPTER 2 LITERATURE REVIEW.....	7
2.1 Introduction.....	7
2.2 Magnetorheological Fluids	7
2.3 Magnetorheological Elastomers	9
2.3.1 Elastomer Matrix	10
2.3.2 Magnetic Particles	12
2.4 Fabrication of Magnetorheological Elastomers.....	18
2.5 Epoxidized Natural Rubber as Matrix	21
2.6 The Application of MRE	24
2.7 Physicochemical Characterization of MRE.....	25
2.7.1 Curing Profile Behavior	25
2.7.2 Microstructure and Elements	27
2.7.3 Magnetic Properties of MRE.....	28
2.7.4 Thermal Properties of MRE	29
2.7.5 Chemical Group of ENRs based MRE.....	32
2.8 Rheological Properties of MRE.....	33

2.9 Summary and Opportunity	36
CHAPTER 3 METHODOLOGY	37
3.1 Introduction.....	37
3.1.1 Raw Materials	39
3.1.2 Sample Fabrication.....	39
3.2 Physicochemical Characteristics	42
3.2.1 Curing Analysis.....	42
3.2.2 Morphological and Elemental Analysis	43
3.2.3 Magnetic properties	44
3.2.4 Chemical Bonding Analysis.....	44
3.2.5 Thermal Properties	45
3.3 Rheological Analysis	45
3.3.1 Rheological Measurement.....	45
CHAPTER 4 RESULTS AND DISCUSSION.....	47
4.1 Introduction.....	47
4.2 Physicochemical Characterization.....	47
4.2.1 Curing Profile Behavior of ENRs based MRE.....	47
4.2.2 Microstructural and Elements	51
4.2.3 Magnetic Properties of ENRs based MRE	59
4.2.4 Chemical Bonding of ENRs based MRE	61
4.2.5 Glass Transition Temperature of ENR-based MRE.....	63
4.2.6 Thermogravimetric of ENR based MRE.....	65
4.3 Rheological Properties of ENRs based MRE	70
4.3.1 Strain Amplitude Sweep Test.....	70
4.3.2 Magnetic Field Sweep Test	79
CHAPTER 5 CONCLUSIONS AND RECOMMENDATION	84
5.1 Conclusions	84
5.2 Recommendations.....	87
REFERENCES	89

APPENDICES99

LIST OF FIGURES

Figure	Title	Page
2.1	Structure of the magnetic particles in MRF before and after supplied of external magnetic field	8
2.2	Different types of matrices used by MRE researcher	11
2.3	Percentage of shapes of magnetic particles used by MRE researchers.	15
2.4	Spherical shapes and flaky shapes of CIPs	16
2.5	Anisotropic structure at different volume of magnetic particles of CIPs	17
2.6	Microstructure of isotropic of CIPs at 10 wt% and 70 wt %.	18
2.7	Schematic diagram for the fabrication of MRE	21
2.8	Schematic diagram for epoxidation process	23
2.9	Curing phase in curing characteristics of rubber properties	26
3.1	Fabrication of Epoxidized Natural Rubber 25 and 50 Based Magnetorheological Elastomers	38
3.2	Conventional double roll-mill	39
3.3	Samples of ENR 25 and 50 based MRE with various weight of CIPs	42
3.4	The microstructures of the CIPs with the irregular shapes under 500x magnification	43
3.5	Particle size distribution of CIPs	44
3.6	Rotational Rheometer for rheological analysis	46
4.1	Curing curves of ENR based MRE with different CIPs content: (a) ENR 25 based MRE (b) ENR 50 based MRE	48
4.2	Microstructures of ENR based MRE with 0wt% of CIPs (i) ENR 25 (ii) ENR 50	52
4.3	Microstructures of ENR based MRE with 10wt% of CIPs (i) ENR 25 (ii) ENR 50	53
4.4	Microstructures of ENR based MRE with 30wt% of CIPs (i) ENR 25 (ii) ENR 50	54
4.5	Microstructures of ENR based MRE with 50wt% of CIPs (i) ENR 25 (ii) ENR 50	55
4.6	Microstructures of ENR based MRE with 70wt% of CIPs (i) ENR 25 (ii) ENR 50	56

4.7	EDX graphs of sample ENR 50 based MRE with (a) 0wt% (b) 70wt%	58
4.8	Hysteresis loops of ENRs based MRE with various weights of CIPs contents (a) ENR 25 (b) ENR 50	60
4.9	The FTIR spectra of chemical bonding between ENR 25 and 50 based MRE with CIPs content (a) ENR 25 (b) ENR 50	62
4.10	Thermal glass transition temperature of (a) ENR 25 and, (b) 50 based MRE with variation weights of CIPs	64
4.11	Thermal features of Thermogravimetric curve of ENR 25 and 50 based MRE with variation weights of CIPs (a) ENR 25 (b) ENR 50	66
4.12	The storage modulus of the ENR 25 and 50 based MRE at different weights of CIPs under various strain of amplitude at 2A (a) ENR 25 (b) ENR 50	71
4.13	The loss modulus of the ENR 25 and 50 based MRE at different weights of CIPs under various strain of amplitude at 2A (a) ENR 25 (b) ENR 50	72
4.14	The loss factor of the ENR 25 and 50 based MRE at different weights of CIPs under various strain of amplitude at 2A (a) ENR 25 (b) ENR 50	73
4.15	The storage modulus of the ENR 25 and 50 based MRE at different current used at 70wt% CIPs (a) ENR 25 (b) ENR 50	75
4.16	The loss modulus of the ENR 25 and 50 based MRE at different current used at for 70wt% CIPs (a) ENR 25 (b) ENR 50	76
4.17	The loss factor of the ENR 25 and 50 based MRE at different current used at 70wt% CIPs (a) ENR 25 (b) ENR 50	77
4.18	The magneto-induced storage modulus of ENR 25 and 50 based..... MRE under magnet	79
4.19	The mechanism of magnetic flux flow within ENR based MRE matrix that contains calcium stearate and CIPs	80

LIST OF TABLES

Table	Title	Page
2.1	Saturated magnetization of MREs with different elastomers and weight percent of magnetic particles	29
3.1	Formulation of ENR 25 based MREs for different CIPs content	40
3.2	Formulation of ENR 50 based MREs for different CIPs content	40
4.1	The cure and scorch time of ENR 25 and 50 based MRE	50
4.2	The minimum torque, maximum torque and torque differences values of ENR 25 and 50 based MRE	51
4.3	Elemental results of ENR 25 based MRE for different weight of CIPs	57
4.4	Elemental results of ENR 50 based MRE for different weight of CIPs	57
4.5	The magnetic properties of ENR 50 and 25 based MRE for various wt% CIPs	61
4.6	The parameter of thermal degradation ENR 25 based MRE for various wt% CIPs	67
4.7	The parameter of thermal degradation ENR 50 based MRE for various wt% CIPs	68
4.8	The MR effect of ENR 25 and 50 based MRE with different weight of CIPs	81

CHAPTER 1

INTRODUCTION

1.1 Background of study

Magnetorheological elastomer (MRE) is regarded as a smart material group having rheological properties that allow it to be controlled by the application of a magnetic field. In MRE, the carrier medium is solid instead of liquid, and it is thus considered the solid state of magnetorheological fluid (MRF). MRE can be classified as a new group of smart material following the proliferation of MRF. It is capable of preventing leakage and magnetic particle sedimentation and thus exhibits superlative performance. Studies by magnetorheological (MR) researchers have shown that MRE can reinstate the passive rubber and be applied in certain fields such as automotive, civil, and medical. Besides, MREs find application in vibration and noise control devices such as seismic isolator, automotive shock absorber, prosthetic devices, and tunable and adaptive mount engine. Li *et al.* [56] studied the performance of the adaptive engine mount utilizing MREs and showed that it was efficiently working at a wide frequency range compared with the traditional method of regulating the magnetic field supplied. In addition, according to Gong *et al.* [81], MRE has a strong sensitivity response to a magnetic field, and they found that the time response of tunable automotive mount was less than 10 milliseconds.

It is acknowledged that MREs can be classified as a composite material whose rheological properties depend on three important elements, namely, the rubber matrix, magnetic particles, and additives. Selecting the types of curing condition is one of the important steps in considering the best performance in MRE [4–6]. Two types of MRE curing condition have been recognized in terms of magnetic particle dispersion: isotropic and anisotropic. In the former, the magnetic particles are uniformly distributed in the matrix polymer as no magnetic field is applied during the curing process. Meanwhile, the latter creates an MRE with its particles aligned like a chain

structure following the external applied magnetic field direction [80]. Previous studies have shown that anisotropic MRE obtained desirable results in magneto-induced storage modulus and MR effect compared to isotropic MRE [60–62]. For instance, Luo *et al.* [41] investigated the performance of MRE under anisotropic and isotropic curing using natural rubber as a matrix. They discovered that the MR effect of the anisotropic MRE (56%) was greater than that of the isotropic MRE (30%). Unfortunately, the anisotropic MRE has several shortcomings, which leaves it suitable for only a limited number of applications [41]. Gong *et al.* [39] identified that the fabrication of anisotropic MRE requires modification in conventional rubber molding equipment, which is referred to as a pre-configuration stage. Li *et al.* [58] gathered all the information regarding the fabrication of anisotropic MRE, where several factors affected the pre-structure in regard to MRE performance such as temperature, curing time, and magnetic field. Therefore, these factors need to be studied thoroughly in consideration to fabricate anisotropic MRE. Yet, the fabrication of isotropic MRE is much easier compared to anisotropic MRE since the existing rubber mold does not require any modification for an application of external magnetic field.

As far as could be ascertained, the selection of the elastomer matrix also needs to be considered in determining the best performance of MRE. To date, different types of elastomers have been discovered by MRE researchers, such as silicon rubber (SiR), natural rubber (NR), polyurethane (PU), and cis-polybutadiene rubber (BR). Among these rubbers, NR-based MRE is a frequently chosen rubber among MRE researchers. According to Ubaidillah *et al.* [67], NR-based MRE promises tremendous potential in tear resistance and is 10 times higher than SiR-based MRE. Li *et al.* [58] also endorsed the properties exhibited by the NR-based MREs. They claimed that NR-based MRE generated high relative MR effect and storage modulus. However, NR-based MREs lack in aging and weathering resiliency in the high temperature range and have low resistance to oil [25]. Recently, a new class of rubber was introduced by MRE researchers known as epoxidized natural rubber (ENR), which is derived from NR and is prepared by chemically modifying NR through the epoxidation process [86–87]. Epoxidation occurs when NR latex reacts with hydrogen peroxide or peracetic acid, converting its carbon–carbon double bonds into epoxy rings [86-87].

ENR 25 filled silica has great potential in green tire application owing to its high wet grip and low rolling resistance [1,86-87], whereas ENR 50 has potential for oil-resistant products [1]. The mol% of hydrogen peroxide significantly influences the compatibility with polar polymers.

1.2 Problem Statement

In new developing era, rubber elastomers have garnered attention from the researchers because of their unique properties, especially for MR materials. Several studies had shown that MRE were already applied in different applications such as tire pressure control and propeller shaft controller [80]. Different elastomers such as SiR, NR, PU, and nitril rubber had shown great potential for MRE study [80,86–87]. However, this rubber also has a few shortcomings such as longer time taken for vulcanization [25], low mechanical toughness [60], and inadequacy in weathering, resilience, and aging, which affect the performance of MRE, especially in rheological properties. Modified natural rubber, acknowledged as ENR, was used as elastomer matrix in this study. Despite using ENR as a passive rubber, active composite was fabricated through the addition of magnetic particles into ENR, which can be applied for the related smart material devices. The composite is known as MRE, which is categorized as a smart material owing to controllable stiffness and damping properties as mentioned earlier. ENR 25 and ENR 50 are commonly used in the study as it is easy to fabricate compared to the other ENRs as the mold to fabricate is already existing. Furthermore, ENR 25 and ENR 50 is already been commercialized by Malaysia Rubber Board (MRB) in which it will be more used in the industry. Utilization of ENR-based MRE may provide many advantages to the end user. First, ENR contains high oil and solvent permeability, which can help carbonyl iron particles (CIPs) disperse homogeneously in the matrix, thereby preventing agglomeration during fabrication process [60,65]. Thus, it may affect the performance of MRE, especially with respect to its rheological properties. Studies have shown that ENR has better oil and solvent permeability compared with others, and this property decreases the air and oxygen permeability across the MR membrane, which can

influence the chain of carbon–carbon bonds in ENR [86-87]. Rohadi *et al.* [83] studied the effect of epoxy in ENR with silica content on the mechanical properties. The results revealed ENR 25, which contains 25% of epoxy in rubber, showed a high value of shear modulus compared with ENR containing 10, 37.5, and 50 mol% of epoxides caused by the better interaction of rubber–filler from ENR containing 25 mol% of epoxides. Thus, the mechanical properties of the ENR 25 were improved. Ka *et al.* [36] investigated the performance of ENR 50 mixed with graphene nano-platelets (GNP) composite in terms of self-healing and mechanical properties. By analyzing the FTIR spectrum, they found that the chemical reaction from the epoxy of ENR 50 and GNP developed a strong hydrogen bonding, which subsequently caused the epoxy rings in ENR 50 to open and enhanced a better self-healing of matrix. Furthermore, Yokkhun *et al.* [70] studied the influence of different (10, 20, 30, 40, and 50) mol% of epoxide with montmorillonite as an additive on cure characterization analysis. They discovered that ENR 50 is capable of increasing the cure time and scorch time because of the amount of epoxy contents in ENR. Subsequently, the rubber–filler interaction and curing performance was enhanced. The above findings confirm that different level of epoxidation of ENR could influence several significant properties such as mechanical properties. However, these studies have not used ENR as a matrix sample of an MRE.

The extant literature reveals that only a few MRE researchers have studied ENR as rubber-based MRE. In 2015, Wang *et al.* [37] first discovered the use of ENR as an MRE matrix. A mixture of ENR with polychloroprene rubber was utilized as the alternative of MRE matrix. Their findings showed that the combination of these two rubbers significantly improves the interfacial adhesion of CIPs in MRE matrix, leading to exceptional field-dependent rheological properties. In the following year, Yunus *et al.* [87] studied the effect of CIPs with ENR 25-based MRE on physicochemical characteristics and rheological properties. Their investigation showed that the distribution of CIPs within ENR 25-based MRE were uniformly distributed, and less agglomeration occurred in the samples. In addition, the magnetic saturation increased from 0.68 to 207.25 emu/g with increasing wt% of CIPs from 0 to 70 wt%. Other than that, MR effect increased from 3.76% to 14.88%. This outcome

demonstrated that ENR 25-based MRE exhibits good rheological properties. Khairi *et al.* [69] discovered the effect of sucrose acetate isobutyrate ester (SAIB) as a plasticizer with ENR 50-based MRE on physicochemical characteristics and rheological properties too. The results demonstrated that the magnetic saturation of the MRE samples increased from 128 to 132 emu/g upon increasing weight percentage of SAIB content. Besides, the MR effect for rheological properties increased up to 22.5% from 13.3% upon increasing the SAIB content up to 10wt%. This showed that the compatibility of SAIB was excellent with ENR 50-based MRE. Consequently, the physicochemical characteristics and rheological properties in their study were improved. Ismail *et al.* [1] evaluated the dynamic properties of ENR 25-based MRE. Their results suggested that ENR 25-based MRE exhibited the highest damping properties compared to MREs fabricated from NR, deproteinized rubber, polyisoprene, and butyl rubber under both active and passive conditions. However, the curing and chemical bonding analysis of their studies were not included. Investigating the fabrication of ENR 50-based MRE alone without additional plasticizer has not been reported heretofore. In 2019, Yunus *et al.* [86] investigated the thermal stability and rheological properties of ENR 25-based MRE with different weight of CIPs. They found that the T_g values of ENR 25-based MRE decreased upon increasing CIPs. Decrease in T_g values from -35.59°C to -36.61°C occurred owing to reduction in the degree of crystallinity of ENR 25-based MRE. Furthermore, the storage modulus of ENR 25-based MRE in strain sweep test were increased upon increasing CIPs and percentage of strain owing to better rubber–filler interaction. Subsequently, the thermal stability and rheological properties of ENR 25-based MRE were enhanced with presence of CIPs. From all reports on ENR-based MRE, the epoxidation level significantly influenced MRE properties, and it is thus worth investigating. For instance, from this study, the researchers can easily choose which ENR as MRE matrix can be chosen to implement in any MRE devices. Therefore, the main technical contribution of this study is to investigate the effect of epoxidation level using ENR 25 and ENR 50 as MRE matrices. The epoxidation level was found to be different for them and noted to vary with mol% percentage produced by ENR. ENR 25 produced 25% of epoxy group, while ENR 50 produced 50% of epoxy group, i.e., different number of epoxy group within ENR may affect the performance in

physicochemical and rheological properties. High number of epoxy group created high number of epoxy rings. Therefore, 10 different weights of CIPs were used in each ENR matrix to analyze the effect of epoxidation level between ENR 25- and ENR 50-based MRE in physicochemical characteristics. Physicochemical characteristics such as curing analysis, microstructure observation, chemical bonding of elastomer, thermal stabilities and magnetic properties of ENR-based MRE were included in this study. Meanwhile, strain amplitude sweep test and magnetic field sweep test were also investigated in detail in this study.

1.3 Objectives

This study was conducted with the aim to investigate the effect of epoxidation level of ENR 25- and ENR 50-based MRE. The primary objectives of this study are enumerated as follows:

- i. To analyze the effect of epoxidation level on physicochemical characteristics of ENR 25- and ENR 50-based MREs corresponding to curing profile, morphology, thermal, magnetic properties, and chemical bonding properties.
- ii. To evaluate the rheological properties of ENR-based MREs under dynamic shear loading in presence and absence of magnetic field.

1.4 Scope of study

- i. All the ingredients of ENR 25- and ENR 50-based MRE samples as well as weight of CIPs (0,10,30,50,70 wt%) were determined in accordance with conventional rubber process and literature review that provided by the previous journals.
- ii. Physicochemical characterizations of ENR 25- and ENR 50-based MRE such as curing profile, morphology structure, thermal stabilities, and chemical bonding analysis were investigated in the absence of magnetic field.
- iii. Mechanical properties such as hardness, elongation, tensile, and tear strength were not investigated in this study.

- iv. The rheological properties analysis of ENR 25- and ENR 50- based MRE were in shear mode only

CHAPTER 2

LITERATURE REVIEW

2.1 Introduction

This chapter discusses the investigation on difference in epoxidation level between ENR 25- and ENR 50-based MRE as well as the advancements in research on MRE. The literature review covers the differences in raw materials of MRE, and it also includes different types of elastomer and magnetic particles. This chapter further discusses MRE's fabrication process, applications, and properties. It then presents an overview of physicochemical characteristics, including curing behavior, morphology, magnetic properties, thermal stabilities, and chemical bonding and its elements. Hence, different types of elastomers and magnetic particles that had been investigated and their influence in field-dependent rheological properties are also described in the literature review.

2.2 Magnetorheological Elastomers

As stated earlier, likewise MRFs, MREs are identified as a smart material group. The main difference between MRE and MRF is their carrier medium, which is in the solid state in the former and in the liquid state in the latter. MRE is therefore also considered the solid analogue of MRF. Other differences between MRE and MRF is that the properties of MRE that can be altered with the application of magnetic field [65,69,87]. MRE samples can be prepared through mixing of raw material such as elastomer rubber matrix with micron-sized magnetic particles. Usually, elastomer is in rubber state in which the rubber can be extensible, compliant, and can return to its original shape. MRF problems such as issues in sedimentation and sealing can be

overcome by replacing MRF by MRE in any MR devices as the latter contains solid elastomer as its carrier medium and the presence of magnetic particles helps to firm the elastomers during vulcanization process.

Since their introduction, MREs have garnered massive attention from MR researchers, who are continuously investigating the importance of MRE in MR devices. In 1996, Jolly and his colleagues [9] discovered MRE. They conducted an investigation on MREs with quasistatic dipolar model in order to identify the modulus changes in MRE. So far, two types of MREs have been identified based on the distribution of magnetic particles within elastomer matrix, namely, anisotropic and isotropic. The former needs to undergo a pre-configuration process, wherein the MRE samples are exposed to the magnetic field at high temperature used, and the magnetic particles are aligned parallel with magnetic field direction. On the other hand, in the isotropic MREs, the magnetic particles are homogeneously distributed within the elastomer matrix. This is because isotropic type does not involve any pre-configuration process and is directly vulcanized after mixing.

2.2.1 Elastomer Matrix

High performance of MRE devices depends on the selection of matrices itself. Consequently, selection of material is vital to develop any devices for a long-term usage. Moreover, high performance of matrices leads to optimum design of the MRE devices. Variations of polymers in MREs have been reported in a few studies. In MRE polymers, the matrices are divided into two common group, namely, synthetic and natural rubber. Appropriate matrices lead to achieve enticing magneto-induced storage modulus, loss factor, and MR effect. Xu *et al.* [33] stated that the selection of matrices is the most crucial part in MRE fabrication as it has major impact on physical, mechanical, and rheological properties. During MRE fabrication, the polymer of matrices is mixed with magnetic particles, forming a solid rubber product.

As reviewed by Ubaidillah *et al.* [60], the polymers of matrix are classified into three categories, namely, saturated and unsaturated rubber, thermoset, and

thermoplastic. Figure 2.2 shows the different percentages of rubber that were used in the study presented in Ref. [60].

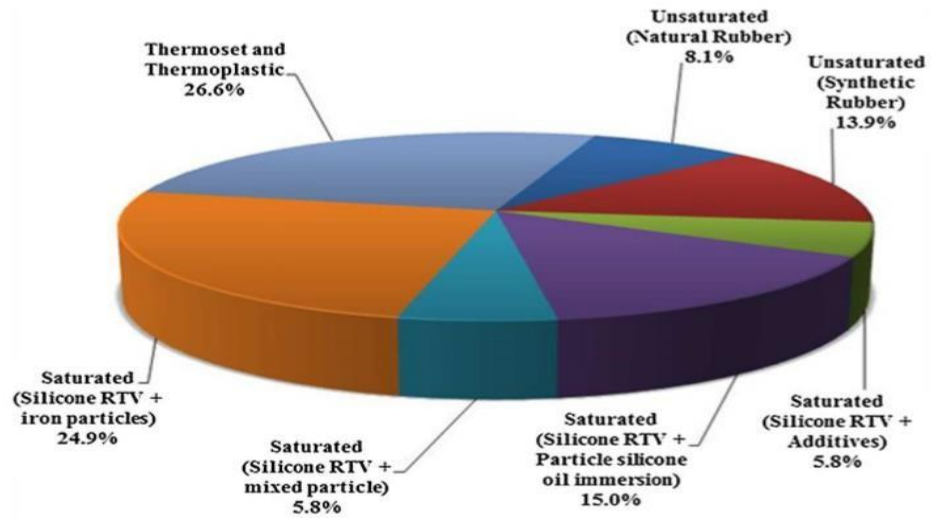


Figure 2.2: Different types of matrices used by MRE researcher [60]

While saturated elastomers (e.g., silicone rubber) do not naturally undergo vulcanization, unsaturated elastomers (e.g., NR and synthetic rubber) need to undergo vulcanization process. This process entails high-temperature vulcanization. Silicone rubber can be fabricated at the room temperature by room temperature vulcanization. Bose *et al.* [55] reported that the percentage of using silicon oil in MRE research was 51.5% compared with other polymers, as SiR is easy to fabricate and has low viscosity, which can make the magnetic particles penetrate easily into SiR during mixing process. These advantages enhanced the MRE performance as the magnetic force among the magnetic particles can be easily induced and released [63–65]. Since silicone rubber has a problem in blending of particles, several additives such as silicone oil and dimethyl silicone were used to help silicon blend well with magnetic particles. Gong *et al.* [81] observed that silicone oil improved the dispersion of fillers, which made magnetic particles emend well with silicone rubber and consequently produced up to 15% of MR effect in field-dependent rheological performance test. This observation was corroborated by Cheng *et al.* [17], who used dimethyl silicone as an additive in fabrication of silicone rubber. They found that the loss factor in field-dependent rheological test was 0.36 MPa, meanwhile without dimethyl silicone was

0.16 MPa. In addition, silicone rubber also has a problem during vulcanization process, where this matrix needs to undergo an elaborate vulcanization process, which can make the SiR become soft elastomer with low stiffness and short fatigue life and thus limit MRE applications.

To overcome this problem, polymers such as unsaturated synthetic rubber (13.9%) and synthetic polymers (26.6%) have also been used by MRE researchers as these rubbers have high performance in regard to field-dependent rheological properties of MRE. According to Ubaidillah *et al.* [60,67], the most frequently rubber used in MRE fabrication is SiR followed by PU rubber. PU rubber also has its own unique characteristics that are desirable in MRE application. Ka Wei *et al.* [36] found that MR effect by using PU rubber as matrix was 121%, which was higher compared with SiR, which produced 26%, as demonstrated by Gong *et al.* [81]. However, PU rubber is a synthetic rubber, which is not greenly rubber type, and thus, it can lead to global warming. After PU rubber, NR has been chosen by MRE researchers as a matrix owing to several attractive features that affect the field-dependent rheological properties. NR has high durability characteristic owing to high fatigue life. Chokanandsomat *et al.* [49] found that besides having a high fatigue life, NR also has several other advantages, for example, NR gives optimum results in resistance to tearing when hot and good dynamic performance. Furthermore, Khimi *et al.* [74] found that the tensile strength for NR was 6.5 MPa, which was 10 times higher than SiR, whose tensile strength was only 0.7 MPa. Li *et al.*'s [56,58] study also corroborated this finding as they discovered that the loss tangent in NR-based MRE was 20% higher than SiR. These advantages can be utilized in a certain application of MRE as this rubber promising a good performance in physical and field-dependent rheological properties. However, NR also has several disadvantages such as poor air permeability, low resistance to oil, and low wet skid, and these disadvantages can affect the performance of field-dependent rheological properties [87].

Epoxidized Natural Rubber (ENR) was a new rubber that produced by the Malaysia Malaysian Rubber Board (MRB), and commercially, ENR is known as Ekoprena. Two types of Ekoprena have already been commercialize by MRB, which

are Ekoprena 25 (ENR 25) and Ekoprena 50 (ENR 50). These types of ENR are differentiated according to mol% of epoxide. ENR is produced from the NR latex through epoxidation process, a chemical process whereby the carbon–carbon double bond turns into epoxy group with help of hydrogen peroxide or peroxide acid as shown in Figure 2.8.

It is worth noting that ENR has different unique properties compared with NR in terms of damping ability, gas permeability, and low rolling resistance [86-87]. In addition, ENR also gives significant effect in mechanical properties such as elongation and compression [1].

Research has shown that epoxidation process can enhance the compatibility with polar polymers and produce resilience to low temperatures. Consequently, the mechanical properties from the epoxidation process are improved. According to Baker *et al.* [96], ENR has the ability to create high strength and damping properties as it can experience strain crystallization. Damping ability is referred to the loss factor, and which it is important for MRE researchers in creating excellent MRE tools such as vibration damper.

Moreover, researchers have claimed that the level of epoxidation gives significant effect to the ENR. According to Rohadi *et al.* [83], the concentration of hydrogen peroxide influenced the mechanical and physical properties of polymers. In addition, the effect of epoxy level with silica on ENR 50, which contained 50 mol% hydrogen peroxide, has high glass transition temperature (T_g) compared to ENR 10, 25, and 37.5. They also found that increasing the epoxidation level of ENR improved the rubber–filler interaction, thereby producing better mechanical properties. Moreover, they also studied the effect of level epoxidation with shear modulus of the ENR. Based on their research, the shear modulus increased when using up to 25 mol% and decreased when using 37.5 and 50 mol%. In addition, Yokkhun *et al.* [70] studied the influence of different epoxy concentrations of epoxide, ranging from 10 mol% to 50 mol%, with montmorillonite as an additive, on cure characterization analysis. They discovered that ENR 50 could increase the cure time and scorch time owing to the

amount of epoxy contents in ENR. Nie *et al* [73] investigated ENR 50 with chitin nanocrystals composites in order to improve the mechanical properties such as tensile strength. From their experiments, they found that the tensile strength increased up to 1.19 MPa, which was twice compared to ENR without chitin nanocrystals composite. This shows that ENR was good in compatibility with other composites. According to Wei *et al.* [36], ENR 50 can also be used as compatibilizer with GNP. Their result showed the thermal stability of ENR 50 as compatibilizer was lower compared to non-compatibilized systems, whereas due to low thermal stability of oxygen on ENR 50. The above findings show that different epoxidation levels of ENR could influence several significant properties such as T_g , mechanical properties, and physical properties. However, the above-mentioned studies did not use ENR as a matrix constituent of an MRE.

In 2015, the use of ENR as a matrix constituent of an MRE was first reported by Wang *et al.* [37], who investigated the effect of combining ENR and polychloroprene rubber in an MRE. They discovered that the combination of different matrices leads to better adhesion of CIPs within the matrix, subsequently displaying an excellent field-dependent rheological performance. These outcomes demonstrated that ENR has excellent properties as a matrix of MRE. That said, their research focused on rheological, hardness, and tensile properties. In the following year, Yunus *et al.* [87] studied the effect of different CIP concentration on characteristics and rheological properties using ENR 25 as an elastomer matrix for the MRE. They found that the magnetic saturation values increased with increasing mass fraction of CIP. However, the study covered only the presence of CIP with different loadings of ENR 25 as the matrix. Khairi *et al.* [69] investigated MRE fabricated from ENR 50 with SAIB as a plasticizer additive, focusing on the physicochemical and rheological properties of MRE. Their results demonstrated that ENR 50 is highly compatible with SAIB and can provide a high MR effect of up to 37%. Thus, adding a plasticizer into an ENR 50-based MRE has significant effects on its physicochemical and rheological performance. Ismail *et al.* [1] evaluated the dynamic properties of ENR 25-based MRE. Their results suggested that ENR 25-based MRE exhibited the highest damping properties compared to MREs fabricated from NR, deproteinized rubber,

polyisoprene, and butyl rubber under both active and passive conditions. However, the curing and chemical bonding analysis of their experiments were not reported. Investigating the fabrication of ENR 50-based MRE alone without additional plasticizer has not been reported yet. Yunus *et al.* [86] analyzed the thermal stability and rheological properties of ENR 25-based MRE with different CIP compositions. From their studies, the weight loss of ENR 25-based MRE was high, especially at 70 wt% of CIP. From all reports on ENR-based MRE, the epoxidation level significantly influenced MRE properties, and it was found to be beneficial to the study.

2.2.2 Magnetic Particles

Magnetically permeable particles, otherwise known as magnetic particles, are one of the components that play a vital role in producing the best performance of MREs. Magnetic particles act as fillers in the elastomers to achieve the best performance of investigation, especially the rheological properties. Since past few centuries, many researchers have tried to probe magnetic particles in various experiments concerning their shape, size, and type. From previous studies, these factors are believed to influence the performance of MREs as these factors have been implicated in MRE investigations. In MRE research, there are two types of magnetic particles commonly investigated by researchers, namely, soft and hard magnetic particles.

Soft magnetic particles are more commonly used by researchers in their study compared with hard magnetic particles. Iron sand is one example of a soft magnetic particle, while examples of hard magnetic particles include iron oxide, barium ferrite, nickel and strontium ferrite [60]. Semilova *et al.* [65] and Song *et al.* [66] found that hard magnetic particles also have two different types of shapes, which are cylindrical particles and rod-shaped particles [60,67]. However, this form has not been well investigated by researchers, though it is expected that these shapes may affect the performance of MRE [69,73]. Stepnova *et al.* [95] investigated storage modulus and loss modulus in their experiment by using irregular shapes of hard magnetic particles. From this experiment, the researchers demonstrated that the storage modulus and loss modulus increased with an increasing magnetic field. However, large residual

deformation was produced by high magnetic remnant, which can influence the MR performance. In addition, Ubaidillah *et al.* [60] discovered the advantageous properties of CIPs and magnetite. In their study, CIP produced a high value of magnetic properties and field-dependent rheological properties, while magnetite produced low magnetic saturation and high remnant magnetism. High remnant magnetism can in turn lead to low MR effect and storage modulus. Ubaidillah *et al.* [60,67] reported that in their study, hard magnetic material continuously magnetized even when the magnetic field was removed. Meanwhile, soft magnetic particles automatically lost magnetization when the magnetic field was released. This is because the magnetic particles were not fully demagnetized when the magnetic field was applied investigation, especially the rheological properties. Since past few centuries, many researchers have tried to probe magnetic particles in various experiments concerning their shape, size, and type. From previous studies, these factors are believed to influence the performance of MREs as these factors have been implicated in MRE investigations. In MRE research, there are two types of magnetic particles commonly investigated by researchers, namely, soft and hard magnetic particles.

Soft magnetic particles are more commonly used by researchers in their study compared with hard magnetic particles. Iron sand is one example of a soft magnetic particle, while examples of hard magnetic particles include iron oxide, barium ferrite, nickel and strontium ferrite [60]. Semilova *et al.* [65] and Song *et al.* [66] found that hard magnetic particles also have two different types of shapes, which are cylindrical particles and rod-shaped particles [60,67]. However, this form has not been well investigated by researchers, though it is expected that these shapes may affect the performance of MRE [69,73]. Stepnova *et al.* [95] investigated storage modulus and loss modulus in their experiment by using irregular shapes of hard magnetic particles. From this experiment, the researchers demonstrated that the storage modulus and loss modulus increased with an increasing magnetic field. However, large residual deformation was produced by high magnetic remnant, which can influence the MR performance. In addition, Ubaidillah *et al.* [60] discovered the advantageous properties of CIPs and magnetite. In their study, CIP produced a high value of

magnetic properties and field-dependent rheological properties, while magnetite produced low magnetic saturation and high remnant magnetism. High remnant magnetism can in turn lead to low MR effect and storage modulus. Ubaidillah *et al.* [60,67] reported that in their study, hard magnetic material continuously magnetized even when the magnetic field was removed. Meanwhile, soft magnetic particles automatically lost magnetization when the magnetic field was released. This is because the magnetic particles were not fully demagnetized when the magnetic field was applied.

Soft magnetic particles, proper magnetic particle size, and high availability of the product are the main reasons why CIPs were used in MRE research area. As reviewed by Ubaidillah *et al.* [60,67], the values of storage modulus, loss tangent, and MR effect increased during MRE investigation when used these criteria of CIP [86–87]. When the field-dependent rheological properties increase, it will help MRE application such as vibration and damping to improve in a better way.

Choosing a suitable size and shape of magnetic particles is a crucial step that needs to be taken in fabricating desirable MRE. Generally, the size of magnetic particles can be classified into three common groups, namely, 0.1 to 10 μm , 10 to 100 μm , and above 100 μm [69]. The size of the CIPs most frequently used by researchers is 0.1 to 10 μm . This is because, the small size of magnetic particles can easily penetrate to the matrix during fabrication [71]. Furthermore, small size of magnetic particles would produce good interfacial fraction between CIPs and matrix. Boczkowa *et al.* [34] investigated the impact of size and shapes of magnetic particles on MR effect. They found that the spherical-shaped CIP with average diameter of 6–9 μm had a high value of MR effect compared with irregular-shaped CIPs having a 70 μm in diameter. This is because CIPs with spherical shapes can easily penetrate the matrix during mixing process and spherical-shaped CIPs were uniformly distributed compared with irregular-shaped ones. In addition, Lokander *et al.* [59] studied the influence of different sizes of iron particles. They found that large size of magnetic particles showed low result in storage modulus in the absence of magnetic field. However, the magnetic particles increased once the magnetic field was applied. In

addition, they found that, the loss factor decreased upon increasing the magnetic field and iron particles [87].

Despite the selection of magnetic particle size, researchers have also explored the different types of shapes, which it can influence the performance of field-dependent rheological properties, as shown in Figure 2.3. Ubaidillah *et al.* [67] they reviewed that the most frequently used particle shape in MRE fabrication was spherical, (91.9%), followed by irregular shapes (6.0%), cylindrical and wire (1.3%), and lastly cubic shapes (0.7%). Most MRE researchers use spherical shapes because it is easily accessible and already commercialized. In addition, spherical shapes also can move freely during mixing process in the fabrication of MRE and easy to align during the pre-structure alignment for anisotropic MREs [87]. Besides, a few researchers have also explored irregular shapes in their study. The most common size of irregular shapes (Figure 2.4) that was used by researchers was between 30–60 μm [67]. Steptova *et al.* [71] examined the field-dependent rheological properties of MRE by using hard magnetic filler. They found that the storage modulus increased after using hard magnetic filler, where the shape of magnetic filler used was irregular shapes as shown in

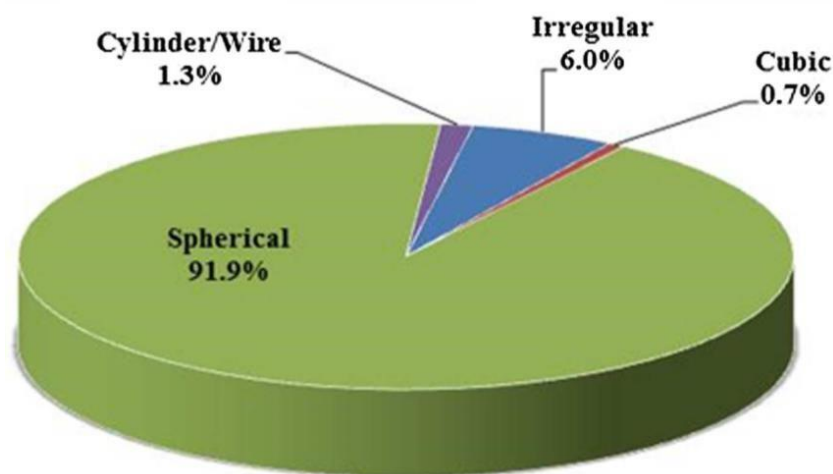


Figure 2.3: Percentage of shapes of magnetic particles used by MRE researchers. [60]

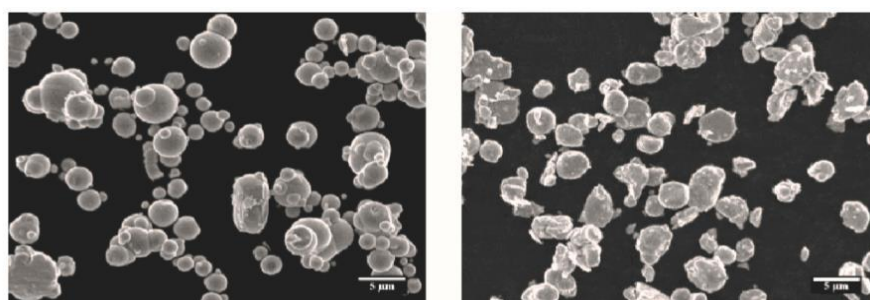


Figure 2.4 (a): Spherical shapes of CIPs [9]

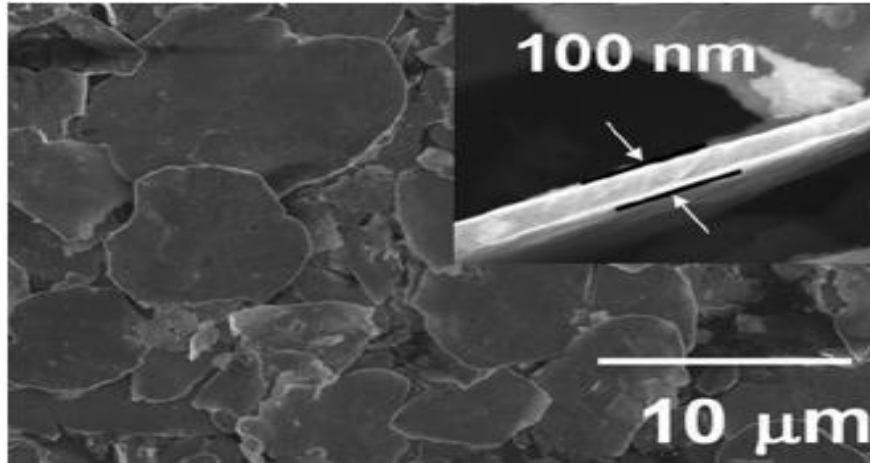


Figure 2.4 (b): Flacky shapes of CIPs [9]

The particle distribution of magnetic particles consists of two categories, namely, uniformly distributed and align structure columns. The former is otherwise known as isotropic distribution, while the latter is known as anisotropic, which can be seen in Figure 2.5. A number of researchers have investigated the particle distribution for isotropic and anisotropic types of particles in MR material studies to understand how it can affect the field-dependent rheological performances. Liu *et al.* [18] examined the mechanical and structural properties of anisotropic and isotropic types by using poly(styrene-*b*-ethylene-co-butylene-*b*-styrene) as MRE matrix. They found that the storage modulus for anisotropic type was higher than isotropic owing to the formation of chain-like structure, which can affect the permeability of magnetic particles in MRE. In addition, Lu *et al.* [79] also investigated the isotropic and anisotropic types by using NR in MRE. From their experiment, the MR effect value of anisotropic was bigger than isotropic with good performance with regard to field-dependent rheological properties. For the anisotropic, magnetic particles need to undergo pre-configuration process, whereby an external magnetic field is applied to the magnetic field, producing a chain-like structure.

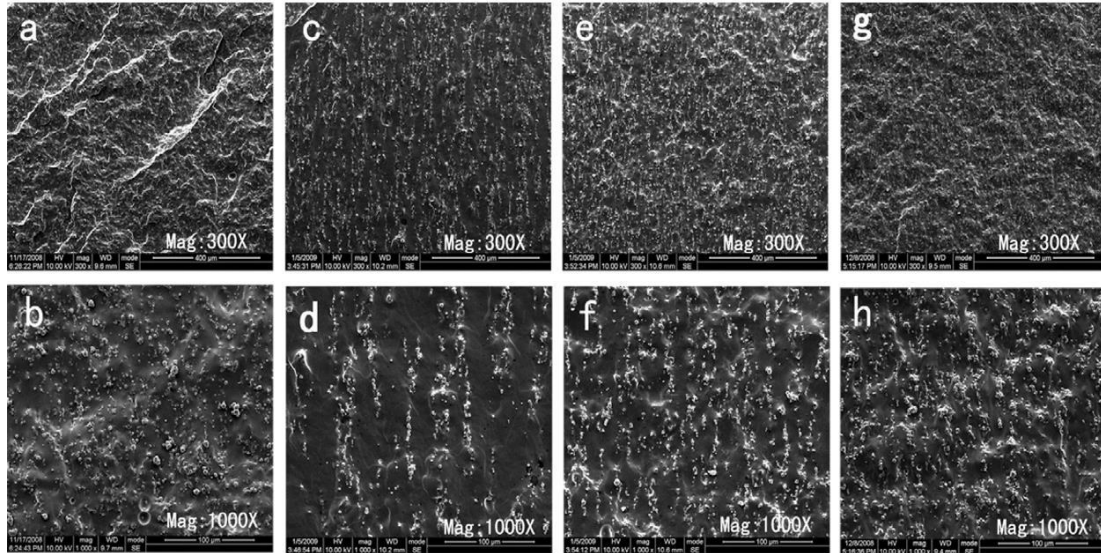


Figure 2.5: Anisotropic structure at different volume of magnetic particles of CIPs.

[78]

However, fabrication of isotropic type is easier compared with anisotropic as for the former, the pre-configuration process is not necessary. Wang *et al.* [37] remarked that isotropic MRE can be produced in large quantity as compared with anisotropic owing to the simplicity of its fabrication process. Xu *et al.* [33] found that by using SiR, the MR effect and storage modulus were higher in isotropic than anisotropic type, as depicted in Figure 2.5. In addition, Wang *et al.* [37] supported the finding that MR effect for anisotropic type reduced when CIPs increased from 10% to 30%. Meanwhile, for isotropic type, the MR effect reduced at 50% of magnetic particles contents. In terms of device applications, isotropic is more suitable compared to anisotropic. This statement was supported by Li *et al.* [58] and Zhang *et al.* [54], who found that the sensing device that were used in their experiment in isotropic section is excellent compared with anisotropic in terms of storage modulus and MR effect.

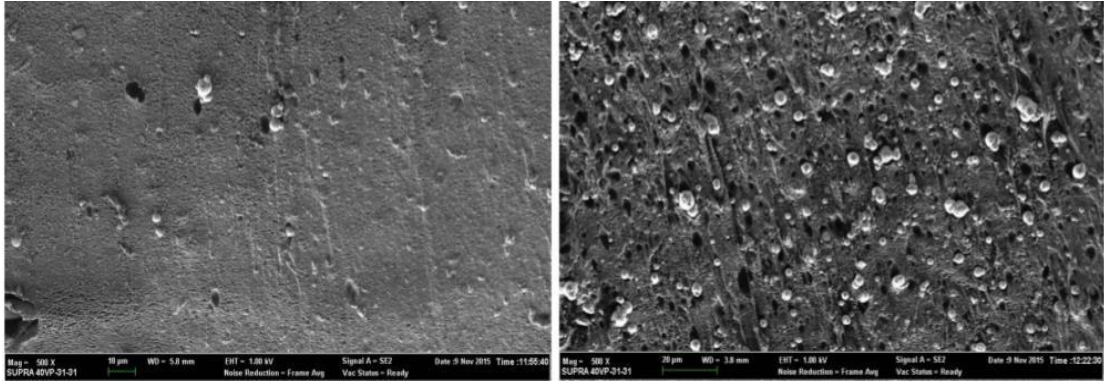


Figure 2.6: Microstructure of isotropic of CIPs at 10 wt% and 70 wt %. [87]

2.4 Fabrication of Magnetorheological Elastomers

In MRE fabrication, two categories have been identified with respect to the temperature of curing or vulcanization, namely, curing at room temperature and high temperature. Curing is a chemical process applied in polymer chemistry to produce a good mechanical property, and it involves a crosslinking process through polymer chains. Saturated elastomer matrices such as SiR and PU undergo a curing process at room temperature. According to Rajpal R *et al.* [27], the fabrication of SiR-based MRE was simple compared with other matrices as they can mix easily with several molecules, additives, and magnetic particles at room temperature. Usually, silicone oil is used as an additive in the fabrication of SiR-based MRE as silicon oil can improve the dispersion of the filler [87]. When all the mixtures are completely mixed, the final mixture will be poured and cured it in a mold that is already provided.

The unsaturated elastomers such as NR and ENR undergo a curing process at a certain high temperature. This is because the unsaturated rubber already exists in a solid while saturated rubber in a liquid condition. The fabrication of NR based MRE involving a rubber compounding process and vulcanization process. A double roll-mill and curing machine will be used in fabricating the NR based MRE. Rubber compounding or rubber formulation is a process whereby certain chemical properties were added into a rubber producing a desirable rubber material [57]. The raw rubber usually has poor mechanical properties such as hardness and elongation. Furthermore,

the raw rubber was easily attacked by oxygen which can cause the rubber easily to degrade and affect the properties of rubber [69]. To overcome this problem, the rubber will be endured by rubber compounding and vulcanization process. To produce the best performance of MRE, several additives will be added in the rubber compounding process of MRE fabrication. The function of an additive is to improve the adhesion of rubber and magnetic particles [89]. In the selection of additives, several aspects such as environment-safety, process-ability, and mechanical and physical properties need to be taken into consideration as these factors can affect the behavior and rheological properties of MRE [67–69]. Wang *et al.* [37] noted that the addition of additives in MRE fabrication impacted the process ability and physical and mechanical properties, which were required for producing huge values of MR effect compared with no addition of additives.

Fan *et al.* [75] asserted that the sulfur content may modify the effect of crosslink density of matrix-based MRE. They varied the sulfur content from 0.1 to 5 phr and found that the loss factor and storage modulus decreased when crosslink density was increased by an increment of sulfur content. This is because increasing sulfur content makes the mobility of the molecular chains limited, and the energy was dissipated when the crosslink density was increased. The usage of plasticizers in the MRE fabrication greatly influences the performance with regard to physical and rheological properties. This statement was substantiated by Chokanandsomat *et al.* [49], who analyzed the influence of plasticizers in the fabrication of NR-based MRE. They reported that the plasticizer acted as a lubricant, which made the molecular chain of rubber move easily and thus made the MR effect, storage modulus, and loss tangent increasing when an increasing amount of plasticizer. *Khairi et al.* [69] also supported the statement whereby in their study of ENR 50 based MRE by using sucrose acetate isobutyrate ester (SAIB) as an additive. In their study, they found that increasing of SAIB amount increased the thermal stability of MRE which consequently the degradation of MRE became lower.

Carbon black is also one of the substances that were used during the fabrication of MRE. The function of carbon black is usually a emphasize filler that usually adds up

on the tire and other products. As reported by *Fan and co-workers* [75], the usage of carbon black affects MRE performance where the tensile strength was 15.16 MPa compare with non-carbon black was 9.89 MPa. This statement is also supported by *Chokanandsomat et al.* [49] where they varied the value of the carbon black in MRE fabrication. From the experiment, they found that the rheological properties such as MR effect and loss tangent were increased when increasing the amount of carbon black. This is because of the carbon black act as an agent in MRE fabrication to improve and strengthen the chain between magnetic particles and matrix.

In the fabrication of MRE, two types can be classified during fabrication which are the isotropic type and anisotropic type. Both need to undergo a vulcanization process to make the rubber more durable. The process of vulcanization makes the mechanical properties especially tensile and extensibility excellent compare rubber without vulcanization process. Three main stages were involving in anisotropic types which were rubber compounding, pre-configuration, and vulcanization. Different between anisotropic and isotropic is the presence of the pre-configuration process. Pre-configuration process whereby the magnetic field and temperature also known as magneto heat couple device were supplied to the uncured rubber before undergoes the vulcanization process. When the magnetic field and temperature was supplied, the monomer of the magnetic particles was magnetized and forming a chain-like structure called anisotropic type as stated at Figure 2.7

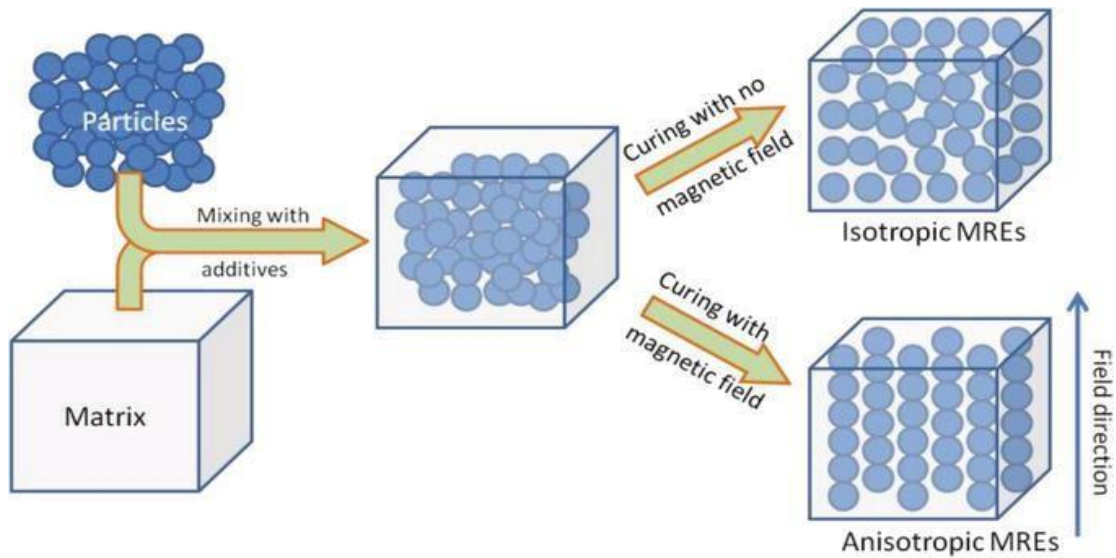


Figure 2.7: Schematic diagram for the fabrication of MRE [58]

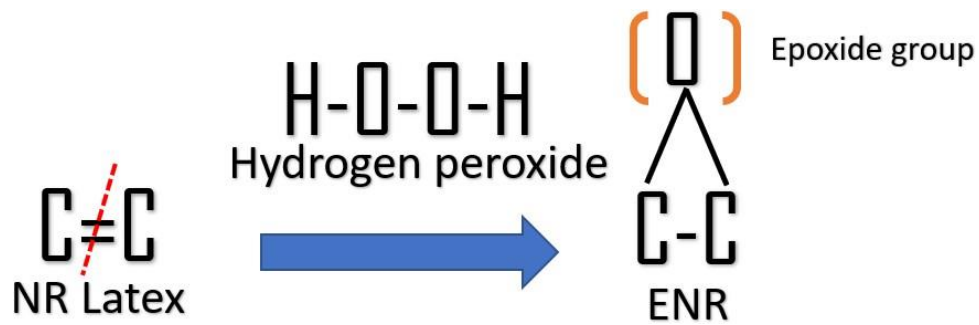


Figure 2.8: Schematic diagram for epoxidation process.

2.6 The Application of MRE

In the era of globalization, MREs have been investigated by researchers as one of the promising candidates that can be applied in a diverse range of applications. Several scholarly articles have reported that MREs have been applied in several applications such as in automotive, civil engineering, medical, military and defense industries [60]. Three main areas have been identified by MRE researchers that offer great potential when implementing MRE. One of them is vibration and noise control device, especially in vehicle applications such as tunable and adaptive engine mounts, seismic isolator, prosthetic devices, and automotive shock absorbers [60,69,86].

Several international MRE researchers had studied about the vibration and noise control devices, for example, Fu *et al.* [64] examined the impact buffer in MRE. They found that the maximum acceleration was created when MRE was applied in impact buffer. In addition, Ginder *et al.* [4] designed and investigated a tunable automotive bushing for vibration for MRE. They found that the stiffness and damping increased until 25% when applied to the current up to 5 A. Behrooz *et al.* [15] also investigated the stiffness and isolator under different currents used in which they applied it in a civil structure in a base isolation system. They conducted their experiment under a shear strain of 1% with excitation frequency of 0.1 Hz. In their study, the isolator increased up to 57% within the loops.

Another device that related with MRE is sensing device which is used as magnetostriction, magnetoelasticity, magnetoresistance and thermal resistance properties [75]. Several MRE researchers had proposed and applied sensing device in MRE, and one of them is Bica *et al.* [16], who investigated a magneto-resistor sensor using graphite MRE and found that the electrical conductivity of MRE could be adjusted by using magnetic field. Li *et al.* [58] also studied the sensing device in MRE, and they used MRE as a force sensor in their study. Their result demonstrated that MRE-based force sensor could enhance the external force at different force ranges. The above-mentioned studies confirm that MRE has potential to be used in a wide array of applications.

2.7 Physicochemical Characterization of MRE

Different fundamental characteristics of MREs have been investigated by MRE researchers since their introduction in the late 1990s. Physicochemical characteristics such as curing profile behavior, microstructure, magnetic properties, chemical bonding, and thermal and rheological properties have been studied experimentally and theoretically. In the following section, previous studies by numerous researchers on the physicochemical characteristics or properties of MRE are explained in detail.

2.7.1 Curing Profile Behavior

Before proceeding into physicochemical characterization of any MRE testing, curing behavior should be tested. Cure characteristic is the process whereby the polymer chains in rubber are mixed with other additives to create crosslinked segments between rubber polymer chains and other substances. In addition, curing is also known as vulcanization process in rubber industry. In curing or vulcanization process, three stages have been identified so far: induction phase, curing phase, and overcuring phase [16]. Khimi *et al.* [74] recognized three types of overcuring phases, namely, marching, plateau, and reversion type.

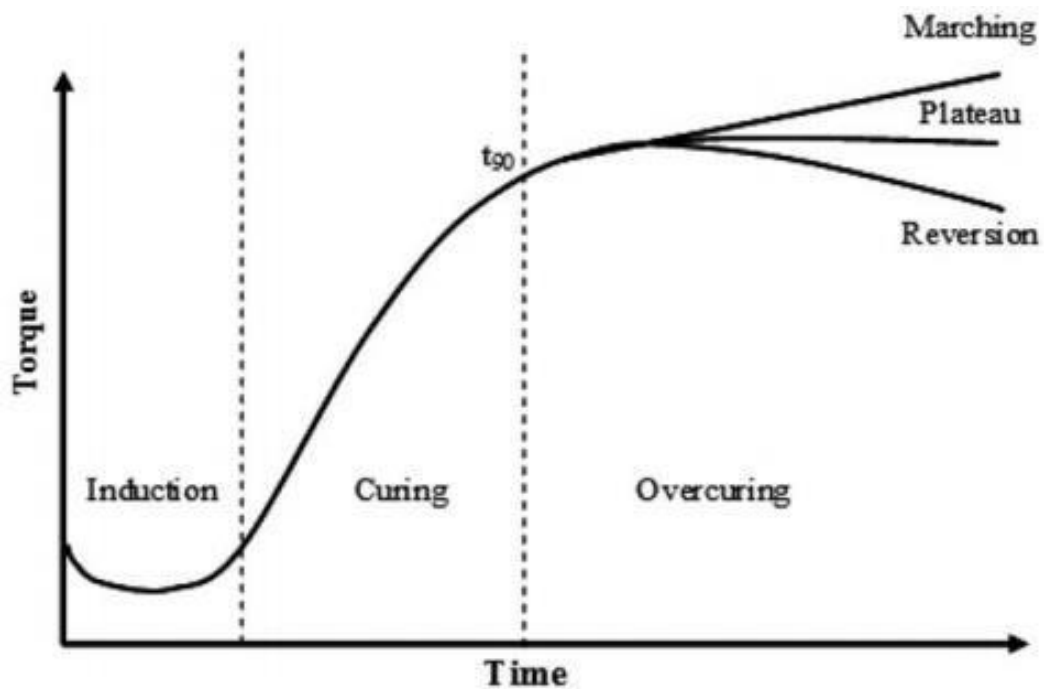


Figure 2.9: Curing phase in curing characteristics of rubber properties [74]

The marching type in at curing profile behavior occurs because of a high probability of crosslinks of monomers, which is attributable to the strong reacting vulcanization agent. Meanwhile, the reversion type occurs when due to the overheating reaction of rubber polymer with other substances the network structure breaks down. In curing profile characteristics, several parameters such as scorch time (t_2), curing time (t_{90}), minimum torque (M_H), maximum torque (M_L), and torque

differences (M_L-M_H) can be obtained only in one graph of curing profile. Different rubber polymers showed different values of these parameters. Interestingly, Yokkhun *et al.* [70] investigated the curing profile at different epoxidation levels of ENR. In their study, different type of ENRs, namely, ENR 10, 20, 30 40, and 50 were used in order to investigate the impact of epoxidation level of ENR on curing characteristics. The researchers found the t_{90} and t_2 time taken decreased upon increasing the epoxidation level of ENR. Moreover, the M_H , M_L and M_H-M_L of ENR 50 showed the best results of these parameters as it is believed that ENR 50 has better interaction with montmorillonite clay nanocomposite compared with other ENRs. In MRE, Khairi *et al.* [69] investigated the properties of curing profile of ENR 50 with different amounts of SAIB as an additive in their study. They claimed that different amounts of SAIB enhanced the performance of t_{90} and t_2 , where t_{90} increased from 4.13 minute to 7.67 minutes, while t_2 increased up to 3.56 minutes. Successful crosslinking between ENR 50 and SAIB enhanced the performance of curing characteristics in this study.

2.7.2 Microstructure and Elements

The morphology of MRE samples in physicochemical characterization is one of the important factors in determine the performance of MRE in rheological properties. Usually, the effect of the morphology in MRE depends on the selection of the right raw material and fabrication process of MRE samples. In morphological analysis, different parameters such as homogeneity of the mixture in MRE, dispersion or agglomeration of magnetic particles, interfacial adhesion between matrix and magnetic particles, and porosity are observed.

As stated earlier, two types of magnetic particle distributions within MRE have been identified by the Wang *et al.* [37], namely, isotropic and anisotropic. In addition to the fabrication process for obtaining good MRE samples, the distribution of magnetic particles should be considered as well. Several reports claimed that the anisotropic type in MRE played a significant role in enhancing the storage modulus and loss modulus with aid of magnetic particle content [34,76,87]. One of the famous

MRE research groups, Li *et al.* [58], investigated the performance of SiR within MRE with anisotropic type and they found the damping capability of the performance in their study can be controlled in wider range and subsequently increased the performance of MR effect in terms of rheological properties. Furthermore, Bcozkowka *et al.* [55] also investigated the performance of PU rubber in microstructure analysis and rheological properties of anisotropic MRE. They found that two different directions of the applied magnetic field, namely, parallel and perpendicular had a significant impact on rheological performance. However, several MRE researchers have agreed that parallel direction of magnetic field enhanced the performance of storage modulus and loss modulus in MREs [86–87].

Yet, MRE researchers have also studied the effect of isotropic type in MRE with various matrices used and found out that isotropic type also attained very interesting outcomes [75]. For instance, Wang *et al.* [58] studied the performance of isotropic and anisotropic types in rheological properties and claimed that isotropic type contributed more prominent MR effect compared with anisotropic type. Furthermore, Xu *et al.* [78] also agreed with Wang *et al.* [58] and claimed that isotropic type with 80 wt% of magnetic particles produced greater MR effect compared with anisotropic type with same amount of magnetic particle used in PU-based MRE.

In addition, the presence of pores within matrix-based MRE also influences the performance of MRE, especially in rheological properties, which usually degrade its performance. However, several MRE researchers had identified the presence of pores within MRE matrix produced high stretching materials capable of producing wider audible frequency applications [76–78]. Furthermore, Ju *et al.* [79] studied the presence of pores within SiR in MRE with different weights of CIPs. They found that the increase of pores within the SiR matrix caused the modulus elasticity to decline, and interestingly, the sample that contained pores formed high MR effect compare with no pores present in SiR-based MRE sample.

2.7.3 Magnetic Properties of MRE

Magnetic properties in MRE are a necessary parameter that need to be examined in any MRE investigation. Magnetic moments are measured as a function of magnetic field, which is known as magnetization. The magnetic properties of the MRE are investigated by using vibration sample magnetometer (VSM). Through the analysis of magnetic properties, important information can be amassed such as saturated magnetization (M_s), retentivity (M_r), and coercivity (H_c), and all this information is presented in a magnetization curve or hysteresis loop. Most MRE researchers take a serious part in M_s values of MRE in which the maximum values of magnetic moments can be taken. As much as could be ascertained, the magnetic moments in the magnetic domain were unable to increase as much as it can as all the magnetic moments have reached the saturated condition, where all the magnetic domains were aligned toward the magnetic field. In addition, when the magnetic field was absent, all the magnetic moments in magnetic domains had different orientations. Thus, the adjacent magnetic domain becomes separated by the domain wall. According to MRE researchers, several factors need to be taken into consideration that influence the values of M_s in MRE, for example, the amount of concentration of magnetic particles. Apparently, different concentration of particles used give different significant effect to the M_s values [87]. In addition, according to Ubaidillah *et al.*'s [60] report, different types of components used that are subjected to magnetic particles give different values of magnetic saturation. They investigated two different types of magnetic particles, which are magnetite and CIPs, with waste tire rubber in MRE. They found that each of these magnetic particles used give different values of M_s in MRE. In addition, a few MRE researchers already investigated the types of magnetic particles such as soft magnetic particle and hard magnetic particle as well as sizes of these types of magnetic particles also played their own significant effect on the M_s values. Table 2.1 shows the saturation magnetization of MREs with different elastomers and weight percent of magnetic particles.

Table 2.1: Saturated magnetization of MREs with different elastomers and weight percent of magnetic particles

MRE Materials	Saturate Magnetization (Ms) (emu/g)	References
SiR + CIPs (30wt%)	180	37
SiR + Magnetic plasticone (30wt%)	60	39
PU + Iron particle (70wt%)	105	37
PU + CIPs (70wt%)	231	36
Waste tyre rubber + CIP (40wt%)	76.08	60
ENR 25 (10, 30, 50, 70wt)	(18.83, 26.97, 101.65, 207.25)	87
ENR 50 + SAIB + CIPs (60wt%)	128	69

2.7.4 Thermal Properties of MRE

The prime purpose of using the thermal analysis is to investigate the thermal degradation, thermal phase transition, polymer decomposition, and glass transition temperature of the samples. However, in MREs, the thermal analysis test has not been discovered broadly since MREs are still new to be explored, and thus, there is a dearth of information about MREs. Usually, researchers using a normal rubber compounding process use thermal analysis in their investigation. This is because, they test their application such as tires through the thermal analysis and ascertain whether is they are safe to be used or not for the customers. Thus, thermal analysis is important for MREs for different potential applications.

Boscowa *et al.* [15] were the first group of researchers to perform thermogravimetric analysis (TGA) in MREs by using urethane rubber as matrix. From their investigation, they discovered that magnetic particles interacted each other and with urethane rubber, which subsequently enhanced the thermal stability of MREs. This is because the magnetic particles and polymer matrix were closely attached together, which made the heat flow easily through the samples. The value of the T_g in the TGA was influenced by the amount of the magnetic particles used in the experiment. This statement was supported by Gong *et al.* [39], who used two different weights of CIPs (60 and 80 wt%) in their study. They found that there was comparison of thermal properties with different weight of CIPs mixed with PU. Based

on the results, two degradation stages had been formed at temperature range of 250°C to 300°C and 350°C to 400°C. From this investigation as well, the temperature of the samples increased when the weight of CIPs increased. In TGA, there are two terms known as T_{onset} and T_{end} . The former represents the temperature where the polymers start to degrade, while the latter shows the end of the temperature after degradation.

Different polymers that were used in the experiments also influenced the T_g values. A number of researchers have used different kinds of polymers matrix in their study, for example, ENR. Khairi *et al.* [69] they investigated ENR 50 with help of SAIB as an additive in their study. Based on the result, the mass loss was occurred between temperature range 300°C to 500°C, and the weight of samples increased above the 500°C. From their study, it can be concluded that ENR 50 and SAIB chemically reacted with each other, and the mass decomposition occurred through this reaction. This observation was corroborated by Harun *et al.* [8], who investigated the epoxidation level of ENR 25 and ENR 50 with nanocomposite electrolyte as a plasticizer. They found that the change of T_g was higher at ENR 50 compared with ENR 25. This is because, ENR 50 contains higher polarity compared with ENR 25, which contributed to the higher contents of epoxide. In addition, ENR is one of the polymer matrices that is easily mixed with the other substances. This statement was supported by Sarkawi *et al.* [95], who found that the T_g value of ENR increased when silica was added together. This is because the interaction between epoxy group of ENR and silane group from silica reacted together in forming high values of T_g . Besides, the carbon-carbon double bond (C=C) from ENR strengthens the chains of ENR, consequently leading to the good thermal analysis.

Besides, differential scanning calorimetry (DSC) has also been used in MRE investigation. The purpose of using this machine is to determine the thermal transition of the samples, such as phase transition and the amount of heat flowing through MREs. From the previous report, adding magnetic particles mixed with polymers matrix increased the melting temperature [95]. However, the T_g values dropped in the range of 1°C–5°C. This is because the limitation for magnetic particles to move in the matrix chain was finite. According to Wu *et al.* [45], the T_g value of PU-based MREs with different weight of CIPs decreased when the CIPs were added increasingly from

5 to 60 wt%. However, the phase separation of the samples increased. Besides, Sun *et al.* [8] also discovered the thermal stability properties of cis-polybutadiene rubber of MREs with different weight of CIPs. Based on the result, the T_g value decreased from 89.5°C to 82.21°C and 88.5°C to 78.81°C when the magnetic particles were added increasingly. From the result, they explained that the mobility between CIPs and matrix decreased due to the reduction of distance between magnetic particles and matrix. Recently, Yunus *et al.* [86] investigated the ENR 25 with different number of CIPs used. They observed that the T_g shifted to negative values as CIPs were increased from 0 wt% to 70 wt%. The values shifted from -34.9°C to -36.6°C because of the interaction between polymers and the magnetic particles. When CIPs were added, they were entrapped in the polymers and made the molecular mobility limited. From the analysis performed using the TGA and DSC experiment, it could be seen that different polymer matrices have their own T_g value properties and can contribute to various effects.

2.7.5 Chemical Group of ENRs based MRE

Fourier transform infrared spectroscopy (FTIR) testing of MREs is important in analyzing the properties and performance of MREs. This test is used for examining the chemical interaction between two or more materials in a sample, which consequently affects the performance of MRE, especially with regard to MR effect. Furthermore, through chemical interaction of the sample, researchers can determine the chemical group and condition of the samples, which involve epoxy group, ether group, hydrogen group, carbon-carbon double bond group, stretching carbon bond, asymmetric and symmetric bond. These compounds are observed by the researchers, especially when they use rubber as a matrix in their study.

The FTIR testing analysis has been done by several researchers who examined the interaction of the rubber compound with other additives. For example, Rohadi *et al.* [83] investigated the presence of silica as an additive in ENR 25 in their study. They noted that pure silica and ENR 25 interacted with each other as the silica produced silanol groups were attached to the chains of backbones of ENR 25. ENR 25 has their own superior, where it can present in two strong peaks, i.e., 878 cm^{-1} and 839 cm^{-1} of

wavelength. These peaks are shown due to asymmetric and symmetric stretching of vibration of the epoxy rings in ENR 25. Besides, the amount of the epoxy group in the matrix could also influence the interaction between matrix and other substances. This finding was supported by *Yangthong et al.* [70], who studied three different matrices, namely, NR, ENR 25, and ENR 50 and used geopolymer as their additives. The researchers observed that ENR 50 shows a great interaction compared with others as it contains high amount of the epoxy group, which is adequate for the geopolymer attached to the epoxy group. Besides, the intensity of NR is 1.135, which is higher than ENR 25 and ENR 50. This is because the changes of the carbon–carbon double bond in oxirane rings are less compared with ENR. The formation of the ENR comes from NR latex that reacts with hydrogen peroxide and peracetic acid through epoxidation process, where the carbon–carbon double bonds turn into epoxy group. As analyzed by *Chuayjuljit et al.* [94], the presence of epoxy rings in the sample helped the interaction of additives in order to improve their performances. The intensity of ENR 30 and NR with multiwall carbon nanotubes showed that the intensity of the ENR is 1.13, which was lower than NR, which had an intensity of 2.70. This was because the epoxy rings in the ENR 30 were enough to support the acidity of the multiwall carbon nanotubes, which consequently prevented the samples from corroding and influenced the mechanical testing properties.

2.8 Rheological Properties of MRE

More than a decade ago, MRE's rheological properties had been discovered by MRE researchers, and it has been reported that the rheological properties can be amended by the external magnetic field. Particularly, rheological properties are defined as study the flow and deformation of liquid and solid of the materials with the application of external force [45]. In addition, the rheological behavior was known as viscoelastic materials. Viscoelastic materials are derived from the combination of viscous liquid and the elastic solid. First, the viscoelastic material starts with the flow of liquid as liquid material when they are subjected to a very low deformation. Then, the material starts to behave as a solid as repetition of deformation is applied toward

the materials. From this phenomenon, stress strain was created independent of time. When external force is applied, the materials (deformed body) will undergo relaxation process, where in this situation the stress value become decrease until the force recede from the process [60,67,87]. Moreover, the relationship of strain stress with viscoelastic has been elaborate in the Kevin-Voight Voigt model. Thus, this relationship is also known as linear viscoelasticity as stated in Equation 2.1.

Where G is the shear modulus complex, γ is the shear strain, η is the dynamic viscosity, and t is time. The delayed deformation when external force is removed can be given through relaxation time as Equation 2.2.

$$\alpha = G\varepsilon + n \frac{ds}{dt} \quad (\text{Eq 2.1})$$

The linear viscoelastic region (LVE) properties of MRE are critical measurements that need to be taken before proceeding to frequency sweep test and magnetic sweep test. LVE is determined by exposing the materials to dynamic or harmonic loading. MRE researchers have reported that LVE has two different states whether in constant stress or strain. Usually, constant strain is applied in oscillating machine owing to the ease in its implementation. Readers must be informed that MREs are famous as a viscoelastic material that it can store and dissipate the energy during deformation. Capability for the viscoelastic material to retain energy temporarily is known as storage modulus, while loss modulus represents the energy loss during deformation in form of heat and viscous properties. The relationship of storage modulus and loss modulus can be seen in the following equation (Equation 2.2 and 2.3).

$$G^* = G' + iG'' \quad (\text{Eq.2.2})$$

$$\tan \delta \equiv \frac{G''}{G'} \quad (\text{Eq.2.3})$$

Apparently, if the value of complex modulus is the same with storage modulus, and at the same time the loss modulus become zero, the material is recognized as completely elastic. For the elastic solid case, the energy stored in the sample during deformation process will be released concurrently when the deformation is fully reversed. In addition, if the complex modulus value equivalent with loss modulus means that the material samples are in completely viscous condition. The storage modulus and loss modulus correspondingly depend on the frequency and temperature used. According to Yunus *et al.* [86], it is believed that the storage was increased. According to their results, the storage modulus increased when the number of CIPs increased, which is up to 1.38 MPa due to entangled of CIPs within ENR itself. Moreover, the loss modulus and loss factor from their study is same in which 10wt% and 30wt% of CIPs used was increased steadily and for 50wt% to 70wt% was increased dramatically compared with others. *Khairi et al.* [69] also investigated the properties of ENR 50 with incorporation of SAIB as an additive in their study. According to their analysis of rheological properties, the storage modulus value increased up to 1.05 MPa upon adding SAIB (10 wt%). Similarly, the loss modulus and loss factor increased with of SAIB as an additive. Wang *et al.* [37] also investigated the properties of MRE by using ENR mix with polychloroprene rubber (CR). They found that mixing ENR with CR created high storage modulus (1.7 MPa) when using the CIPs up to 40 vol% on isotropic type compared with anisotropic with just only 1.3 MPa with the same number of CIPs. This pattern is also similar with loss modulus and loss factor analysis in which the initial value increased upon increasing CIPs. Based on the analysis above, different epoxidation levels give different result, especially in regard to storage modulus, loss modulus, and loss factor analysis.

Other than these parameters, the MR effect is one of the crucial parameters that need to be investigated by MRE researchers, and the equation can be referred at Equation 2.4. MR effect can be recognized through the magnetic field sweep measurement. It can be determined as the ratio of magneto-induced storage modulus and zero storage modulus. The equation is stated below, which uses the shear storage modulus as response parameters. Several MRE researchers had studied the analysis of

magnetic field sweep test by using ENR as their matrix. In 2015, Wang *et al.* [37] demonstrated that the MR effect of ENR mixed with CR increased upon increasing volume of CIPs. From their observation, the MR effect increased from 61.33% to 134.93% when 30 vol% of CIPs was used. Another MRE research group, Yunus *et al.* [86], had studied the performance of magnetic field sweep test by varying wt% of CIPs using ENR 25. They claimed that MR effect steadily increased from 0 wt% to 70 wt%. It was noted that MR effect increased from 2.50% to 20.00%. Next, Khairi *et al.* [69] investigated the performance of magnetic field sweep test by varying the concentration of SAIB with ENR 50. They found that the increment of MR effect started from 13.3% to 22.9% upon using different concentrations of SAIB as their additive. From this analysis, it is clear that different ENR samples used in MRE give different significant effect toward the magnetic field sweep test.

$$MR\ effect = \frac{(G^F_{max} - G^F_0)}{G^F_0} \times 100\% \quad (Eq.2.4)$$

2.9 Summary and Opportunity

Author and Title	Research	Remarks
<p>Rohadi et al (2014) Effect of epoxidation level in silica filled epoxidized natural rubber</p>	<ul style="list-style-type: none"> - High glass transition (T_g) for ENR 50 is higher than ENR 10, 25 and 37.5 	<ul style="list-style-type: none"> - The sample is not made up for MRE. - The magnetic properties are not investigated
<p>Yokkhun et al (2014) Influence of epoxidation level in ENR molecules on cure characteristics and dynamic properties.</p>	<ul style="list-style-type: none"> - The cure time and scorch time for ENR 50 is higher than ENR 10 and 25 	<ul style="list-style-type: none"> - The ENR sample is not for MRE application as not added any magnetic particles
<p>Wang et al (2015) Effects of rubber/magnetic particles interaction on the performance of magnetorheological elastomer (MRE)</p>	<ul style="list-style-type: none"> - Combination of ENR with polychloroprene rubber led to better adhesion of CIPs 	<ul style="list-style-type: none"> - The author does not mention which ENR based MRE was used - More focusing on mechanical property not rheological study
<p>Yunus et al (2016) Rheological properties of isotropic magnetorheological elastomers featuring epoxidized natural rubber</p>	<ul style="list-style-type: none"> - Studied the effect of CIPs with different weight of CIPs 	<ul style="list-style-type: none"> - The author only used ENR 25 based MRE and do not discuss any of the epoxidation level on research
<p>Khairi et al (2017) The field-dependent complex modulus of magnetorheological elastomers consisting of sucrose acetate isobutyrate ester (SAIB)</p>	<ul style="list-style-type: none"> - Studied the effect of SAIB for ENR 50 based MRE 	<ul style="list-style-type: none"> - The author only focusing additive of SAIB in their study and do not compare any ENRs for epoxidation level

CHAPTER 3

METHODOLOGY

3.1 Introduction

This chapter elaborates on the experiments with ENR 25- and ENR 50-based MREs with different apparatus used in this research. The experimental procedure such as preparation of raw material, fabrication of MRE samples, physicochemical characteristics, and rheological properties are explicated in this chapter. To achieve the objective of the research, five different samples from each ENR-based MRE were prepared. The physicochemical characteristics of ENR 25- and ENR 50-based MRE that were studied are curing profile behavior, morphology, chemical bonding and its elements, magnetic properties, and thermal properties. Furthermore, the rheological properties of ENR 25- and ENR 50-based MRE were investigated in two conditions corresponding to the steady state and dynamic state. All the parameters used in the experiment were followed from the selection of literature reading. Figure 3.1 illustrates the flowchart of this study

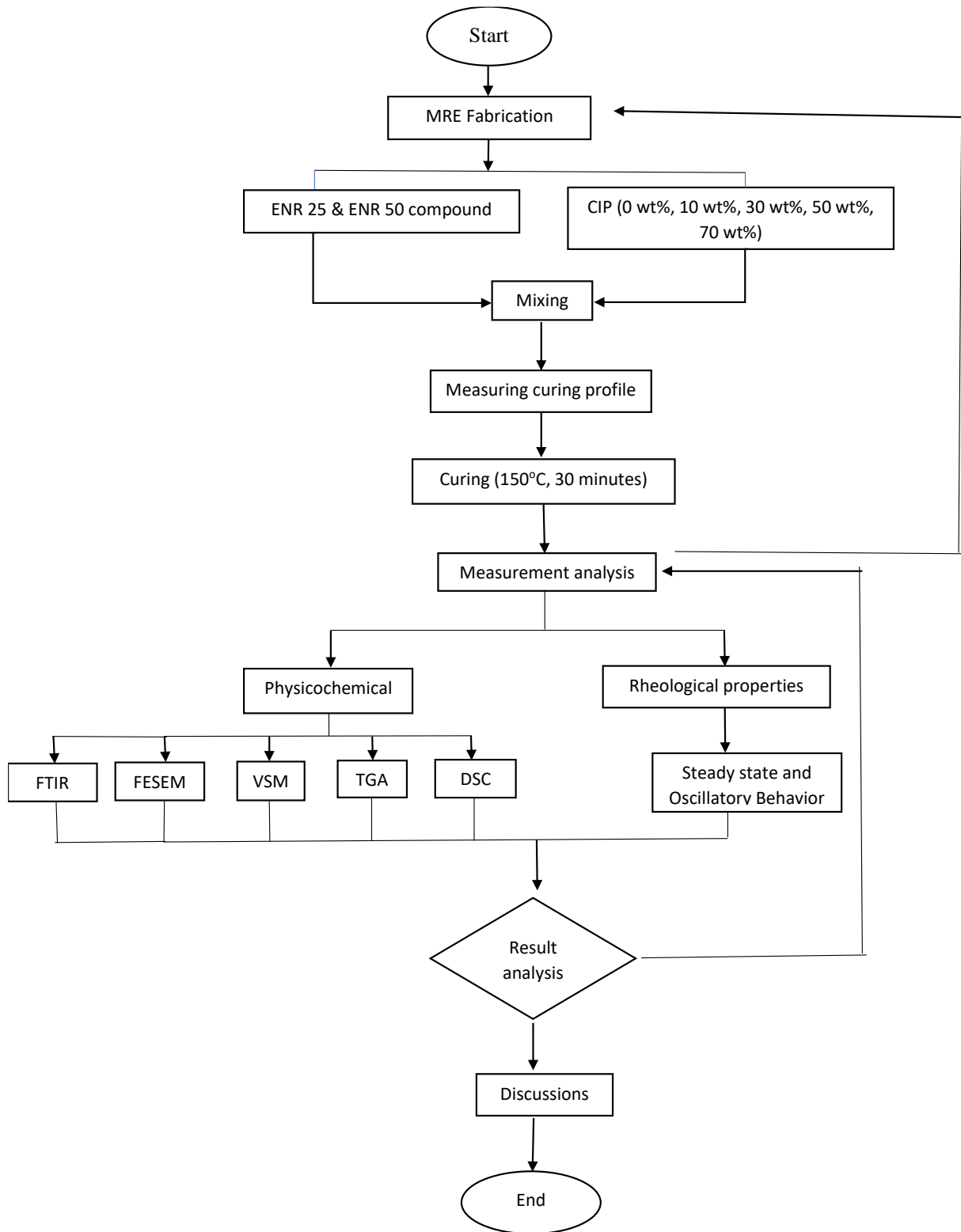


Figure 3.1: Fabrication of Epoxidized Natural Rubber 25 and 50 Based Magnetorheological Elastomers

3.1.1 Raw Materials

As stated earlier, the raw rubber used in this study is the epoxidized natural rubber, i.e., ENR, and two types of ENR have been identified: ENR 25 and ENR 50. These two rubbers are different in terms of the mol percentage (mol%) of epoxidation level. ENR 25 and ENR 50 were supplied by MRB, RRIM Research Situation. The Mooney viscosity of ENR 25 and ENR 50 are 110 and 85 Mooney units, respectively. Meanwhile, T_g values of ENR 25 and 50 are -47°C and -24°C , respectively.

CIP type C3518 (Sigma Aldrich, Singapore) were used in this study as magnetic particles. CIPs are present in powder form, which has irregular shapes containing more than 97% of iron (Fe) with density 7.86 g/mL. The particle size distributions of CIPs were experimentally measured through laser light scattering using Particle Size Analyzer (PSA) instrument (Malvern, Zetasizer Nano-ZSP).

3.1.2 Sample Fabrication

Fabrication of MRE samples generally consists of two main stages, namely, mixing process and vulcanizing or curing process. The conventional double roll mill used is illustrated in Figure 3.2.

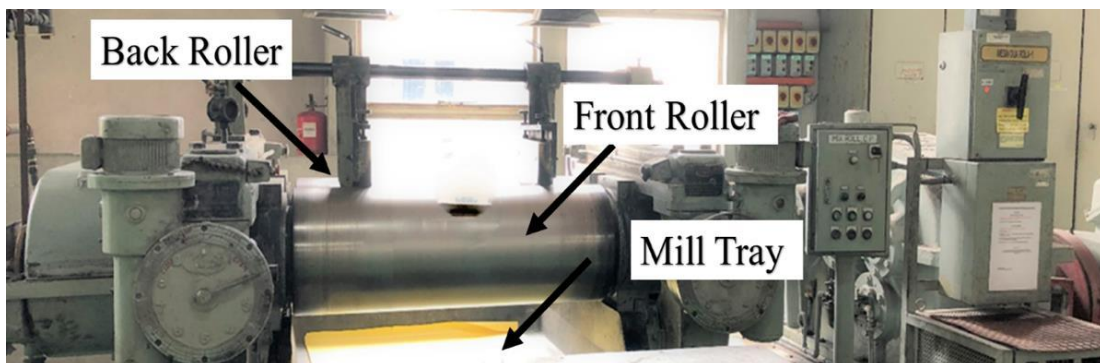


Figure 3.2: Conventional double roll-mill

MRE samples were fabricated by preparing all the ingredients of ENR compound. Ingredients such as carbon black, aromatic oil, zinc oxide, stearic acid, sulfur, N-Cyclohexyl 1-2-benzothiazole (CBS), and calcium stearate were added together with ENR 25 and ENR 50. Next, CIPs with different number were added at the last stage of mixing, and final product can be referred in Figure 3.3. The compositions of ENR-based MRE are listed in Table 3.1 and Table 3.2.

Table 3.1: Formulation of ENR 25 based MREs for different CIPs content

Compounding Ingredients	MRE/ENR 25				
	0 wt% CIPs	10 wt% CIPs	30 wt% CIPs	50 wt% CIPs	70 wt% CIPs
ENR 25 (phr)	100	100	100	100	100
Carbon Black (phr)	19	19	19	19	19
Aromatic Oil (phr)	5	5	5	5	5
Zinc Oxide (phr)	5	5	5	5	5
Stearic Acid (phr)	2	2	2	2	2
Sulfur (phr)	2.3	2.3	2.3	2.3	2.3
CBS (phr)	0.8	0.8	0.8	0.8	0.8
Calcium Stearate (phr)	3	3	3	3	3
Total (%)	100	90	70	50	30
CIPs (wt %)	0	10	30	50	70

Generally, phr is the unit measurement used by rubber chemists to calculate the amount of the ingredient used in producing the rubber compound. For, all the ingredients in the fabrication of ENR-based MRE, phr was used as a measurement unit except for the CIPs, which was measured in terms of weight of percent (wt%).

As stated earlier, ingredients such as carbon black, aromatic oil, zinc oxide, stearic acid, sulfur, CBS, and calcium stearate are required in the processing of rubber compound as these additives enhance the properties of the gum rubber. This is

because rubber such as NR and ENR can be easily attacked by oxygen, which would contribute to limited usage of rubber, especially in mechanical applications. Thus, these additives were added to improve the process ability and physicochemical and mechanical properties, as these additives have their own function and role in the fabricated rubber compound.

Table 3.2: Formulation of ENR 50 based MREs for different CIPs content

Compounding Ingredients	MRE/ENR 50				
	0 wt% CIPs	10 wt% CIPs	30 wt% CIPs	50 wt% CIPs	70 wt% CIPs
ENR 50 (phr)	100	100	100	100	100
Carbon Black (phr)	19	19	19	19	19
Aromatic Oil (phr)	5	5	5	5	5
Zinc Oxide (phr)	5	5	5	5	5
Stearic Acid (phr)	2	2	2	2	2
Sulfur (phr)	2.3	2.3	2.3	2.3	2.3
CBS (phr)	0.8	0.8	0.8	0.8	0.8
Calcium Stearate	5	5	5	5	5
Total (%)	100	90	70	50	30
CIPs (wt %)	0	10	30	50	70

phr = parts per hundred of rubbers

The function of stearic acid and ZnO is to enhance the process ability of the rubber compound. They acted as activators, which helped the other accelerators to react effectively. Meanwhile, the aromatic oil helped in improving dispersion of fillers and known as plasticizer. CBS was used in this study as it can accelerate the crosslinking reaction during mixing process. Sulfur acted as crosslinking agent, which helped the rubber forming a network through crosslinking formation.

Vulcanization characteristics were tested after curing profile for the ENR/CIPs sample by using moving die rheometer (MDR) (MDR 2000 on COM1) with standard RHEO. This process is vital for rubber compounding as it can determine the accurate

curing profile for the same. Besides, vulcanization process also helps the monomers of the rubber to be well-crosslinked together, which is needed in rubber industry for enhancing the quality of their products (ASTM D4818-21).

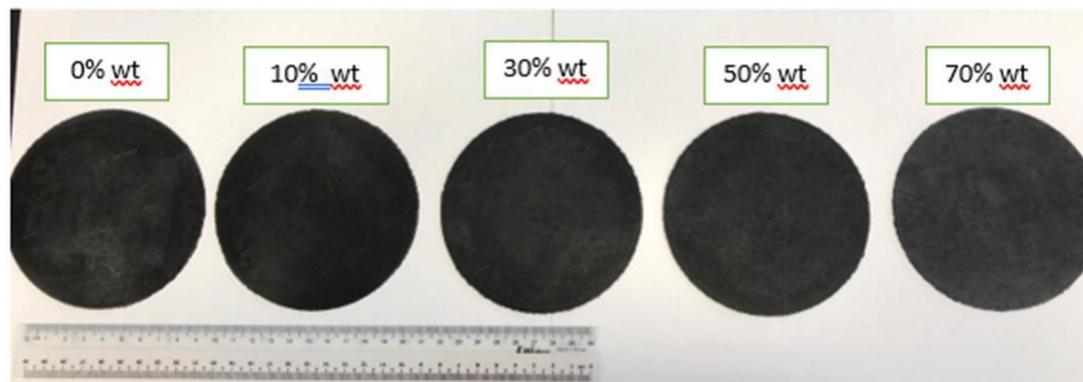


Figure 3.3: Samples of ENR 25 and 50 based MRE with various weight of CIPs

3.2 Physicochemical Characteristics

Samples of ENR 25- and ENR 50-based MRE were analyzed in terms of physicochemical characteristics. It is important for MRE researchers to know the properties of the MRE samples before proceeding to the rheological properties.

3.2.1 Curing Analysis

In this study, the curing profile of the ENR 25- and ENR 50-based MRE was acquired by using a MDR 2000 from Alpha Technologies at 150°C under conditions of 0.833 Hz and 2.79% strain for 30 minutes. This device is useful in determining the accurate curing profile for rubber compounding. The cure time (t_{90}), scorch time (t_2), minimum torque (M_L), maximum torque (M_H), and differences in torque ($M_H - M_L$) were obtained in this experiment.

3.2.2 Morphological and Elemental Analysis

The microstructure of ENR 25- and ENR 50-based MRE samples was observed via field-emission scanning electron microscopy (FESEM) (Model: Zeiss Supra 55 VP, China) in order to examine the morphology and distribution of CIPs within MRE samples. The sample was cut into a dimension of 5 mm × 5 mm × 1mm and coated with a thin layer of gold. The device was operated under acceleration of 5 kV in voltage, and 500x of magnification was used for obtaining the best capture of CIPs within both ENR matrix-based MRE samples. Furthermore, all MRE samples were observed through energy dispersive X-ray spectroscopy (EDX), which is also equipped with FESEM. This study was conducted to determine the elements of MRE samples. The microstructure of CIPs can be referred to in Figure 3.4. The size distribution of CIPs particle size analyzer is included in Figure 3.5.

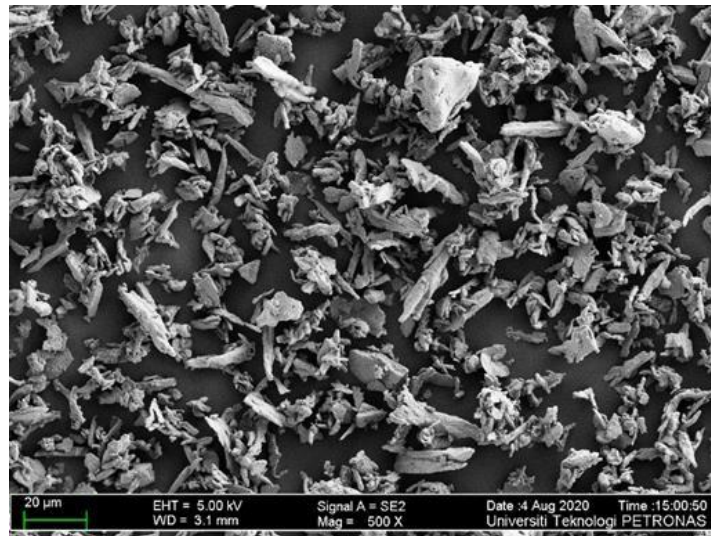


Figure 3.4: The microstructures of the CIPs with the irregular shapes under 500x magnification.

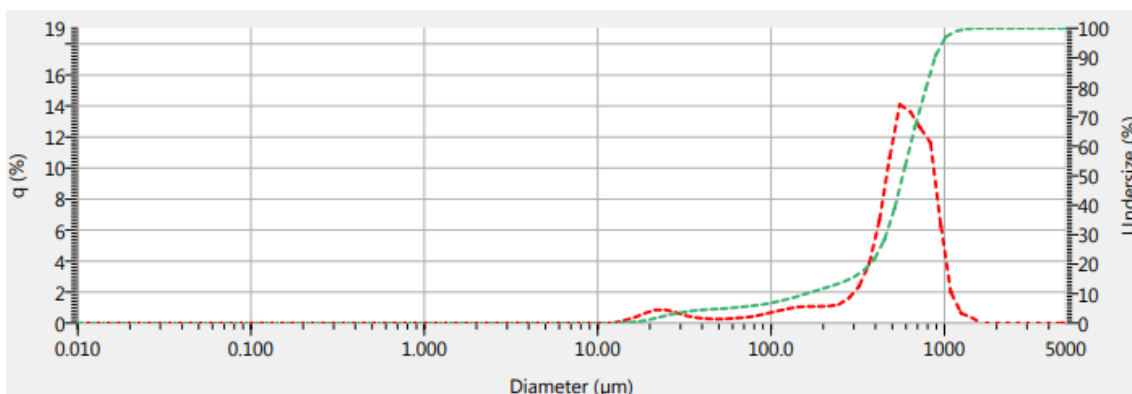


Figure 3.5: Particle size distribution of CIPs.

3.2.3 Magnetic properties

The magnetic properties were analyzed by using vibrating sample magnetometer (VSM) (Lake Shore 7400 Series VSM system, United States). This analysis was conducted to determine whether the magnetic flux can flow through MRE samples. From the hysteresis loop, the magnetic saturation (M_s), retentivity (M_r), and coercivity (H_c) were obtained after applying maximum value of magnetic field. The magnetic properties of MRE samples were measured from -0.8 to 0.8 KOe or equivalent with -8000 to 8000 Gauss.

3.2.4 Chemical Bonding Analysis

The chemical bonding between ENR matrix in MRE with CIPs and other compounds was analyzed using FTIR (Model: FTIR Frontier, China) to identify the chemical groups and bonds in ENR matrix based MRE. All MRE samples were cut to 40 mm and placed in the provided mold. Frequency range of 400 cm^{-1} to 500 cm^{-1} was used in this study to obtain desirable results of ENR matrix in MRE.

3.2.5 Thermal Properties

The thermal properties of ENR 25- and ENR 50-based MRE were studied using TGA and DSC in order to determine the thermal behavior and thermal glass transition of the samples, respectively. The mass of the samples was approximately measured in range of 8–10 mg for both the tests. In case of TGA, The MRE samples were heated at temperature between 25°C to 600°C under constant heating rate of 10°C/min. Meanwhile, for DSC, the MRE samples were cooled from 0°C to 100°C under nitrogen atmosphere.

3.3 Rheological Analysis

The field-dependent rheological properties of the ENR 25- and ENR 50-based MREs were measured for the rheological analysis. The analysis was conducted under dynamic oscillatory state, and the experimental details are explained in the next subsection.

For rheological analysis, the samples were prepared by cutting the disk into thin cylindrical film having a diameter of 20 mm and the thickness 1 mm using steel plunger. Rotational Rheometer (MCR 302, Anton Paar Compony, Germany) located at Universiti Teknologi Malaysia, Kuala Lumpur (UTM) was used in this research to investigate the rheological properties of ENR 25- and ENR 50-based MREs. Two different controllers were identified in the rotational rheometer, namely, current controller (MRD 70) and temperature control device (Viscotherm VT2, Anton Paar, Germany). The current controller generated the magnetic field perpendicular to the direction of shear flow in test area. Meanwhile, the temperature control device was used to measure the temperature and control the temperature to be at 25°C.

The MRE samples were sheared at 100 s^{-1} with a constant shear rate at zero magnetic field for 30 s before performing the oscillating analysis. In addition, this

step was expected to make sure the magnetic particle was in uniform distribution within each sample. Besides, this step was likely to reduce the residual stress in the samples. This was followed by preliminary magnetic energizing process for 30 s to ensure the homogenous static interaction between CIPs within MRE samples.

After the pre-conditioning step, the sequence of oscillatory test was allowed to proceed. The dynamic oscillatory test was performed with increments in strain and current. In addition, the dynamic shear was applied for calculating the shear storage modulus, G' , loss modulus, G'' , and the loss factor, $\tan \varphi = G''/G'$, as a function of the strain amplitudes.

The main purpose to perform the strain amplitude test was to determine the LVE of each MRE sample. For strain sweep test, the strain was used from range 0.01% to 25% with constant frequency of 1 Hz. The current was increased from 0 to 5 A with increment of 1 A for each measurement. Meanwhile, for the magnetic field sweep test, magnetic fields with varying strengths were applied when varying the current from 0 to 5 A. For this test, the strain amplitude needs to be constant, and 1 Hz of constant frequency were used in magnetic field sweep test correspondingly (ASTM-D6204)

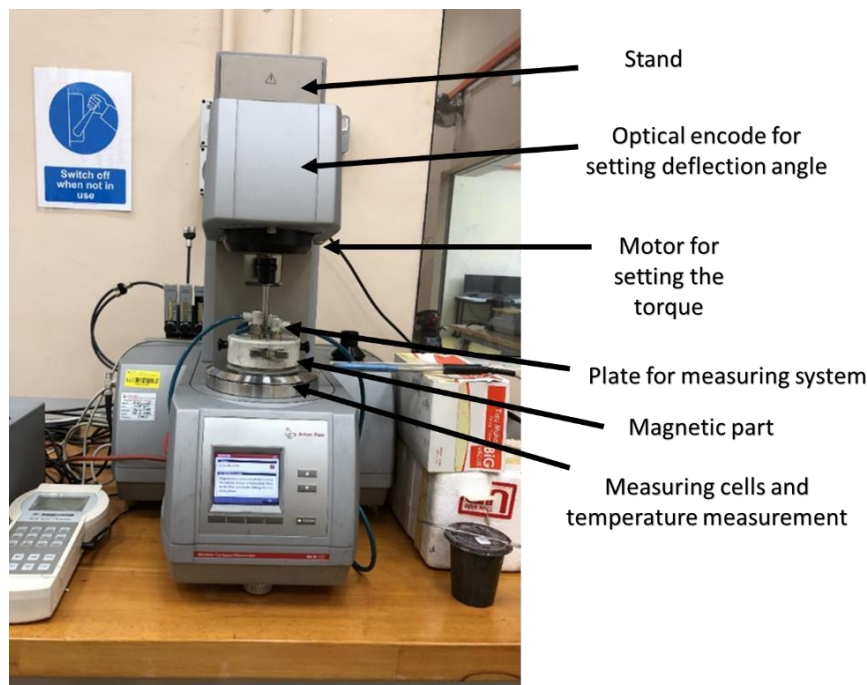


Figure 3.6: Rotational Rheometer for rheological analysis

CHAPTER 4

RESULTS AND DISCUSSION

4.1 Introduction

This chapter presents the results of data collection from the MRE/ENR 25 and MRE/ENR 50 samples. Two different sections discussing these results include physicochemical characteristics and field-dependent rheological parts. The first section explains the curing profile behavior, morphology of microstructure, elemental compositions, magnetization of matrix, thermal stabilities, and chemical elements in both samples. Curing profile was investigated for both ENR to make sure is really cure with other substances. Meanwhile, the morphology of microstructure was investigated to study the arrangement of the ENR matrix with CIPs. Furthermore, magnetic properties were studied as they are necessary for identifying the responsiveness of samples to external magnetic fields. In addition, the thermal stabilities are essential for both ENR as it will be easier to understand the MRE's characteristics in relation to temperature. Lastly, in physicochemical characteristics, chemical elements analysis for both ENRs was tested in this study, which is vital for researchers to identify which elements were involved.

4.2 Physicochemical Characterization

4.2.1 Curing Profile Behavior of ENRs based MRE

Figure 4.1 (a) and (b) show the curing curves of MRE samples with different constituent ENR and CIP composition. Generally, three phases can be identified from a vulcanization curve.

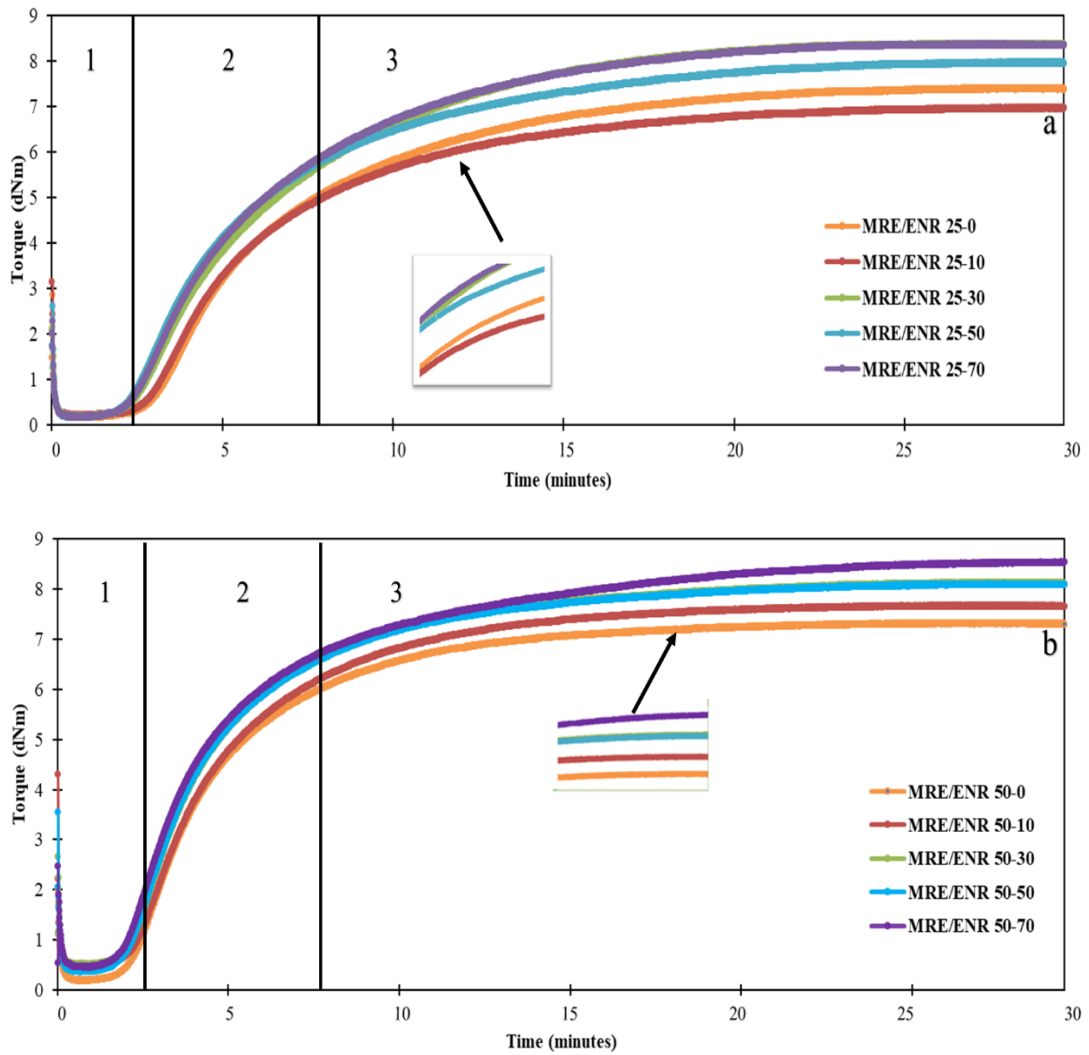


Figure 4.1: Curing curves of ENRs based MRE with different CIPs content: (a) ENR 25 (b) ENR 50

The first phase is recognized as an induction, which occurred in the first three minutes of the curing process [74]. During this phase, the curing curve showed an equilibrium torque value at less than 1 dN.m. This was certainly ascribable to slow chemical reactions between the ENR matrix with CIP and other additives. The second phase is known as the curing phase, which occurred between minute 3 and minute 8 for the MREs fabricated from ENR 25 and ENR 50. During this phase, the rubber molecular chains started to form a network structure between the polymers and the

fillers. The last stage is known as the overcuring phase [74]. The overcuring reaction depends on the type of rubber used, scale of temperatures, and vulcanization agents. The curing curve then plateaus at beyond 15 minutes, signifying that all the MRE samples have reached the equilibrium in the curing process.

From the curing curves, specifically the curing phase of the curve, two values can be derived: (i) optimum curing time (t_{90}) and (ii) scorch time (t_{s2}). The former represents the time taken for the rubber compound to achieve 90% of the maximum obtainable torque during the curing process, corresponding to 90% of the rubber having been vulcanized. The latter refers to the time taken for the rubber polymer to be exposed to the vulcanization temperature before the vulcanization process. The t_{90} and t_{s2} values of MRE samples are presented in Table 1. The t_{90} values increased with higher composition of CIP for both types of MRE, which is simply due to the CIP acting as a filler in the MRE composite. As CIP content increased, more CIP would entangle with the rubber chains, and consequently the t_{90} increased. However, the t_{90} of MRE/ENR 50 is considerably shorter than MRE/ENR 25. This could be due to the breaking of the carbon–carbon double bond (C=C) by adjacent epoxy groups in ENR 50. High number of epoxy group that contain in ENR 50 can easily break the C=C bond when increasing of time taken during curing process. MRE/ENR 25 took a long time to cure compared to MRE/ENR 50, regardless of CIP content.

The t_{s2} exhibited a different trend from t_{90} , where it decreased upon increasing CIP composition, as shown in Table 4.1. From the sample with 0 wt% CIP to the sample with 70 wt% CIP, the MRE/ENR 25 had its t_{s2} decrease from 4.19 minutes to 3.37 minutes, while the MRE/ENR 50 had its t_{s2} decrease from 3.11 minutes to 2.83 minutes. This is because of the C=C bond being broken and replaced with the epoxy ring from the epoxy group. Generally, the number of epoxide group influences the rate of crosslink, and the higher the number of epoxy rings in the polymer, the more chances of a crosslinking occurring in the ENR itself [75]. Consequently, the scorch time of ENR 50 was less than ENR 25. In addition, the scorch times for both types of MRE were less than five minutes. This is attributed to the presence of calcium stearate in the MRE. The low pH in the ENR can have a large effect on its scorching

characteristics [28]. Hence, a basic compound such as calcium stearate is required to control processing safety [28].

Table 4.1: The cure and scorch time of ENR 25 and 50 based MRE

MRE Samples	Cure Time (t_{90}) [minutes]	Scorch Time (t_{s2}) [minutes]
MRE/ENR 25-0	13.81	4.19
MRE/ENR 25-10	13.91	4.10
MRE/ENR 25-30	14.02	3.60
MRE/ENR 25-50	14.08	3.48
MRE/ENR 25-70	14.36	3.37
MRE/ENR 50-0	10.34	3.23
MRE/ENR 50-10	10.97	3.11
MRE/ENR 50-30	11.22	3.01
MRE/ENR 50-50	11.44	2.92
MRE/ENR 50-70	13.49	2.83

Table 4.2 indicates the minimum (M_L), maximum (M_H), and torque differences ($M_H - M_L$) of MRE/ENR 25 and MRE/ENR 50 with different mass percentages of CIP. M_L refers to the viscosity and elastic modulus of the uncured rubber. M_H represents the hardness of the rubber after the vulcanization process. $M_H - M_L$ is the dynamic shear modulus, which is consequently related to the crosslink density of the MRE samples. For both MRE/ENR 25 and MRE/ENR 50 samples, the M_L showed a similar trend in which the value for M_L increased after increasing the weight percentage of CIPs. Contradicting trend in the values of M_H and $M_H - M_L$ was observed for MRE/ENR 25, where the values decreased as CIP composition increased. Meanwhile, the values exhibited by the MRE/ENR 50-based MRE increased upon increasing CIP composition. This might be attributed to the low number of activated epoxy rings in ENR 25 compared to in ENR 50. Less activation of epoxy content in ENR decreases the rubber–filler interaction as the concentration of CIP increased [1]. Subsequently, this phenomenon adversely affected the crosslink density between ENR 25 and ENR 50 with CIP in the MRE samples.

Table 4.2: The minimum torque, maximum torque and torque differences values of ENR 25 and 50 based MRE

MRE Samples	Minimum Torque (ML) [dNm]	Maximum Torque (MH) [dNm]	Torque Differences (MH-ML) [dNm]
MRE/ENR 25-0	0.18	8.38	8.20
MRE/ENR 25-10	0.17	8.37	8.20
MRE/ENR 25-30	0.16	7.97	7.81
MRE/ENR 25-50	0.16	7.40	7.24
MRE/ENR 25-70	0.21	6.97	6.76
MRE/ENR 50-0	0.18	7.33	7.15
MRE/ENR 50-10	0.47	7.69	7.22
MRE/ENR 50-30	0.50	8.14	7.64
MRE/ENR 50-50	0.36	8.11	7.75
MRE/ENR 50-70	0.46	8.55	8.09

4.2.2 Microstructural and Elements

Figure 4.2 until 4.6 illustrate the microstructure of MRE/ENR 25 and MRE/ENR 50 at different mass percentages of CIP. The CIP were randomly dispersed within both ENR matrices, which confirmed the MRE as being isotropic. More distributed CIP were observed for samples containing high mass percentages of CIP, while no CIP were detected in samples without CIP, as shown in Figure 4.2 (i) and (ii). The dispersion of CIP plays a major role in determining the sustainability performance of the MRE, particularly its magnetic and rheological properties [86]. Furthermore, a uniform distribution of CIP provides a smooth magnetic flux within the ENR 25 and ENR 50 matrices, contributing to favorable magnetic properties and MR effect. However, some porosities and agglomeration of CIP were observed in both ENR-based MRE, as shown in Figure 4.3, Figure 4.4, Figure 4.5, and Figure 4.6. The

porosities can be either beneficial or detrimental to the MRE properties [87]. In addition, the distribution of CIP also favors the agglomeration in the rubber. As evident from Figure 4.3, Figure 4.4, Figure 4.5, and Figure 4.6, the agglomeration of CIP and other additives increased with increasing CIP. Therefore, it can be said that the weight percentage of CIPs in the ENR 25- and ENR 50-based MRE have high potential to create more agglomeration.

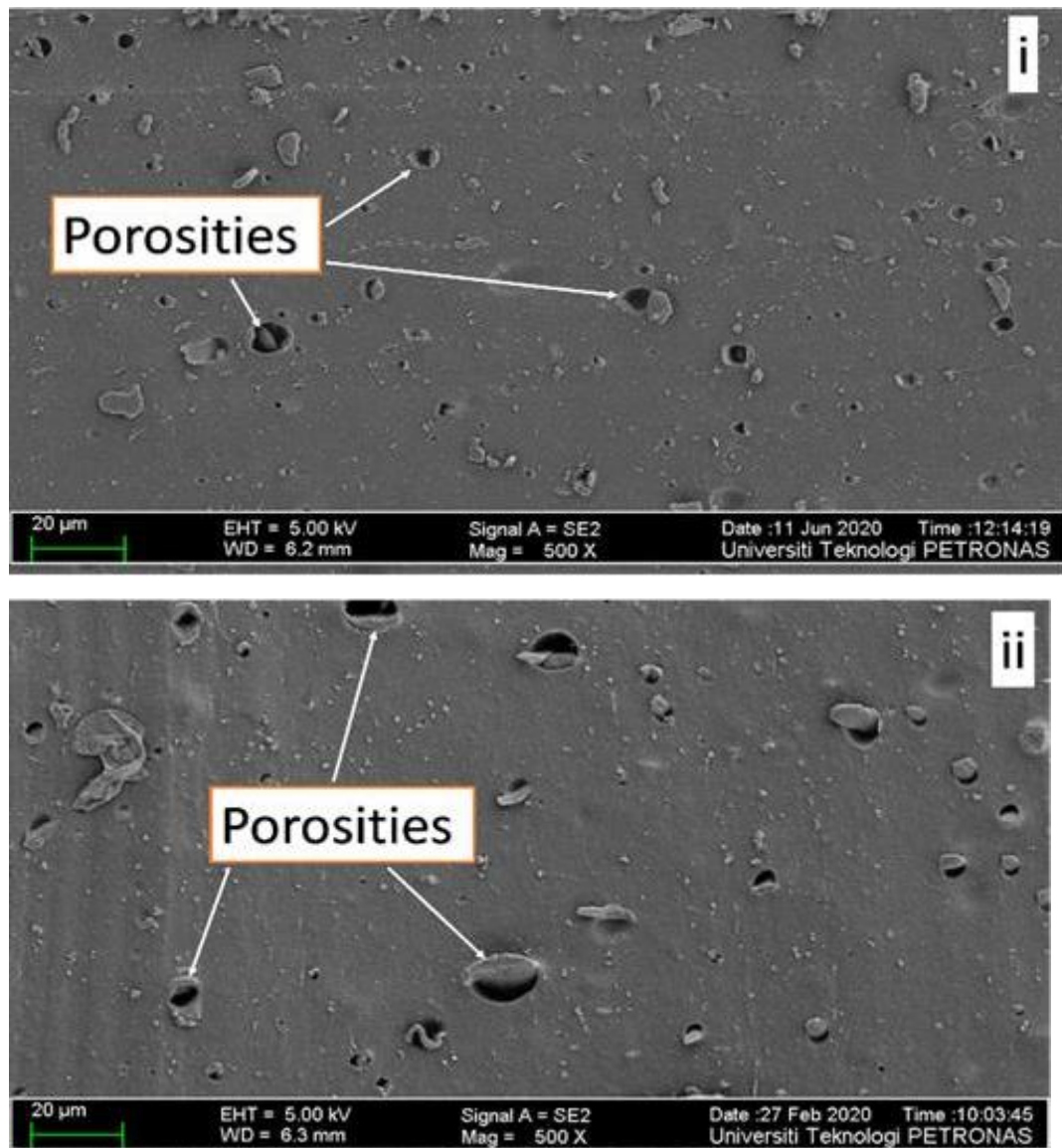


Figure 4.2: Microstructures of ENR based MRE with 0wt% of CIPs (i) ENR 25 (ii) ENR 50

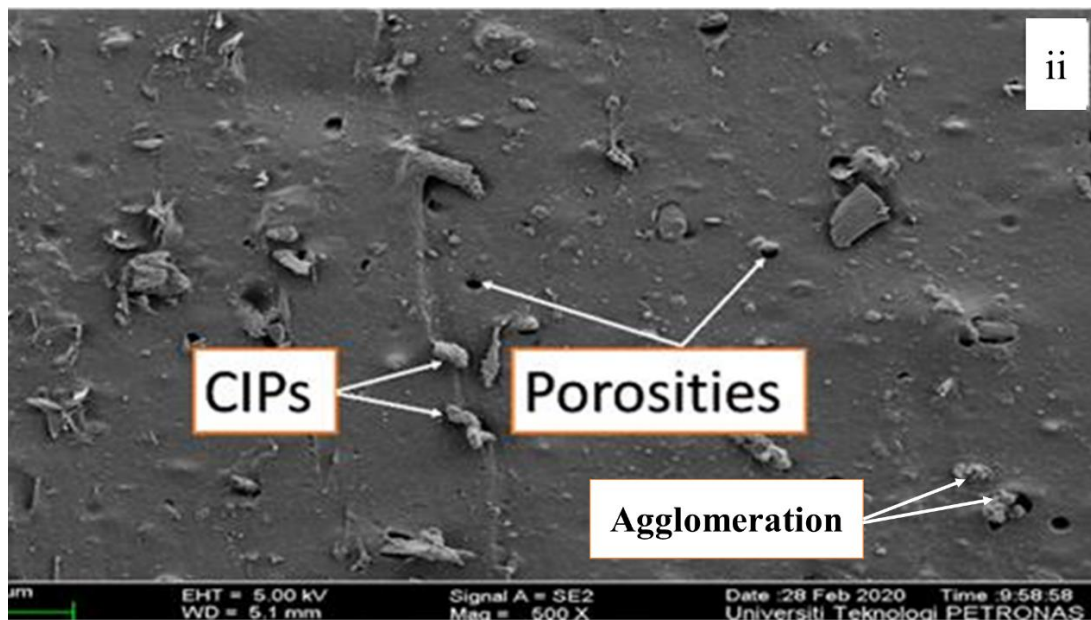
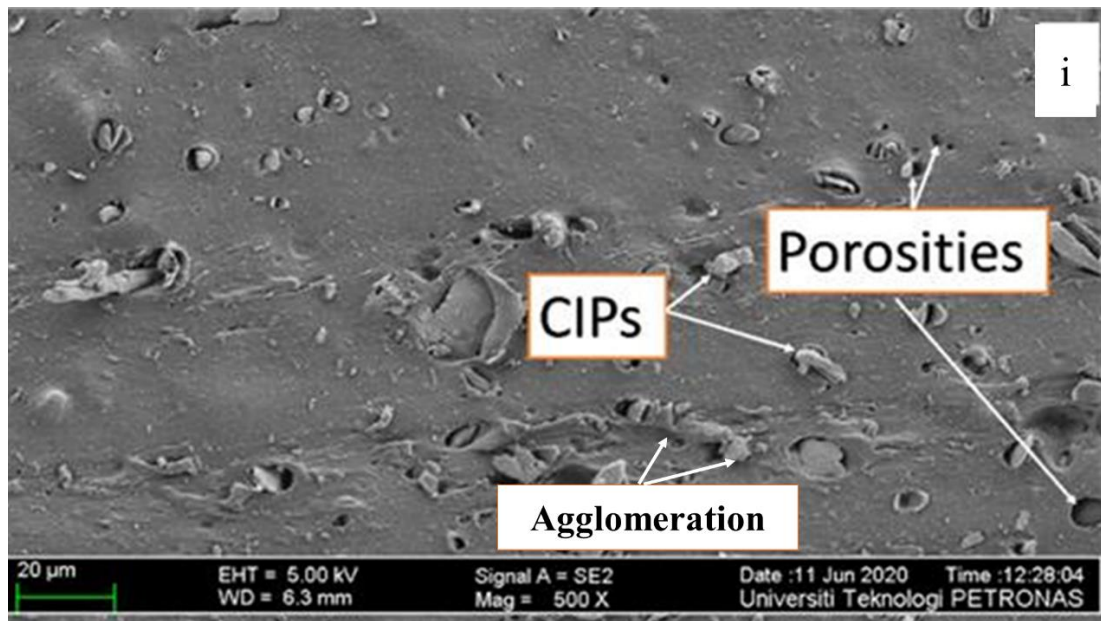


Figure 4.3: Microstructures of ENR based MRE with 10wt% of CIPs (i) ENR 25 (ii) ENR 50

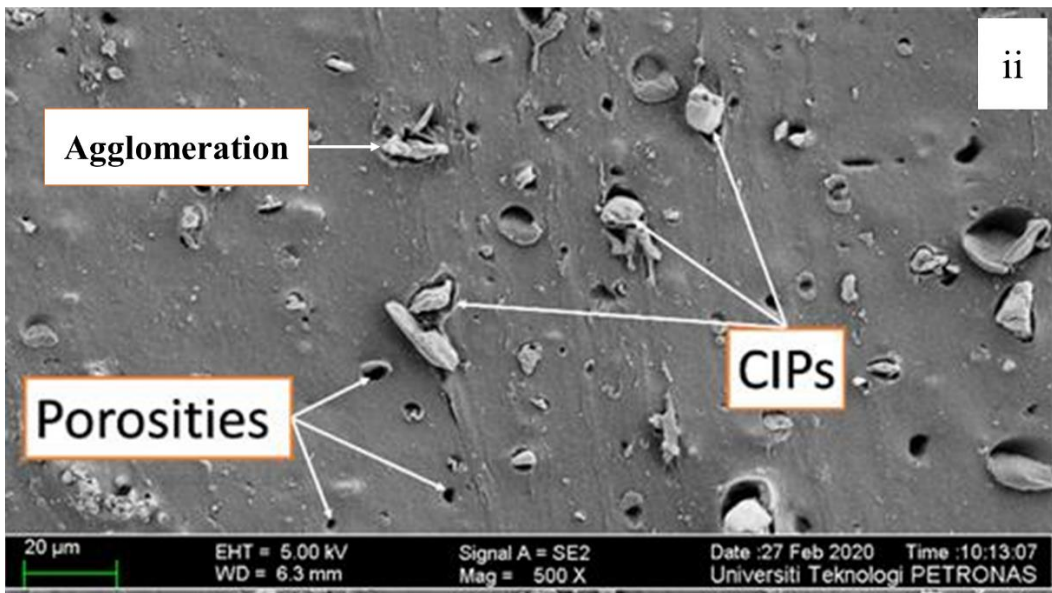
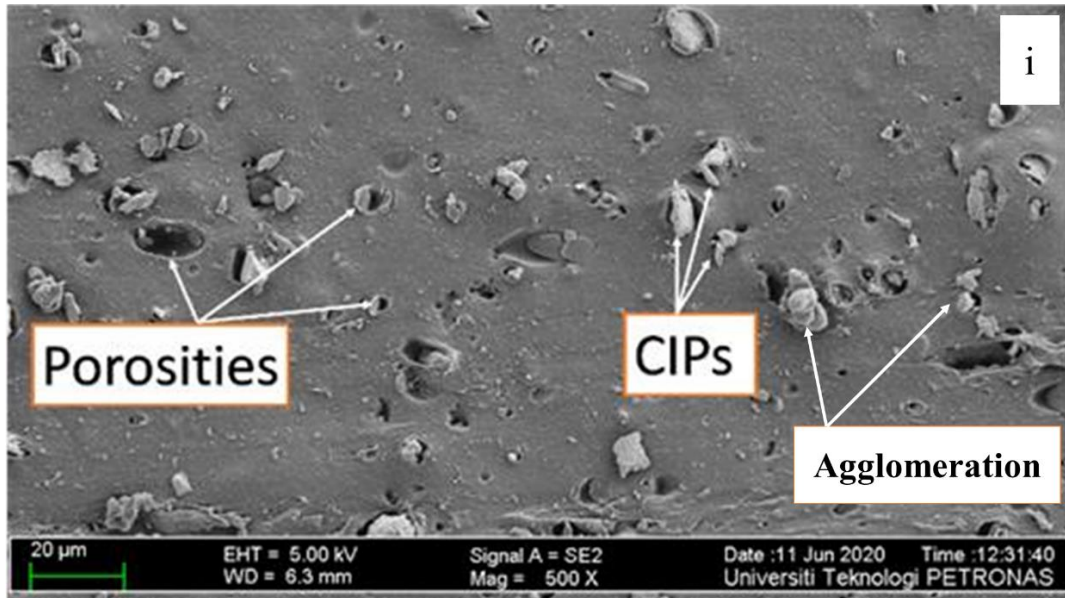


Figure 4.4: Microstructures of ENR based MRE with 30wt% of CIPs (i) ENR 25 (ii) ENR 50

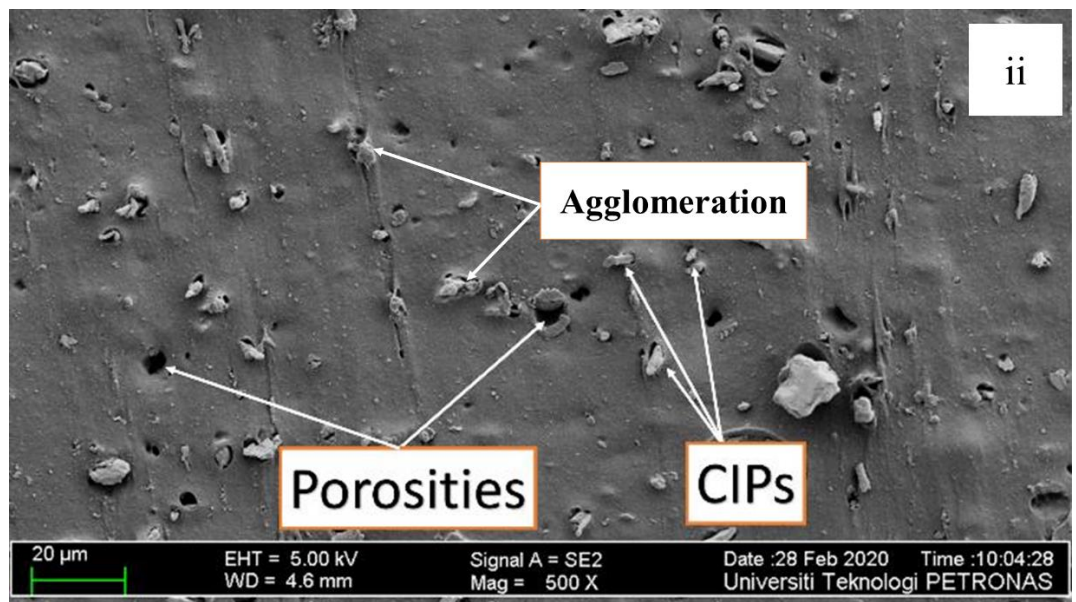
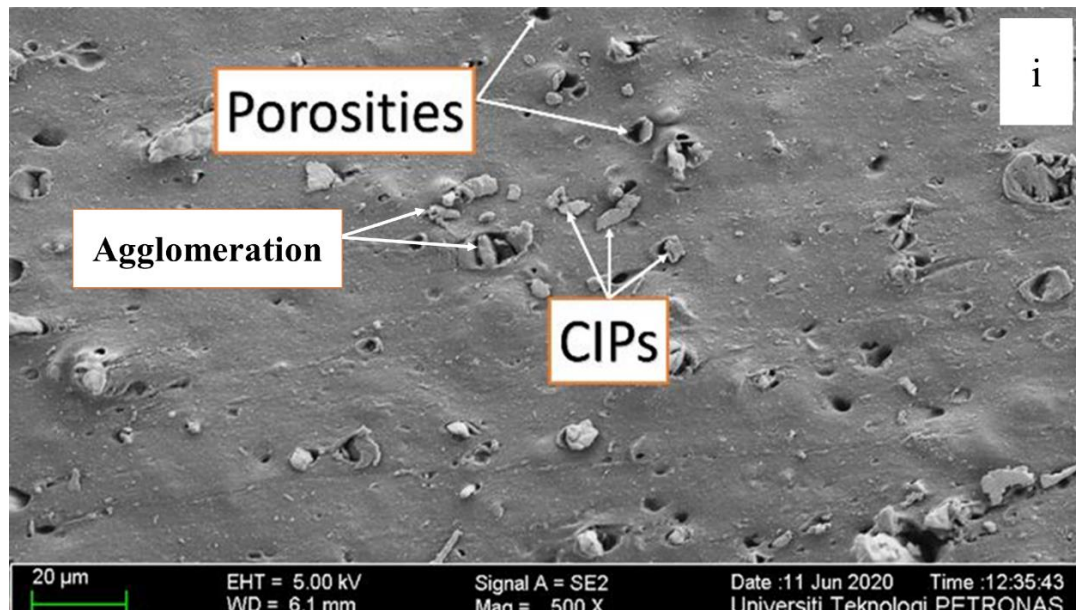


Figure 4.5: Microstructures of ENR based MRE with 50wt% of CIPs (i) ENR 25 (ii) ENR 50

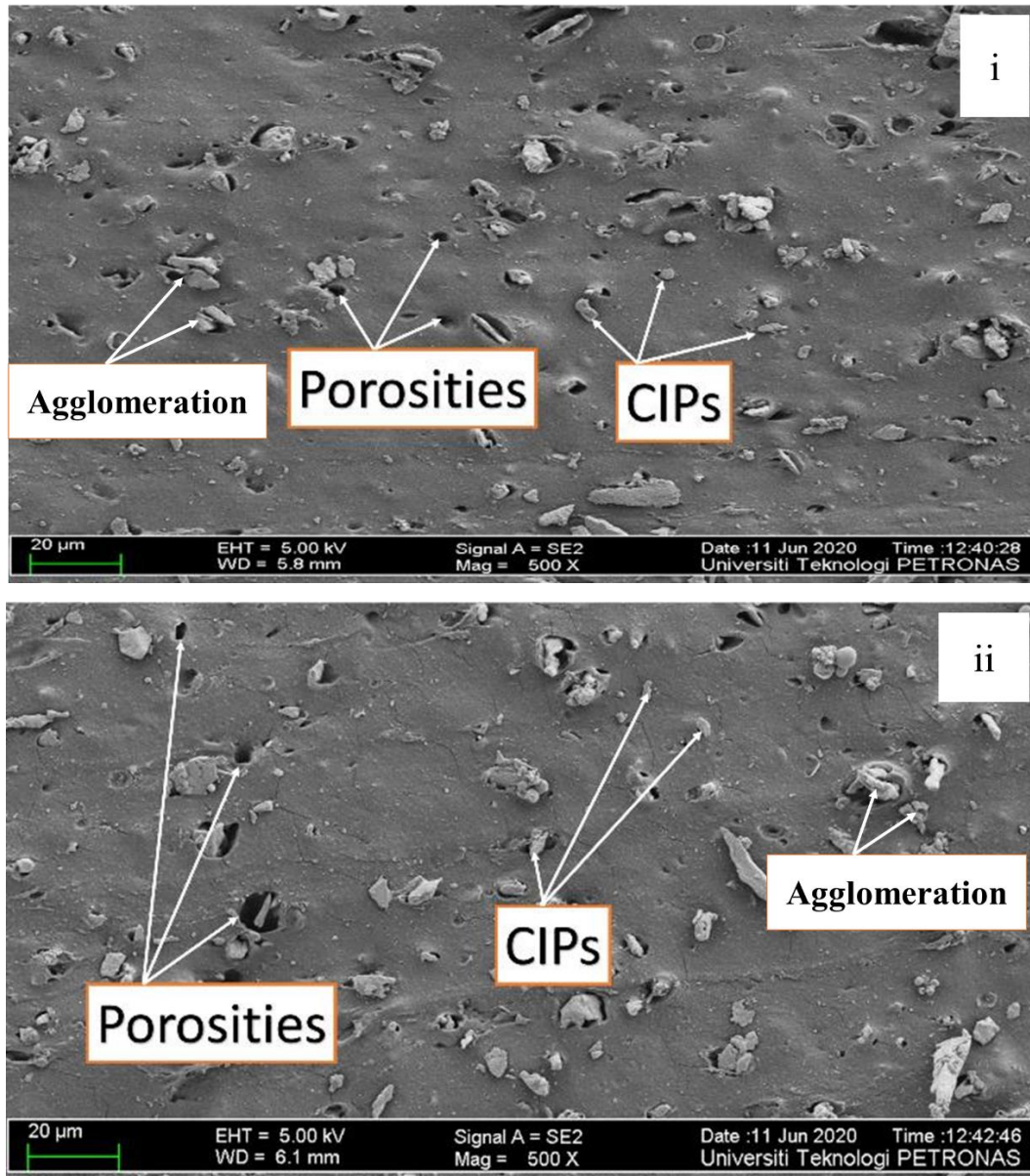


Figure 4.6: Microstructures of ENR based MRE with 70wt% of CIPs (i) ENR 25 (ii) ENR 50

All samples of MRE/ENR 25 and MRE/50 were also examined under the EDX analysis to advocate the presence of CIPs and other elements. The EDX analysis results are depicted in Figure 4.7, Table 4.3, and Table 4.4, wherein all the peaks in EDX figures were presented for all elements in MRE samples. Figure 4.7 represent the peaks that correspond with the elements in MRE samples that existed in 0 wt% and 70 wt% of CIPs.

Table 4.3: Elemental results of ENR 25 based MRE for different weight of CIPs

Elements and CIPs content (wt%)	Fe	C	S	Zn	O	Ca	Cl
0	0.00	81.98	1.95	1.92	12.34	1.51	0.30
10	2.15	79.54	1.98	1.98	13.43	0.92	0.00
30	5.92	79.24	1.70	1.87	9.98	1.29	0.00
50	8.62	78.84	1.60	1.85	9.05	0.04	0.00
70	14.25	73.25	1.65	1.98	8.73	0.14	0.00

Table 4.4: Elemental results of ENR 50 based MRE for different weight of CIPs.

Elements and CIPs content (wt%)	Fe	C	S	Zn	O	Ca	Cl
0	0.00	82.39	1.95	2.59	12.56	0.21	0.30
10	1.95	79.85	1.98	2.56	13.66	0.00	0.00
30	5.81	79.89	1.70	2.19	10.09	0.31	0.00
50	8.55	78.84	1.60	1.68	9.12	0.22	0.00
70	14.21	73.26	1.65	1.97	8.92	0.00	0.00

Table 4.3 and Table 4.4 display the elements that contains different weights of CIPs of ENR 25- and ENR 50-based MRE. Apparently, sample with 0 wt% of CIPs showed that the Fe element in the sample was 0 wt%. It is proved once again that there are no CIPs in the sample. Based on the Table 4.3 and Table 4.4, the wt% of Fe increased from 0.00 to 14.25 wt% for MRE/ENR 25, meanwhile for MRE/ENR 50, it increased from 0.00 to 14.21 wt% as CIPs increased from 0 to 70 wt%. Noticeably, the Cl element was only found in 0 wt% of CIPs. This is probably attributable to the presence of calcium stearate in the samples. Other elements such as carbon, sulfur, zinc oxide, and oxygen that come from the additives, which are already added to rubber compounding, were also found in the EDX results. Carbon had the highest amount in MRE samples. This is due to the presence of carbon black in the sample,

which subsequently enhanced the bonding between ENR 25 and 50 elastomers with CIPs. As a highlight, the microstructure and elements of ENR 25- and ENR 50-based MRE are in parallel and showed that the distribution of CIPs within ENR 25 and ENR 50 matrices were randomly distributed.

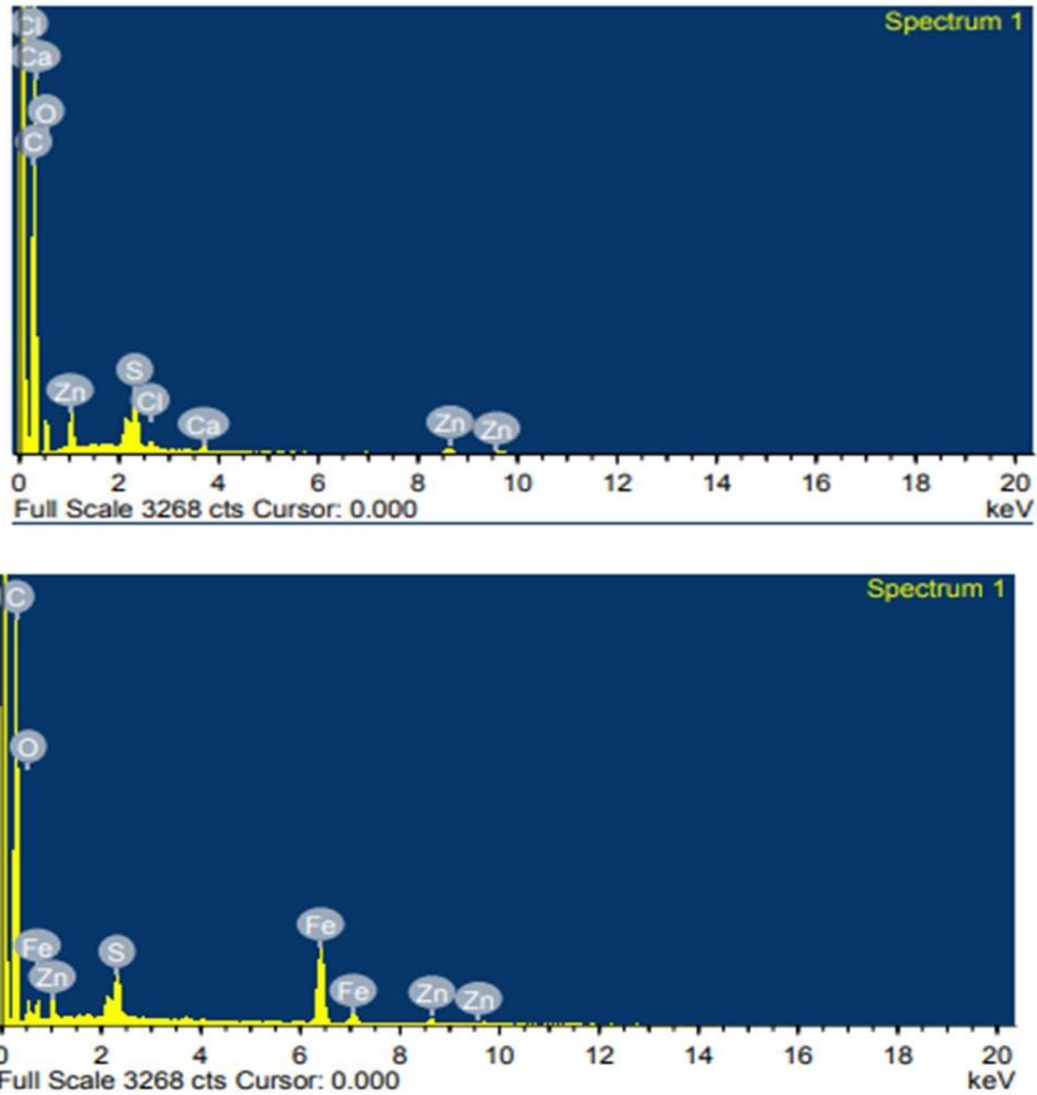


Figure 4.7: EDX graphs of sample ENR 50 based MRE with (a) 0wt% (b) 70wt%

The presence of CIPs is evident in Figure 4.7 (b) in which the Fe peak elements can be identified. Meanwhile, no peak of Fe elements can be seen in Figure 4.7 (a). This proved that the sample of 0 wt% of CIPs is clearly defined, i.e., no CIPs existed

in the samples. In addition, three different peaks of Fe were analyzed in Figure 4.7(b), which concede with 70 wt% of CIPs. Therefore, the EDX results were correlated with microstructural figures for ENR-based MRE. Other than Fe, several peaks were found in the MRE samples such as carbon (C), calcium (Ca), sulfur (S), oxygen (O), zinc (Zn) and chloride (Cl).

4.2.3 Magnetic Properties of ENRs based MRE

Figure 4.8 (a) and (b) depict the hysteresis loops of MRE samples fabricated from ENR 25 and ENR 50 with various masses of constituent CIP. The narrow hysteresis loops were identified in both ENR-based MRE samples, which suggest that all MRE samples have soft magnetic characteristics. The magnetization curves for all MRE samples increased up to 5000 Gauss, beyond which the curve became slender. It is believed that at this moment, the dispersion of CIP within the ENR had reached saturation, and therefore, the magnetic saturation (M_s) may be recorded for that material. At magnetic saturation, the magnetization of MRE samples did not increase further, as all magnetic moments within the magnetic particles were already aligned with the direction of the magnetic field. All these important values such as M_s , retentivity (M_r), and coercivity (H_c) at various mass percentages of CIP in ENR 25- and ENR 50-based MRE are enumerated in Table 4.5.

The M_s values for both ENR-based MREs increased upon increasing CIP content. However, the M_s value for MRE/ENR 25 with 70 wt% of CIPs was at 42.54 emu/g. Meanwhile, the M_s value for MRE/ENR 50 with same weight percentage of CIP was 40.80 emu/g which is less than MRE/ENR 25. This is probably due to the iron from CIP reacting with the oxygen from the epoxy ring and forming iron oxide during the curing process. From the epoxidation process, more oxygen atom will form when the epoxy content increases.

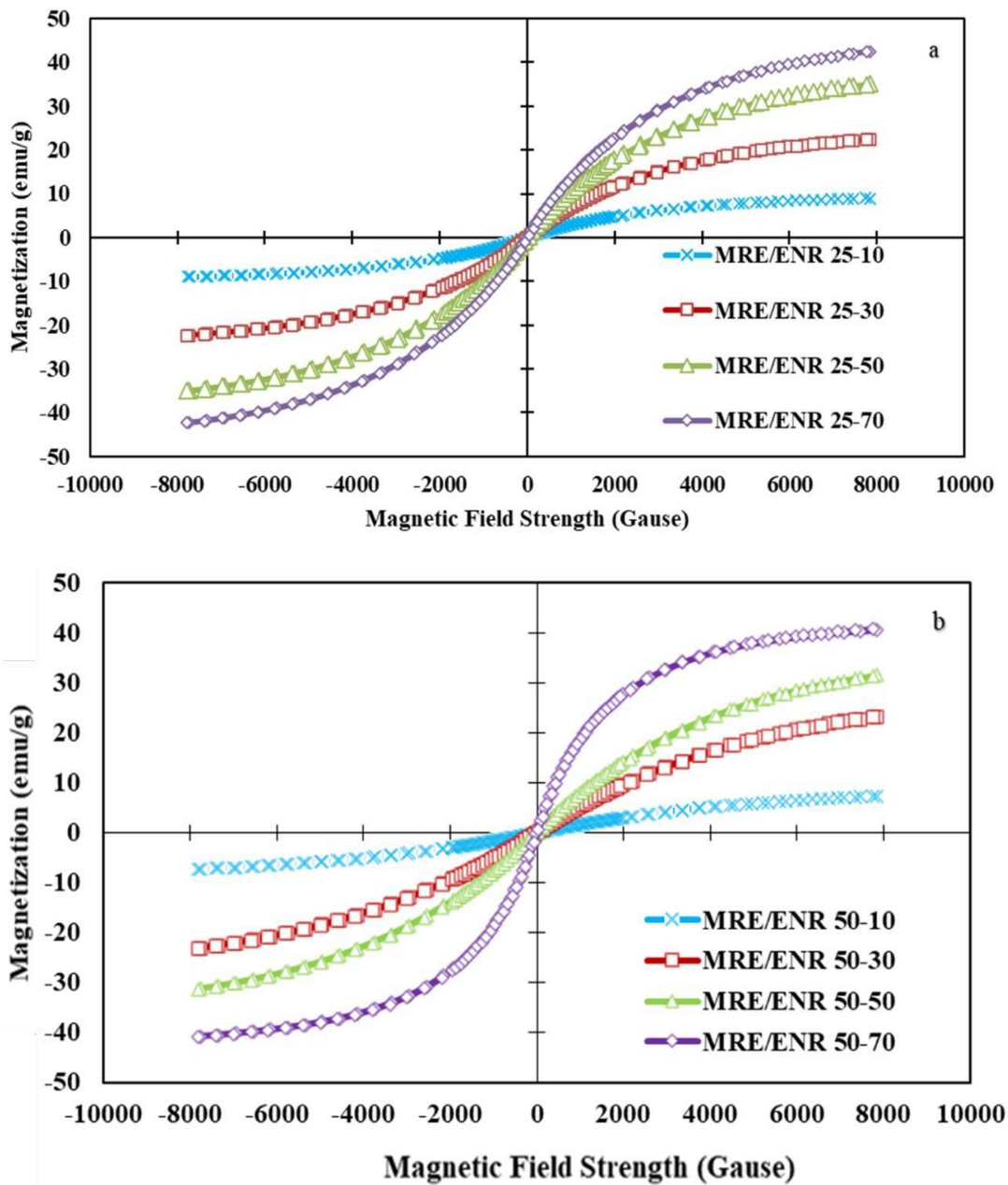


Figure 4.8: Hysteresis loops of ENRs based MRE with various weights of CIPs contents (a) ENR 25 (b) ENR 50

Thus, ENR 50 has more oxygen due to high amount of epoxy ring. Iron oxide is more likely to develop when the number of oxygen atom that could react with iron from the CIP increases. A difference in M_s value for both ENR-based MREs was found, and it adversely affected the performance when implemented on MRE devices.

Meanwhile, the M_r values for MRE/ENR 25 and MRE/ENR 50 showed a similar trend with M_s , where both increased upon increasing CIP composition. The high M_r in ENR-based MRE caused a significant magnetic remanence. Nonetheless, the increment of M_r in all samples is comparatively small in values, which proved that the MRE/ENR 25 and MRE/ENR 50 exhibited soft magnetic characteristics. All the MRE samples of ENR 25 and ENR 50 proved that increasing CIP contributed to the increase in magnetic flux through the samples when magnetic field was applied. Consequently, all the MR samples enhanced the magnetic properties, which is one of the important parameters need to be considered before implementation in MRE devices, and from the results, MRE/ENR 25 is slightly better than MRE/ENR 50 with regard to the magnetic properties.

Table 4.5: The magnetic properties of ENR 50 and 25 based MRE for various wt% CIPs.

MRE samples	Magnetization (M_s) emu/g	Coercivity (H_c) A m⁻¹	Retentivity (M_r) emu/g
MRE/ENR 50-10	7.32	17.41	0.03
MRE/ENR 50-30	23.17	17.33	0.10
MRE/ENR 50-50	31.42	17.30	0.15
MRE/ENR 50-70	40.80	14.73	0.40
MRE/ENR 25-10	8.98	15.81	0.005
MRE/ENR 25-30	22.38	15.70	0.13
MRE/ENR 25-50	35.08	15.45	0.20
MRE/ENR 25-70	42.54	15.23	0.25

4.2.4 Chemical Bonding of ENRs based MRE

Figures 4.9 (a) and (b) depict the FTIR spectra of the chemical interaction between the MRE and the CIP. Different peaks, bonds, and chemical groups have been identified for different mass percentages of CIP.

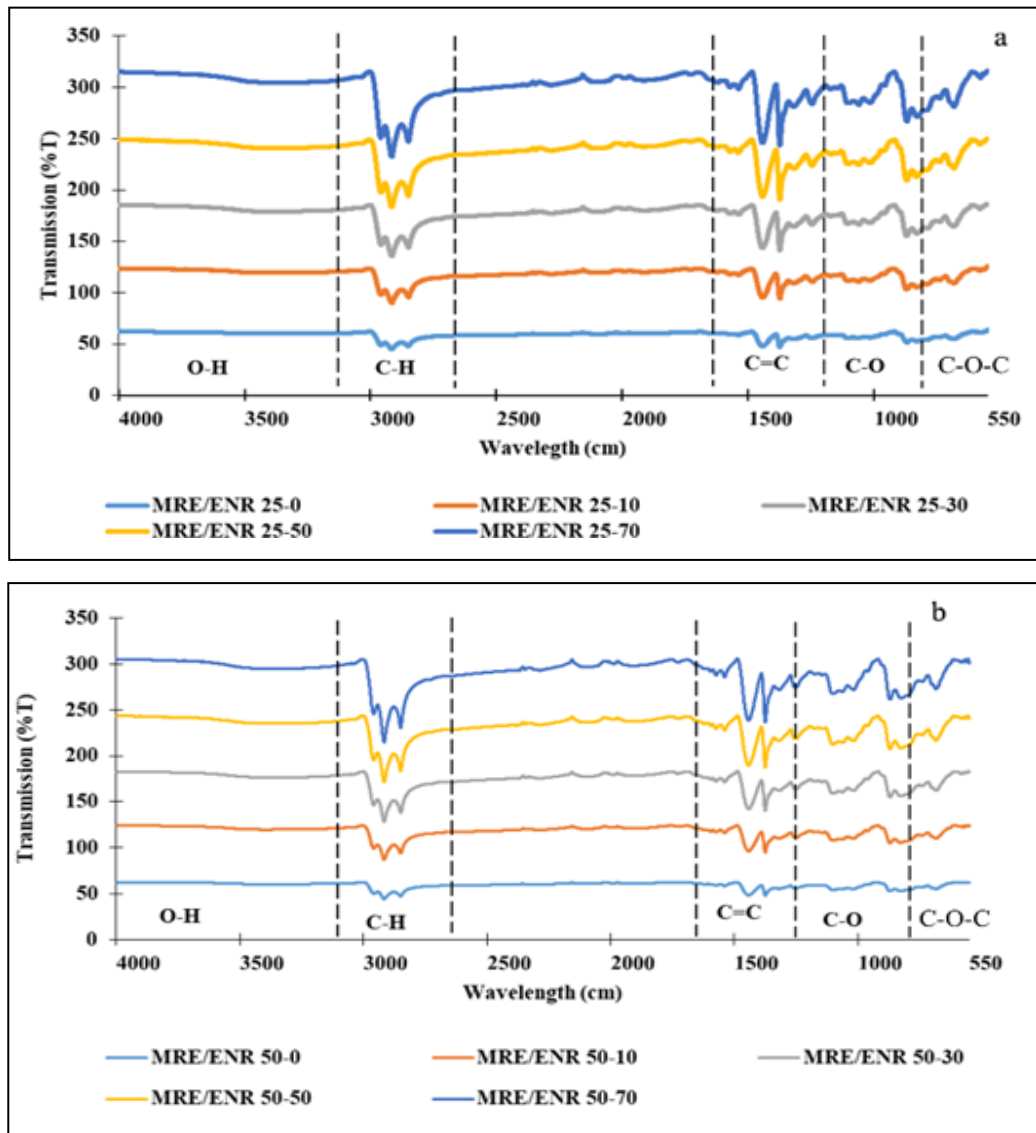


Figure 4.9: The FTIR spectra of chemical bonding between ENRs based MRE with CIPs content (a) ENR 25 (b) ENR 50

The presence of CIP within the MRE samples is evident at the range of 3700 cm^{-1} to 3250 cm^{-1} , where a peak appears at a height correlated with CIP composition, and it was recognized as an O-H signal peak. Meanwhile, the peak appearing at 2700 cm^{-1} to 3200 cm^{-1} and associated with C-H stretching vibration was detected. Both types of MREs had a peak at 870 cm^{-1} , which is associated with the stretching vibration of the C-O-C ring (epoxy group). The chemical interaction between the ENR 25- and ENR 50-based MRE was clearly identified with the peak at 1347 cm^{-1} , where the peak gradually increased with increasing CIP. However, the epoxy peak

from the MRE/ENR 50 (315% transmission) was stronger compared to the peak in the MRE/ENR 25 (304% transmission) .

Furthermore, the peak at 1120 cm^{-1} corresponding to the ether bond also increased in intensity alongside increasing CIP composition. The ether bond was formed from the chemical interaction between epoxy group from ENR and the hydroxyl group from CIP. In addition, the peak around 1245 cm^{-1} , which represents the C–O group, also increased in both types of MRE. This was probably due to the balance of oxygen group causing the epoxy group of the rubber to open up, subsequently creating the strong hydrogen bond between the oxygen and the epoxy group. The higher the epoxy content that can react with the balance of oxygen, the stronger the hydrogen bonding will form. It can be concluded that the number of mol% of epoxidation influenced the formation of hydrogen bonding between the ENR and the CIP. The formation of hydrogen bonding in the MRE composite constrained the polymer chain within it.

4.2.5 Glass Transition Temperature of ENR-based MRE

Figure 4.10 (a) and (b) present the DSC curves of the MRE samples. The MRE samples with different ENR grades show correspondingly different values of T_g , which refers to the temperature where the polymer started to change from soft to rubbery (hard to glassy state). As shown in the figures, all MRE samples displayed an endothermic heat flow, with increasing CIP content. Endothermic is a chemical reaction that the reactant absorbs heat energy from the surrounding. The MRE fabricated from ENR 25 had its T_g reduced from -53.2°C to -55.1°C , while the MRE fabricated from ENR 50 had its T_g reduced from -24.5°C to -26.1°C . This reduction in glass transition temperature was due to the transition phase from glassy to rubbery state, whereby as the CIP content reached 70%, there were more CIPs in the composite than rubber. After increasing the CIP content into the ENR samples, the interaction between CIPs and ENR rubber limits the molecular mobility of the matrix chains. In addition, loaded CIPs that entangled between matrix polymer chain decreased the free space from polymer chain.

The MRE/ENR 50 had a lower T_g than the MRE/ENR 25. This is attributed to the fact that the number of epoxy groups in MRE/ENR 50 is higher than MRE/ENR 25. As stated in the result, high number of epoxy group can soften the rubber compared to a smaller number of epoxy groups. The epoxide group content in the composite had a significant impact on its thermal property, and it has been shown that the T_g of ENR increases with increasing concentration of CIPs [86–87].

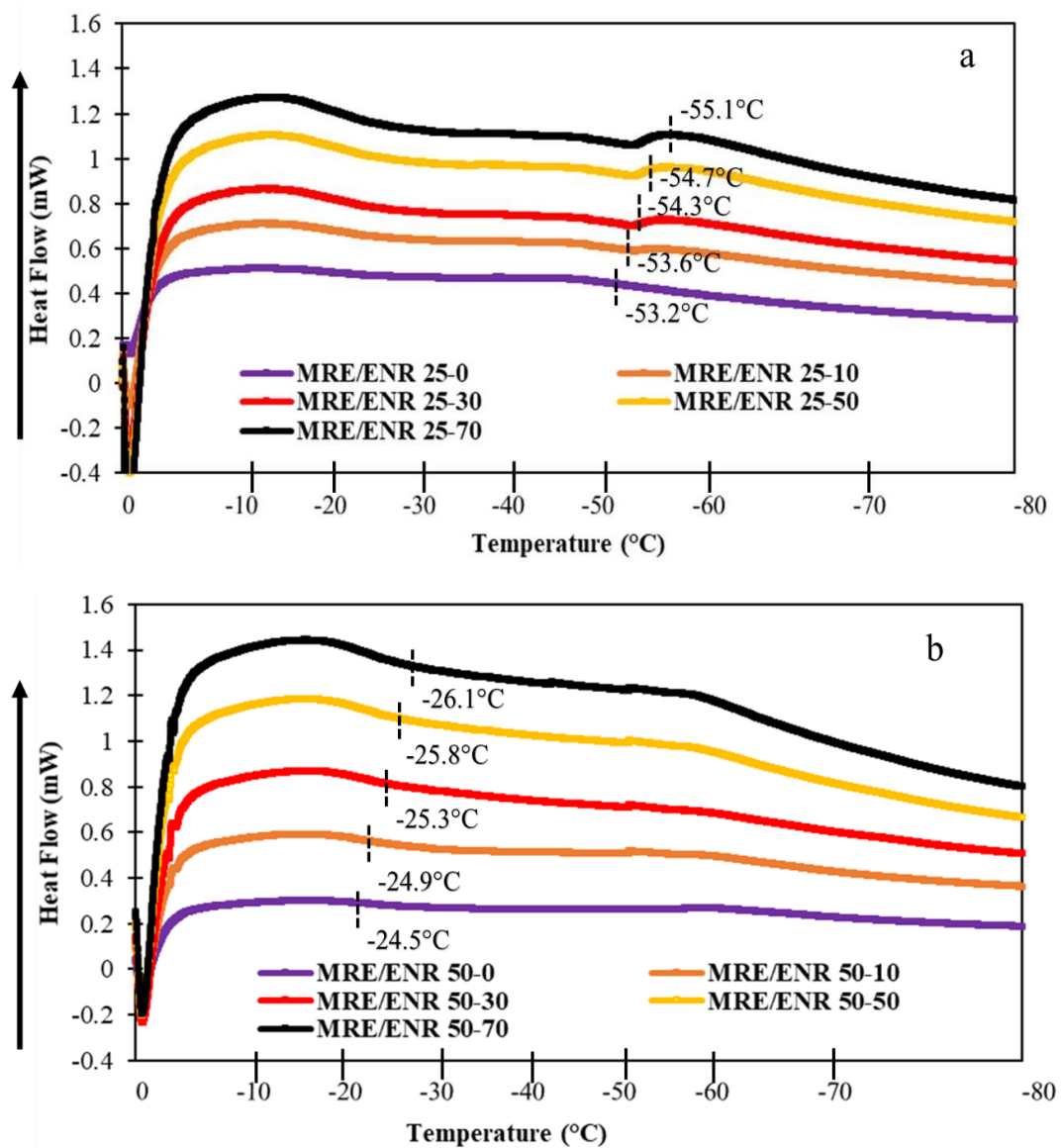


Figure 4.10: Thermal glass transition temperature of (a) ENR 25 and, (b) 50 based MRE with variation weights of CIPs

4.2.6 Thermogravimetric of ENR based MRE

As can be seen in Figure 4.11 (a) and (b), two degradation stages were identified for both ENRs. The first occurred from 336°C to 361°C, and the second occurred from 361°C to 432°C for ENR 25 based MRE. Meanwhile ENR 50, the first occurred from 341°C to 370°C, and the second occurred from 370°C to 454°C. In the first degradation stage, the mass of the sample saw a small reduction for both types of MRE, which is likely due to the decomposition of volatile compounds. Volatile compounds are unstable and could easily vaporize when the suitable conditions are met, as mentioned in the literature [38]. The second stage of degradation may be attributed to polymer degradation. Both types of MRE decomposed slowly at this temperature range, which has been speculated to be due to the CIP retarding the decomposition process in the MRE samples [86–87]. CIPs only start to decompose at 1000°C [4,17,39,40]. Evidently the ENR matrix containing CIP degraded at higher temperature compared to ENR without CIP.

Table 4.6 and Table 4.7 summarize the parameters that were measured during the thermal degradation temperatures of the MRE. The important parameters that pertain to the study are T_{onset} , T_{max1} , T_{max2} , and T_{end} . T_{onset} represents the temperature where the sample began to degrade, while T_{end} represents the temperature where the sample finished its thermal degradation. T_{max1} and T_{max2} represent the highest temperature where the first and second stage of thermal degradation had occurred, respectively. The results demonstrated that the onset temperature of both types of MRE increase proportionally with CIP composition. The T_{onset} of the MRE fabricated from ENR 25 increased from 336°C to 361°C between the sample with the least wt% of CIP to the sample with the highest wt% of CIP. The T_{onset} of the MRE fabricated from ENR 50 increased from 341°C to 370°C with CIP content. Meanwhile the MRE/ENR50 with different wt% of CIPs began to degrade at a higher temperature than the MRE/ENR25. This could be attributed to the level of epoxidation in both composites. As explained in chemical bonding results, the strengthening of hydrogen bond created from epoxy group and CIPs caused the MRE/ENR 50 to degrade at higher temperature compared with MRE/ENR 25.

Higher the number of epoxy group within the ENR matrix, the stronger hydrogen bond was created. Therefore, ENR 50 is thermally stable than ENR 25 due to the high amount of epoxide group content. As shown in Table 4.6, the T_{max1} , T_{max2} , and T_{end} for the MRE fabricated from ENR 25 are lower than MRE fabricated from ENR 50, indicating higher thermal stability. Moreover, the level of CIP has a significant effect on the thermal degradation the MRE, where all the measured temperatures increased along with increasing CIP composition

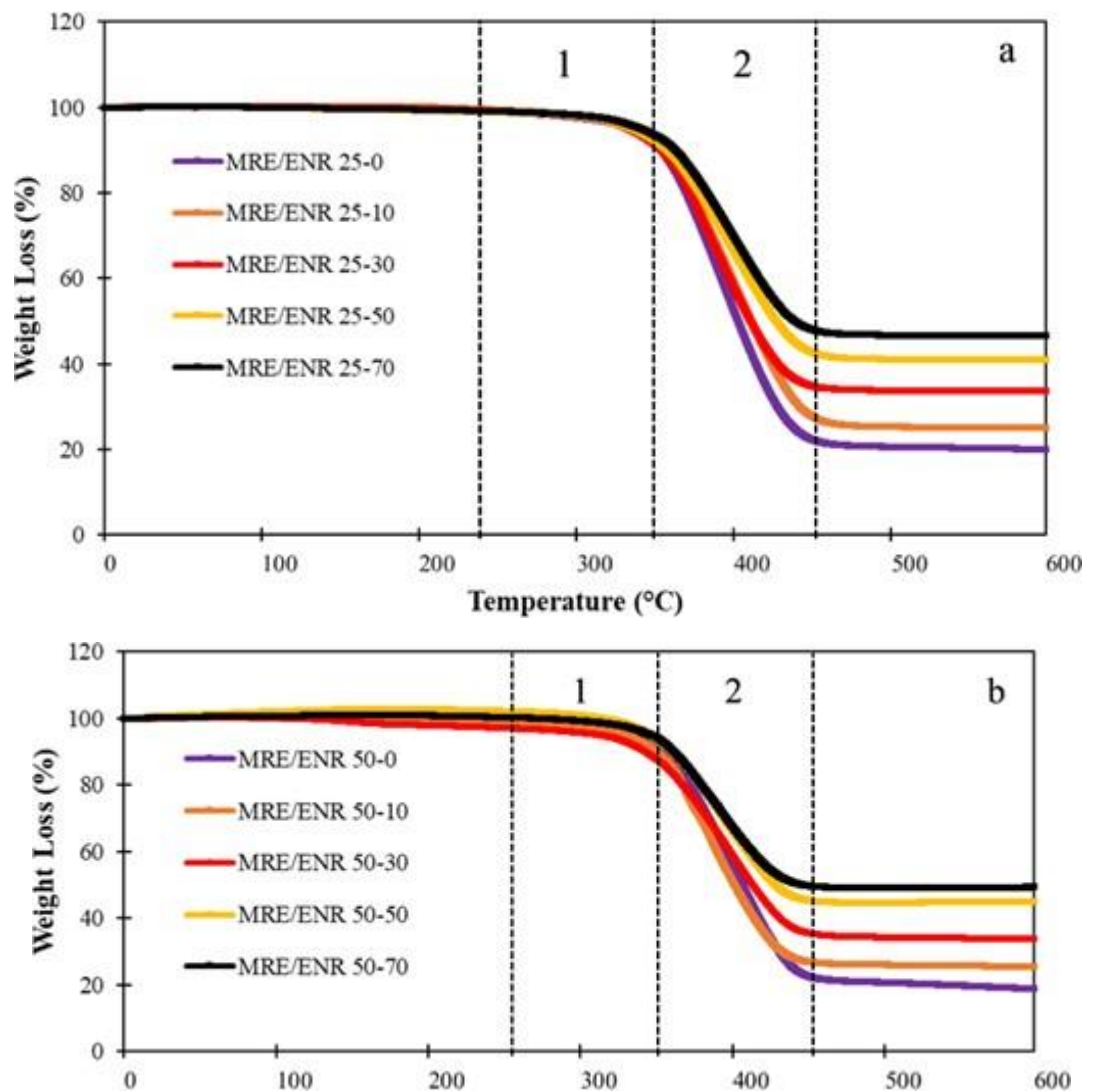


Figure 4.11: Thermal features of Thermogravimetric curve of ENRs based MRE with variation weights of CIPs (a) ENR 25 (b) ENR 50

A similar trend was observed for the amount of residue at the end of the thermal analysis for each sample. The percentage of residue produced by both types of MRE increased with increasing CIP composition. As the CIP composition increased from 0 wt% to 70 wt%, the residue produced by the MRE fabricated from ENR 25 increased from 19.3% to 58.9%, whereas that of the MRE fabricated from ENR 50 increased from 21.3% to 60.3%. The residue from the samples without any CIP was attributed to the incomplete decomposition of several additives in forming the composite [86–87] The presence of CIP in the MRE delayed the process of degradation because it is believed that it constrained the molecular chain of ENR

Some residue remains in the sample holder at the end of the thermal cycle because CIP and a few of the additives only start to degrade at beyond 1000°C [87]. It can be said that the incorporation of CIP into ENR 25 and ENR 50 improved the thermal stability of the resultant MRE. Interestingly, the mass percentage of residue from the MRE/ENR 50 600°C was higher compared to the MRE/ENR 25, especially samples with 70 wt% of CIP. This could be explained by the higher amount of epoxy ring increasing the crosslink density as created from the interaction with CIP. As a result, the motion of the molecular chain becomes more constrained. This was supported by Chuayjuljit *et al.* [14], who investigated the thermal behavior of NR and ENR 30 incorporated with multiwall carbon nanotubes. According to their investigation, ENR 30 was more thermally stable compared to NR, which they claimed was because the epoxide rings in ENR 30 formed a better intermolecular interaction with the multiwall carbon nanotubes

Table 4.6: The parameter of thermal degradation ENR 50 and 25 based MRE for various wt% CIPs.

CIPs content (wt%)	T_{onset} (°C)	T_{max1} (°C)	T_{max2} (°C)	T_{end} (°C)	Residue at 600(°C) (%)
MRE/ENR 25-0	336	354	375	407	19.3
MRE/ENR 25-10	338	357	382	413	29.2
MRE/ENR 25-30	340	358	388	420	39.8
MRE/ENR 25-50	342	360	397	429	52.6
MRE/ENR 25-70	343	361	403	432	58.9

Table 4.7: The parameter of thermal degradation ENR 25 and 50 based MRE for various wt% CIPs.

CIPs content (wt%)	T_{onset} (°C)	T_{max1} (°C)	T_{max2} (°C)	T_{end} (°C)	Residue at 600(°C) (%)
MRE/ENR 50-0	341	359	389	416	21.3
MRE/ENR 50-10	344	362	393	427	31.3
MRE/ENR 50-30	345	363	409	432	42.8
MRE/ENR 50-50	347	367	417	444	53.6
MRE/ENR 50-70	348	370	420	454	60.3

4.3 Rheological Properties of ENRs based MRE

The rheological properties of the ENR 25- and ENR 50-based MRE with different weights of CIPs are deliberated on oscillatory behavior. Several parameters such as weight of CIPs, strain amplitude, and magnetic field, are believed to affect the performance of rheological properties for both ENRs.

4.3.1 Strain Amplitude Sweep Test

Field-dependent rheological properties of ENR 25- and ENR 50-based MRE with different weights of CIPs were investigated under the strain amplitude sweep test. In this study, the variation of magnetic field values was varied with the usage of different currents starting from 0 A to 5 A. The current flow increment was 1 A for each test. The excitation of the amplitudes in each MRE sample was subjected to sinusoidal or harmonic loadings. In this study, the strain amplitude was chosen from the range 0.01% to 25% ramped logarithmically. This range can significantly identify the behavior of rubber through stress–strain analysis, especially for rubber that fill up with fillers such as carbon black and silica. All the MRE samples were examined under the same range with a constant frequency (1 Hz). The results of the storage modulus, loss modulus, and loss factor are demonstrated and summarized in the graphs presented herein.

According to Figures 4.12 (a) and (b), all the samples of MRE/ENR 25 and MRE/ENR 50 showed a similar trend wherein the initial storage modulus was increasing with increasing wt% of CIPs within the ENR matrix. Then, the storage modulus for all MRE samples started to decrease upon application of the strain up to 25%. In addition, it is found that the storage modulus value for MRE/ENR 25 was nearly constant at 0.025%, and for MRE/ENR 50, it is 0.040%, and it is known as linear viscoelastic region, i.e., LVE. At this region, the network structure was not affected by the strain used. Meanwhile, at nonlinear viscoelastic region (NLVE), structure of MRE samples becomes damaged when shear was exerted on samples. It is worth noting these two regions as it can prevent other tests such as frequency sweep

test and magnetic field sweep test from being conducted in the region in which is the structured polymer was already damaged.

According to Figure 4.12, the initial storage modulus increased with increasing wt% of CIPs. The additional of CIPs within the ENR matrix made the ENR rubber become stiff. Adding the CIPs within the ENR matrix caused the distance between CIPs to reduce. Subsequently, the interparticle magnetic force became stronger, and high value of storage modulus was noted. Figures 4.12 (a) and (b) show that the storage modulus for both ENR-based MRE increased with increasing wt% of CIPs, and MRE/ENR 25 produced 0.77 to 0.88 MPa. Meanwhile, the output storage modulus for MRE/ENR 50 ranged from 0.73 to 1.04 MPa with same wt% of CIPs used. Interestingly, the storage modulus for ENR 50-based MRE is 1.04 MPa, which is higher from MRE/ENR 25 with same wt% CIPs used (70 wt%). This is mainly attributed to the strong hydrogen bonding formed from the excess oxygen within the matrix and epoxy group. The more the epoxy content reacts with the balance of oxygen, the stronger hydrogen bonding. The hydrogen bonds limit the movements of the ENR molecular chains when shear is applied, and consequently, the stiffness of the samples increase.

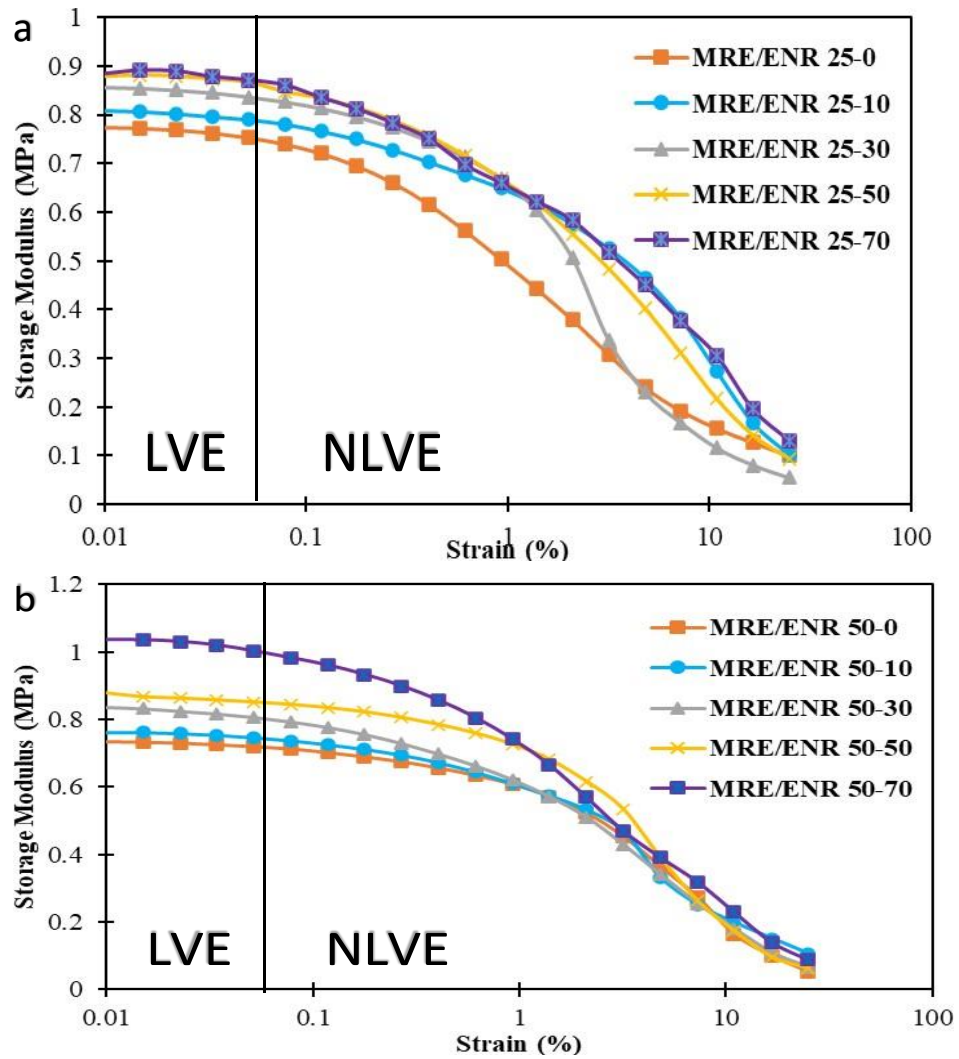


Figure 4.12: The storage modulus of the ENRs based MRE at different weights of CIPs under various strain of amplitude at 2A (a) ENR 25 (b) ENR 50

Figures 4.13 (a) and (b) represent the loss modulus values of MRE/ENR 25 and MRE/50 with various weights of CIPs used at 2A. Both graphs showed a similar pattern where the values of loss modulus for MRE/ENR 25 and MRE/ENR 50 were increased until 0.18% of strain and it was not in order beyond that value. Loss modulus value of MRE/ENR 50 is slightly lesser than MRE/ENR 25 for 70 wt% of CIPs. The loss modulus value for MRE/ENR 50 was 0.098 MPa, which is lesser than

MRE/ENR 25 (0.112 MPa) at the same quantity of CIPs. This is mainly attributed to the formation of hydrogen bond created from the epoxy ring with the oxygen during the fabrication. The hydrogen bond caused less energy dissipated when increasing of strain used. Hydrogen even limited the movements of the ENR molecular chain when shear was applied, and consequently, the stiffness of the samples increased.

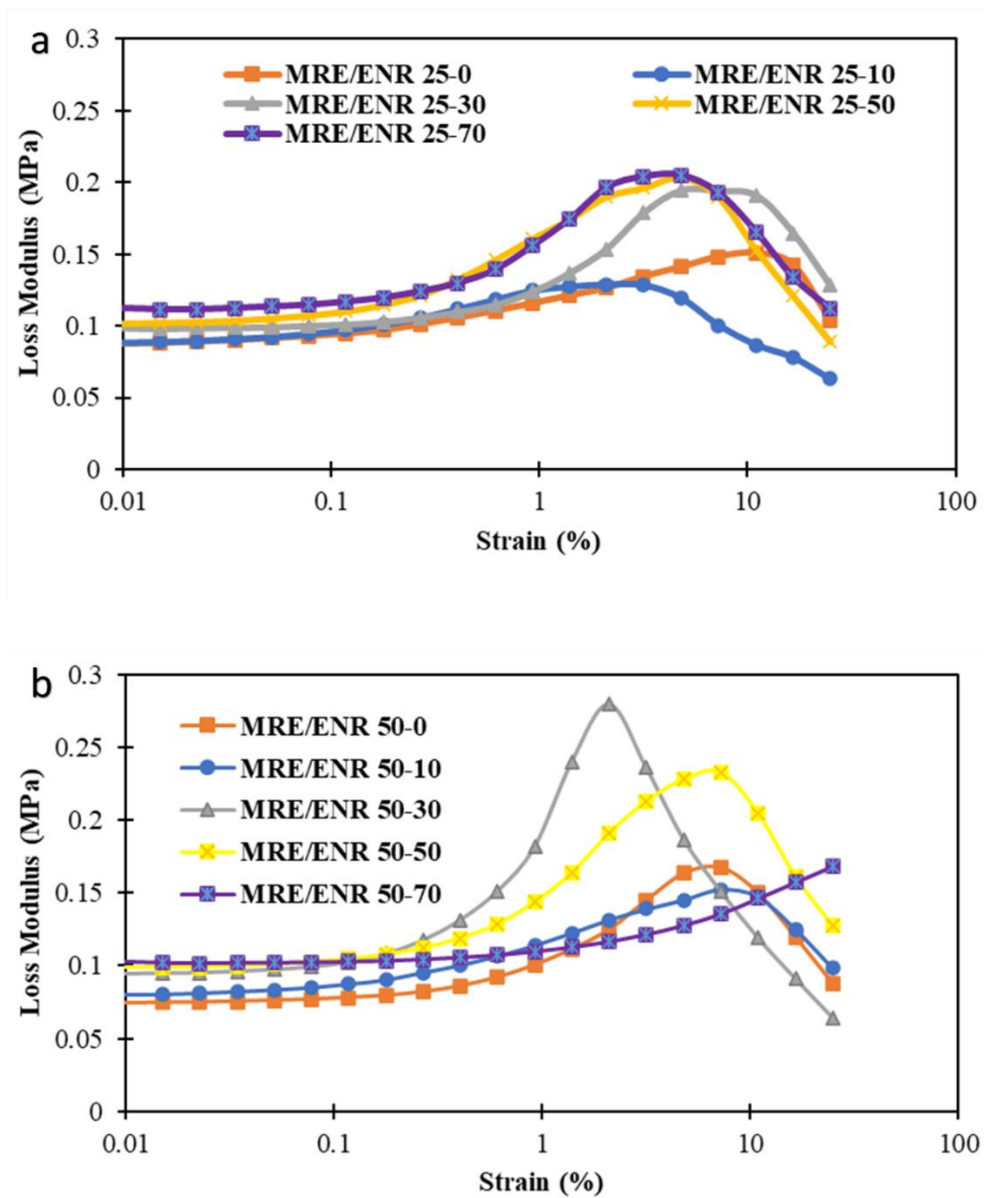


Figure 4.13: The loss modulus of the ENRs based MRE at different weights of CIPs under various strain of amplitude at 2A (a) ENR 25 (b) ENR 50

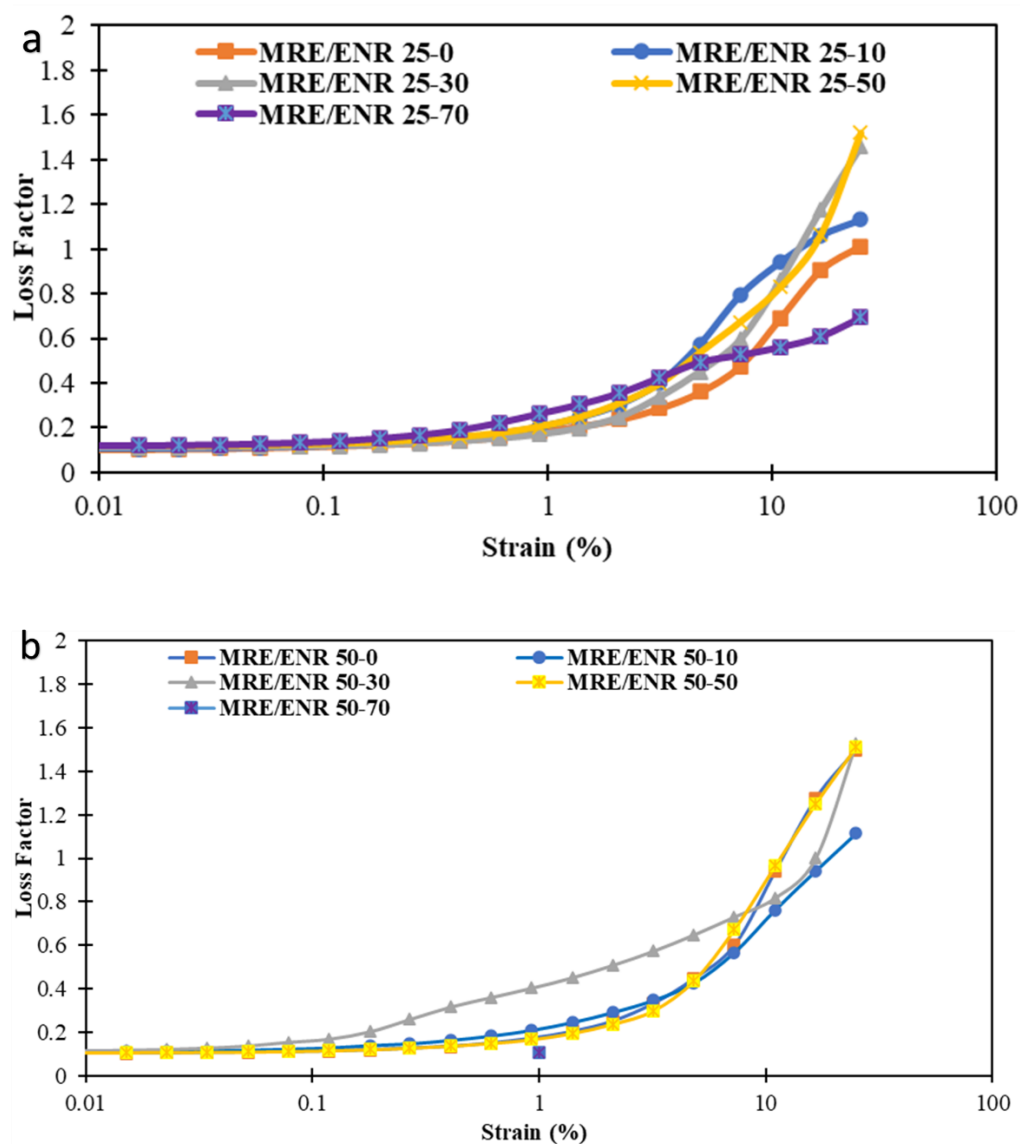


Figure 4.14: The loss factor of the ENRs based MRE at different weights of CIPs under various strain of amplitude at 2A (a) ENR 25 (b) ENR 50

As shown in Figures 4.14 (a) and (b), both ENR-based MRE indicated a different trend at loss factor results. For ENR 25-based MRE, the loss factor values were increased with an increase of CIPs until 2.95% of strain, and then, the order was different beyond the value due to the disruption of the polymer network (NLVE region). Based on the figures above, the initial value for the loss factor insignificantly increasing with increasing wt% of CIPs. This is probably attributed to the reduction in

the distance among the CIPs and the resultant increase in the friction between CIPs and the ENR matrix upon increasing CIP content. The interaction between CIPs and ENR increased and caused the movement of molecular chain of matrix become restricted when strain is applied. Thus, increasing of wt% CIPs within the ENR caused the initial loss factor to increase gradually. In addition, at 70 wt% of CIPs in ENR 50-based MRE show 0.120 MPa, which is higher than ENR 25-based MRE, which only 0.106 MPa. This is attributed to the strong hydrogen bond that was formed through formation of epoxy group and oxygen. As explained in Figures 4.14 (a) and (b), the number of epoxy group within the matrix played significant effect in forming the strong hydrogen bond. The hydrogen bonds limit the movements of the ENR molecular chains when shear is applied.

Figures 4.15 (a) and (b) show the increase of storage modulus in the LVE region with the increment of current up to 3 A and drop at current 4 A and 5 A accordingly, and a similar trend is observed for both ENR based MRE. These results indicate that increasing the current to 3 A can increase the strengthen of bond the among CIPs and the stiffness of the MRE increased. However, when the current for both ENR-based MRE samples increased up to 4 A, the storage modulus decreased. This is probably due to increase in wt% of CIPs, which caused the particles within elastomer become more closer and subsequently the CPVC of CIPs reached saturated condition. Based on the microstructural analysis, all the MRE samples showed the random distribution of particles, which prevents the magnetic flux induced directly to the CIPs and probably few current from current used was hit the calcium stearate, in which calcium stearate is not a magnetic particle. Consequently, the magnetic force reduced, and the stiffness or energy store decreased. Based on the storage value for both ENR at 3 A, ENR 50-based MRE produced 1.03 MPa in contrast with ENR 25-based MRE, which only 0.88 MPa. This is mainly attributed to the fact that interfacial interaction between epoxy content in ENR 50 is more reacted with CIPs contrast with ENR 25-based MRE. Subsequently, the hydrogen bond is created through the interfacial interaction between epoxy and CIPs. High epoxy content generated high number of hydrogen bond produced. The hydrogen bond made the rubber become more stiff and rigid. Therefore, the storage modulus of ENR 50-based MRE at 3 A was found to be higher than ENR 25-based MRE.

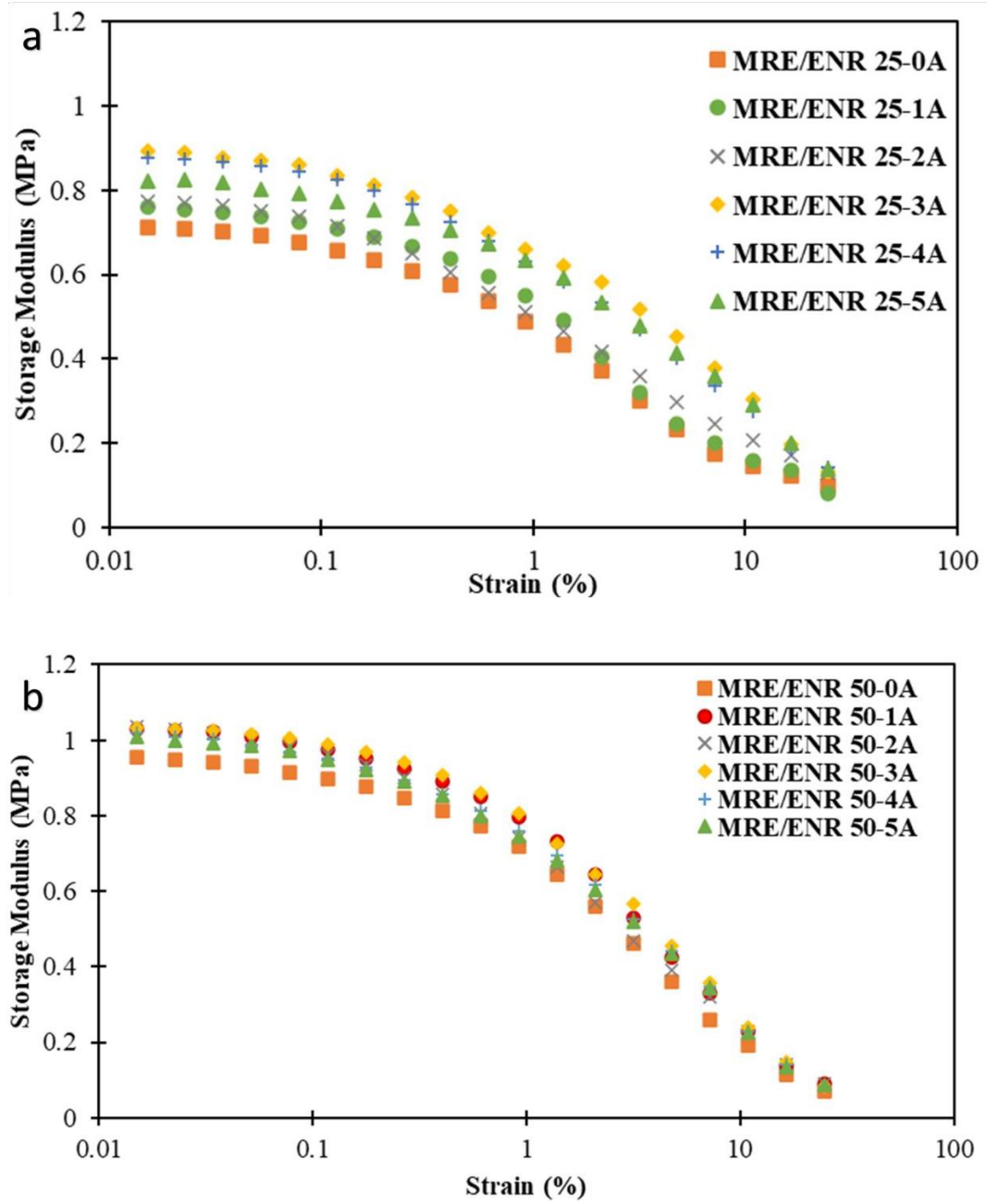


Figure 4.15: The storage modulus of the ENRs based MRE at different current used at 70wt% CIPs (a) ENR 25 (b) ENR 50

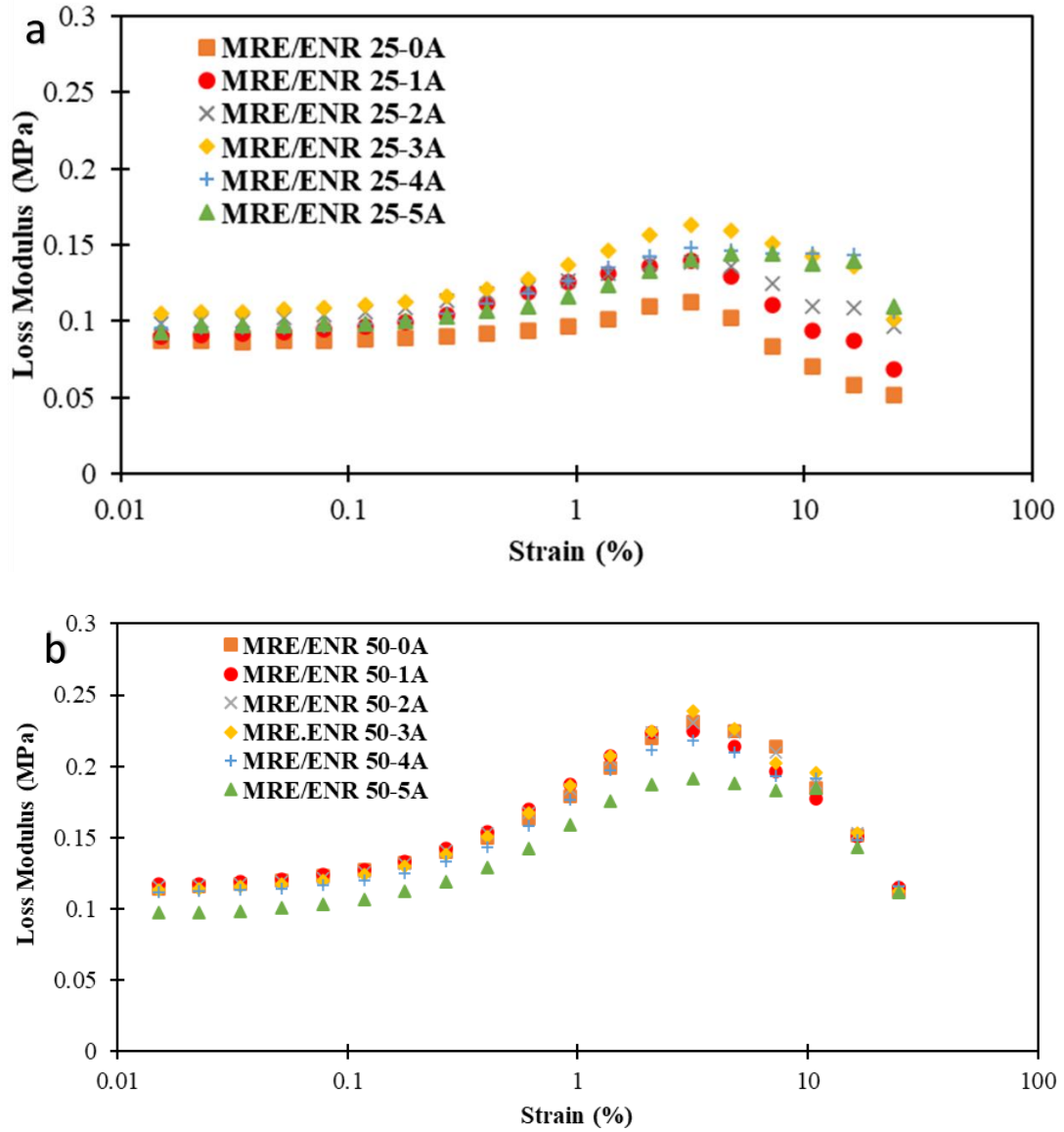


Figure 4.16: The loss modulus of the ENR based MRE at different current used at for 70wt% CIPs (a) ENR 25 (b) ENR 50

Figures 4.16 (a) and (b) represent the loss modulus value for both ENR-based MRE samples. According to both graphs above, an identical trend is observed, in which the initial loss modulus both ENR-based MRE samples increased up to 3 A and dropped at 4 A and 5 A, respectively. Then, loss modulus value for ENR 25- and ENR 50-based MRE become fluctuated starting from NLVE region. Based on the

graph, the initial loss modulus for ENR 50 based MRE at 3 A was 0.106 MPa, which is lesser than ENR 25-based MRE, for which the initial loss modulus was 0.113 MPa. This is mainly attributed to the formation of hydrogen bond incorporated with epoxy content and CIPs within the matrix. The hydrogen bond will strengthen the energy from being dissipated to the surroundings. Consequently, the sample of ENR 50-based MRE was stiffer compared with ENR 25-based MRE.

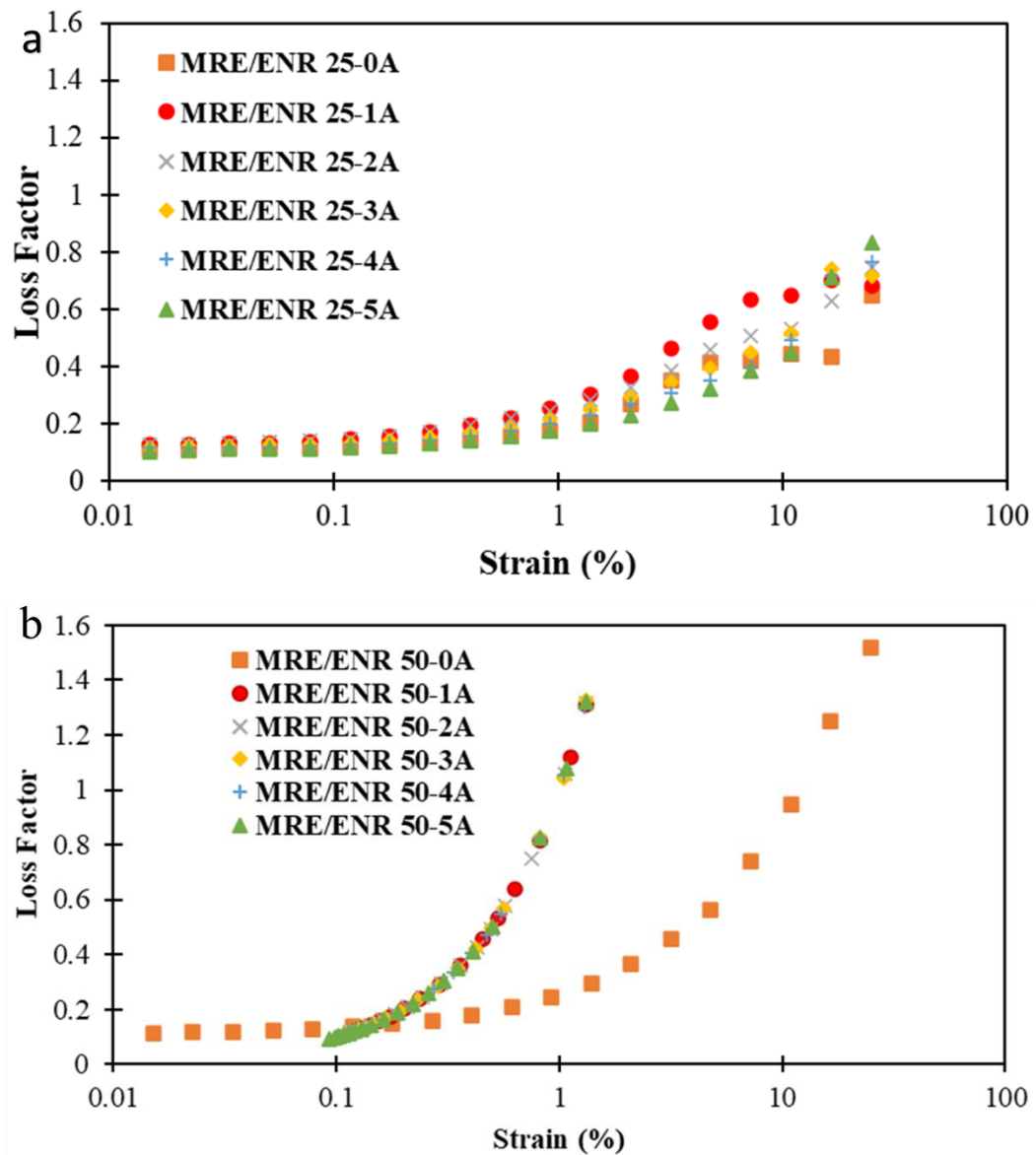


Figure 4.17: The loss factor of the ENR 25 and 50 based MRE at different current used at 70wt% CIPs (a) ENR 25 (b) ENR 50

The loss factor for both ENR-based MRE with different current supplied at the same weight of CIPs is demonstrated in Figures 4.17 (a) and (b). Based on the figures above, ENR 25-based MRE exhibited increasing values of loss factor up to 3 A and decrease after 4 A and 5 A. Meanwhile, the loss factor of ENR 50-based MRE increased until 2 A and dropped from 3 A to 5 A accordingly. The similarity for both ENRs is that they produced high values of loss factor at low current applied. This is mainly attributed to the presence of calcium stearate in both ENRs based MRE. As been illustrated in Figure 4.19, the size of calcium stearate is double from the CIPs and consequently resists the magnetic force when shear is applied. In fact, the huge gap between CIPs has also been analyzed through microstructural analysis for both ENRs. Subsequently, loss factor occurred between CIPs and led to low values of loss factor at small current applied for both ENRs based MRE. Interestingly, the loss factor of ENR 50-based MRE was slightly higher than ENR 25-based MRE, especially at 3 A of current supplied. This is because the epoxy rings in the epoxide group form strong hydrogen bond. Subsequently generated high production value of loss factor in ENR 50-based MRE compared with ENR 25-based MRE.

4.3.2 Magnetic Field Sweep Test

Figures 4.18 (a) and (b) illustrate the relationship between magneto-induced storage modulus with different weights of CIPs for ENR 25- and ENR 50-based MRE. Based on the graphs above, the trends for both of them were different. For ENR 25-based MRE, the initial storage modulus values fluctuated upon increasing the CIPs. ENR 25-based MRE with 70 wt% of CIPs had low initial storage modulus, which is 0.53 MPa, followed by 10 wt% (0.54 MPa), 0 wt% (0.76 MPa), 50 wt% (0.77 MPa), and lastly 30 wt % (0.81 MPa). At first, 0 wt% of CIPs showed 0.71 MPa, followed by 10 wt% (0.74 MPa), and dropped at 30 wt% (0.68 MPa), then 50 wt% (0.58 MPa), and raised again at 70 wt% (0.66 MPa). This is probably due to the shear applied, which is consequently all the MRE samples were having stress. Once shear was applied, the particles caused the dislocation of other particles. Consequently, the magnetic moment was difficult to align especially in less wt% of CIPs. From the microstructural graph discussion, the CIPs were randomly distributed

in both ENRs, and consequently, it was difficult for the magnetic flux to be induced in the samples when the magnetic field is applied. In addition, the size of calcium stearate was double from the CIPs, and it is also one of the factors that affected the storage modulus value of magnetic field sweep test.

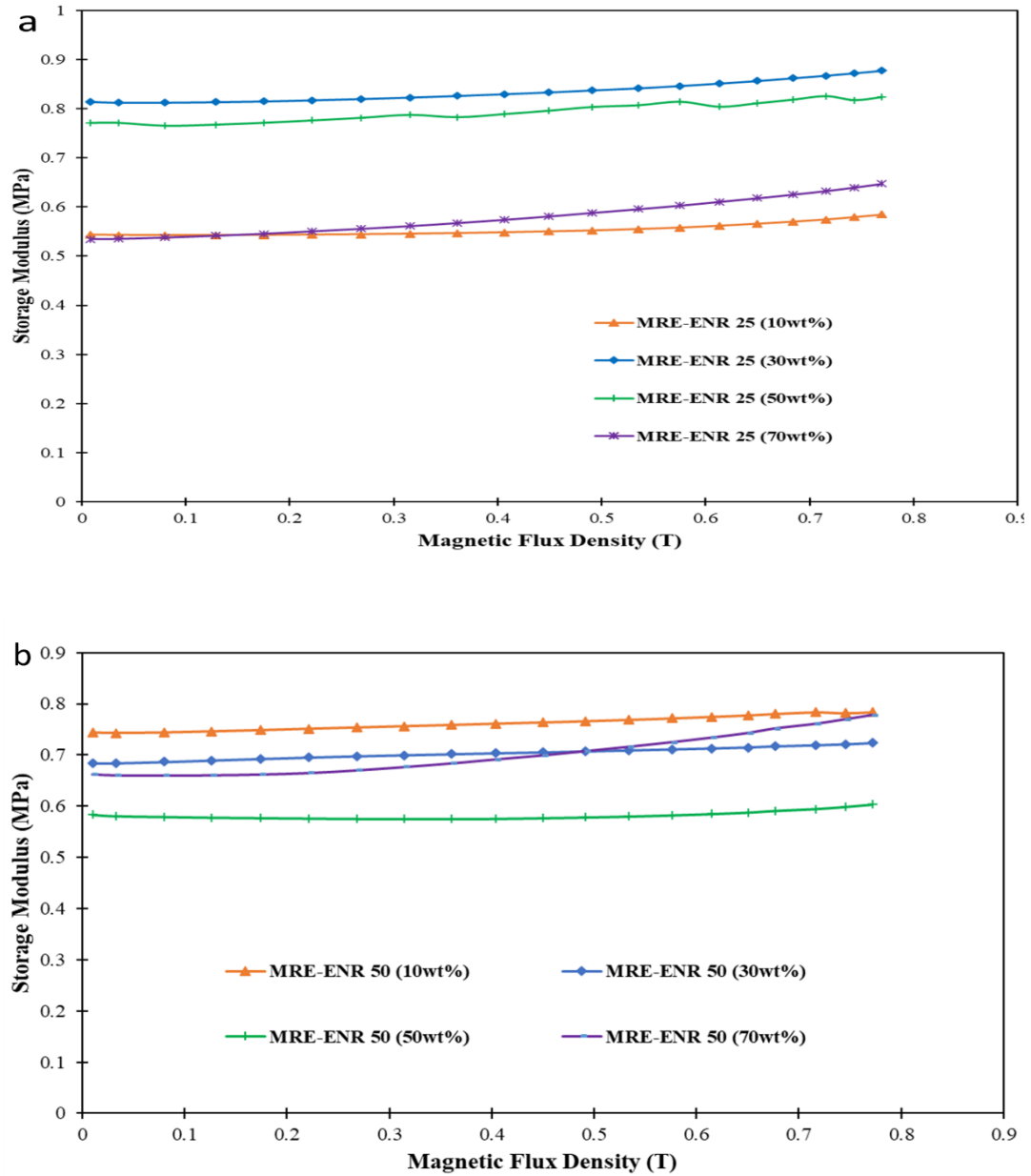


Figure 4.18: The magneto-induced storage modulus of ENR 25 and 50 based MRE under magnetic flux density (a) ENR 25 (b) E

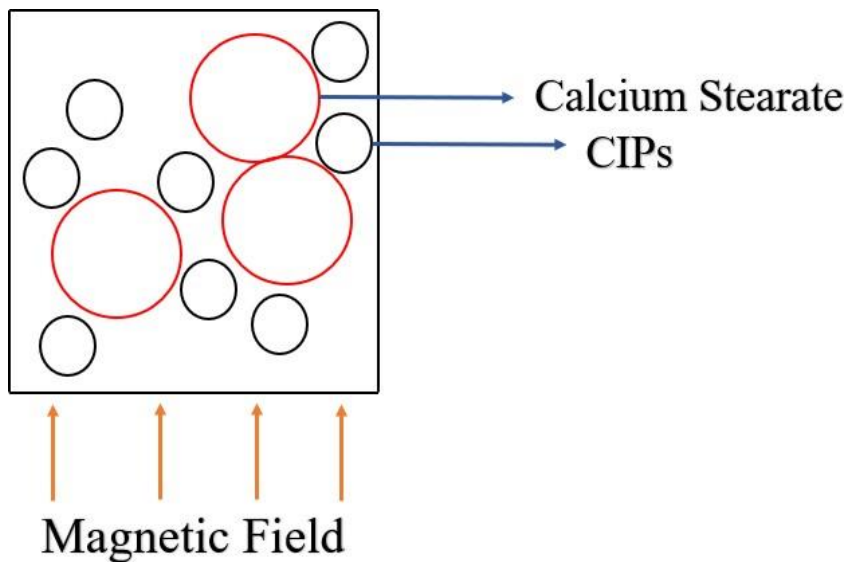


Figure 4.19: The mechanism of magnetic flux flow within ENR based MRE matrix that contains calcium stearate and CIPs

Interestingly, the initial storage modulus of ENR 50-based MRE was 0.66 MPa higher than ENR 25-based MRE, which is only 0.53 MPa at 70 wt% of CIPs. This is because of the numbers of the epoxy group in ENR. The epoxide group in ENR 50-based MRE is higher than ENR 25-based MRE. The chances of epoxy rings that contain ENR 50 probably caused the rings to frequently open because of the number of epoxy rings in ENR 50 is more than ENR 25. Subsequently, the number of hydrogen bond created was more. The hydrogen bonds limit the movements of the ENR molecular chains when magnetic field is applied, and consequently, the stiffness (storage modulus) of the samples increase.

Table 4.8 indicates the MR effect of ENR 25- and ENR 50-based MRE with different weights of CIPs evaluated through rheological analysis. Noticeably, for ENR 25-based MRE, the MR effect increased from 1.88% to 21.08% with a range from 0 to 70 wt% of CIPs. Meanwhile, the MR effect of ENR 50-based MRE enhanced from 2.47% to 17.40% with the same weight percentage of CIPs. Increase in weight percentage of CIPs improved the percentage of MR effect in MRE. This is because of the rise of magnetic force, which was caused by the interaction of magnetic moments of each CIPs. Furthermore, increases in weight percentage of CIPs and magnetic field

could strengthen the magnetic force. Hence, the magnetic moments aligned toward the magnetic field, and greater MR effect was created. In addition, the increase of MR effect in both ENR-based MREs is possibly due to the reduction of interparticle distance among the CIPs. Once the distance among the CIPs was reduced, it easier for the pathway of magnetic flux density to flow the ENR samples. It can be concluded that high wt% of CIPs can generate high magnetic force and significantly improve the performance of MRE, especially in the magnetic properties.

Table 4.8: The MR effect of ENR 25 and 50 based MRE with different weight of CIPs.

MRE Sample	MR Effect (%)
MRE/ENR 25-0	2.47
MRE/ENR 25-10	7.58
MRE/ENR 25-30	7.75
MRE/ENR 25-50	10.02
MRE/ENR 25-70	22.64
MRE/ENR 50-0	1.88
MRE/ENR 50-10	5.33
MRE/ENR 50-30	5.76
MRE/ENR 50-50	8.27
MRE/ENR 50-70	18.18

Based on Table 4.8, the MR effect of ENR 25-based MRE is 22.64%, which is higher than ENR 50-based MRE with only 18.18% using same quantity of CIPs (70 wt%). This is probably due to iron from CIPs reacting with the oxygen from the epoxy ring and forming iron oxide. High chances of oxide layer created when the number of epoxies is increasing. When magnetic field was applied, probably the magnetic flux reached the iron oxide, and only few directly hit the CIPs within the matrix. Consequently, the MR effect for ENR 50-based MRE was slightly lower than ENR 25-based MRE. ENR 50-based MRE samples probably produced high iron

oxide compared with ENR 25-based MRE samples since the former has high amount of epoxy (50%) compared with the latter (25%).

CHAPTER 5

CONCLUSIONS AND RECOMMENDATION

5.1 Conclusions

MRE is regarded as one of the smart material groups, with its rheological properties that allow it to be controlled by the application of a magnetic field. MRE researchers have investigated the potential applications of MREs. MRE devices can be enhanced with different elastomer matrix used, type of magnetic particles, and additives. Since the type of matrix is also one of the factors that affect the performance of MRE, different levels of epoxidation for commercialized ENR (25 and 50) of MRE were investigated in this study, and it has not been reported yet by other researchers. In addition, this research also includes the physicochemical characteristics and rheological properties analysis for both ENRs based MRE. This study will be beneficial for MRE researchers, especially involved in designing MRE-based devices. This research has been concluded in every single test that had been done during the investigation.

As stated earlier, in this research, both ENR 25- and ENR 50-based MRE were successfully fabricated at MRB through conventional rubber using different weight of CIPs. Two processes were used in this study, namely, rubber compounding process and vulcanizing process. Double roll mill machine was used in processing the rubber compound, and MDR machine was used for the curing process of MRE samples. Different additives such as sulfur, ZnO, stearic acid, carbon black, calcium stearate, CBS, and aromatic oil were added together with ENR 25 and ENR 50 matrix and various weights of CIPs (0, 10, 30, 50, and 70 wt%). Next, these mixtures were completely mixed and were cured at 150°C for 30 minutes, and subsequently MRE samples were produced.

From the curing analysis :

- Three phases were identified for all ENR/MRE samples knew as induction phase, curing phase, and overcuring phase.
- The t_{90} for MRE/ENR 50-based MRE was lesser than MRE/ENR 25-based MRE at 70 wt% of CIPs due to the high chances of breaking the C=C by adjacent of epoxy group.
- In addition, the time taken for t_2 for MRE/ENR 50-based at MRE was lesser than MRE/ENR 25-based MRE at the same weight of CIPs.
- Contrasting trends were observed for values of M_H and M_H-M_L for both ENR-based MRE due to the number of activated epoxy rings.

The microstructural and elemental test :

- MRE/ENR 25 and MRE/ENR50 were randomly distributed from 10 to 70 wt% of CIPs.
- Increase in CIPs in MRE/ENR 25 and MRE/50 were clearly prominent from the micrograph pictures and EDX results correspondingly.
- Presence of Fe in all MRE samples that contained CIPs successfully proved the existence of CIPs within the ENR-based MRE, especially in 70 wt%, which produced large quantity of Fe.
- The continuation of agglomeration and porosities in MRE sample were also verified from micrographs picture.

The magnetization result:

- Both ENR-based MREs showed that MRE/ENR 25 and MRE/50 exhibited soft magnetic characteristics.
- Both ENR-based MREs showed the same trend in terms of M_s and M_r , in which the value of these two terms increased upon increasing CIPs.

The different groups of chemicals:

- The peak of epoxy was increased and sharp when increasing the weight of CIPs.
- The peak of epoxy group for MRE/ENR 50 with 0 wt% of CIPs indicated high peak was observed compared with MRE/ENR 25 with no presence of CIPs.
- Strong hydrogen bond was established through the formation of epoxy group from ENR.
- The hydrogen bond in MRE/ENR 50 was broader than MRE/ENR 25 with same number of CIPs used. This was due to the number epoxirane rings in MRE/ENR 50 higher than MRE/ENR 25.

The DSC results:

- T_g for both ENR-based MRE shifted toward negatives values with increasing of CIPs content. This confirmed that the insertion of CIPs with ENR-based MRE influenced the performance of T_g .

TGA results :

- Increase in temperature of both ENR-based MREs showed that the incorporation of CIPs with ENR was successfully formed.
- MRE/ENR 25 started to degrade early compared with MRE/ENR 50 in which the epoxidation level played a significant role particularly in physicochemical characteristics.
- The residue for MRE/ENR 50 had high percentage of residue compared with MRE/ENR 25, specifically at 70 wt% of CIPs. MRE/ENR 50 produced 60.3%, while MRE/ENR 25 showed only 58.9%.

Strain sweep analysis:

- The LVE value identified approximately 0.025% of strain used. The storage modulus of MRE/ENR 50 was higher than that of MRE/ENR 25 with same wt.% of CIPs used (70 wt%). This is mainly attributable to the strong hydrogen bonding that was formed from the excess oxygen within the matrix and epoxy group.

- The hydrogen bonds limit the movements of the ENR molecular chains when shear is applied, and consequently, the stiffness increased.

Magnetic Field Sweep test:

- MR effect for MRE/ENR 25 was slightly higher than MRE/ENR 50 samples. MRE/ENR 25 with 70 wt% of CIPs exhibited 22.18% of MR effect, while MRE/ENR50 exhibited only 18.18%.
- The oxygen that comes from epoxy group reacts with CIPs, and subsequently, iron oxide is produced. High amount of epoxy rings caused high chances oxygen to react with CIPs and formed iron oxide.

As a consequence, all the results including physicochemical characteristics as well as field-dependent rheological properties can be used as a guidance for the MRE researchers especially in fabrication process and experimental analysis. The results showed in this study can be a guideline for the research to implement any MRE devices. From this study, the values of each analysis that already done for both ENR 25- and ENR 50-based MREs only had slight differences. Mostly, MRE/ENR 50 gave high values compared to MRE/ENR 25, especially in storage modulus. However, the MR effect and magnetic properties of MRE/ENR 25-based MRE was found to be better than with MRE/ENR 50. Besides, in this study, the number of CIPs also played a significant role, where increase in wt% of CIPs will give different value. Both ENR-based MREs showed an increasing value, especially in storage modulus and MR effect. In addition, from this study, increase in wt% of CIPs was shown to enhance the performance.

5.2 Recommendations

Several issues had been identified during this investigation during the development of difference level epoxidation between ENR 25- and ENR 50-based MRE. These issued can be used for future work, and these suggestions are summarized as follows:

- i. The best ideal for the ingredients was not found yet in addition to the

composition of additives and magnetic particles. Consequently, several acts such as the amount of additives need to be added, amount of CIPs and carbon black need to be suggested to enhance the properties of both ENR-based MRE.

- ii. In this study, isotropic type was used in investigating the level of epoxidation between ENR 25- and ENR 50-based MRE. The extant literature has confirmed that anisotropic type can affect the performance of physicochemical characteristics and rheological properties. The development of ENR 25- and ENR 50-based MREs of anisotropic type can be further studied.
- iii. In this study, the rheological properties, and physicochemical characteristics of two types of ENR-based MRE were studied. It will be beneficial to study the mechanical properties such as tensile strength, elongation, hardness, and compression test since it is more and less related with the study.

REFERENCES

- [1] Ismail H and Poh B T 2000 Cure and tear properties of ENR 25/SMR L and ENR 50/SMR L blends *Eur. Polym. J.* 36 2403–8
- [2] Yang Z, Peng H, Wang W and Liu T 2010 Crystallization behavior of poly(ϵ -caprolactone)/layered double hydroxide nanocomposites *J. Appl. Polym. Sci.* 116 2658–67
- [3] Alam M N, Kumar V, Lee D J and Choi J 2021 Magnetically active response of acrylonitrile-butadiene-rubber-based magnetorheological elastomers with different types of iron fillers and their hybrid *Compos. Commun.* 24 22–6
- [4] Ginder J M, Nichols M E, Elie L D and Tardiff J L 1999 *Magnetorheological elastomers: properties and applications* *Smart Struct. Mater.* 1999 *Smart Mater. Technol.* 3675 131–8
- [5] Hamzah R, Bakar M A, Khairuddean M, Mohammed I A and Adnan R 2012 A structural study of epoxidized natural rubber (ENR-50) and its cyclic dithiocarbonate derivative using NMR spectroscopy techniques *Molecules* 17 10974–93
- [6] Burfield D R, Lim K L, Law K S and Ng S 1984 Analysis of epoxidized natural rubber. A comparative study of d.s.c., n.m.r., elemental analysis and direct titration methods *Polymer (Guildf)*. 25 995–8
- [7] Díez A G, Tubio C R, Etxebarria J G and Lanceros-Mendez S 2021 Magnetorheological Elastomer-Based Materials and Devices: State of the Art and Future Perspectives *Adv. Eng. Mater.* 23 1–20
- [8] Yang Z, Peng H, Wang W and Liu T 2010 Crystallization behavior of poly(ϵ -caprolactone)/layered double hydroxide nanocomposites *J. Appl. Polym. Sci.* 116 2658–67
- [9] Shilan S T, Mazlan S A, Ido Y, Hajalilou A, Jeyadevan B, Choi S B and Yunus N A 2016 A comparison of field-dependent rheological properties

between spherical and plate-like carbonyl iron particles-based magneto-rheological fluids *Smart Mater. Struct.* 25 1–9

- [10] Pire M, Oikonomou E K, Imbernon L, Lorthioir C, Iliopoulos I and Norvez S 2013 Crosslinking of epoxidized natural rubber by dicarboxylic acids: An alternative to standard vulcanization *Macromol. Symp.* 331–332 89–96
- [11] Shilan S T, Mazlan S A, Ido Y, Hajalilou A, Jeyadevan B, Choi S B and Yunus N A 2016 A comparison of field-dependent rheological properties between spherical and plate-like carbonyl iron particles-based magneto-rheological fluids *Smart Mater. Struct.* 25 1–9
- [12] Zrínyi M 2011 Colloidal particles that make smart polymer composites deform and rotate *Colloids Surfaces A Physicochem. Eng. Asp.* 382 192–7
- [13] Zrínyi M 2011 Colloidal particles that make smart polymer composites deform and rotate *Colloids Surfaces A Physicochem. Eng. Asp.* 382 192–7
- [14] Alam M N, Kumar V, Lee D J and Choi J 2021 Magnetically active response of acrylonitrile-butadiene-rubber-based magnetorheological elastomers with different types of iron fillers and their hybrid *Compos. Commun.* 24 22–6
- [15] Chen L, Gong X L and Li W H 2008 Effect of carbon black on the mechanical performances of magnetorheological elastomers *Polym. Test.* 27 340–5
- [16] Lin T and Guo B 2013 Curing of rubber via oxa-michael reaction toward significantly increased aging resistance *Ind. Eng. Chem. Res.* 52 18123–30
- [17] Cheng B, Lu X, Zhou J, Qin R and Yang Y 2019 Dual Cross-Linked Self-Healing and Recyclable Epoxidized Natural Rubber Based on Multiple Reversible Effects *ACS Sustain. Chem. Eng.* 7 4443–55
- [18] Liu S, Zhou S B, Peng A, Xuan W and Li W 2019 Analysis of the performance and mechanism of desulfurized rubber and low-density polyethylene compound-modified asphalt *J. Appl. Polym. Sci.* 136 1–10
- [19] Cao L, Cheng Z, Yan M and Chen Y 2019 Anisotropic rubber nanocomposites via magnetic-induced alignment of Fe₃O₄/cellulose nanocrystals hybrids obtained by templated assembly *Chem. Eng. J.* 363 203–12
- [20] Mohapatra S and Nando G B 2014 Cardanol: A green substitute for aromatic

oil as a plasticizer in Natural Rubber vol 4

- [21] Kim M S, Liu Y D, Park B J, You C Y and Choi H J 2012 Carbonyl iron particles dispersed in a polymer solution and their rheological characteristics under applied magnetic field *J. Ind. Eng. Chem.* 18 664–7
- [22] Anon Brochure - Response Surface Methodology Training_CORIL.pdf
- [23] Examiner P and Merriam A E C 2000 p a °d nu o
- [24] Ilyas S U, Narahari M, Theng J T Y and Pendyala R 2019 Experimental evaluation of dispersion behavior, rheology and thermal analysis of functionalized zinc oxide-paraffin oil nanofluids *J. Mol. Liq.* 294 111613
- [25] Wahab N A A, Mazlan S A, Ubaidillah, Kamaruddin S, Ismail N I N, Choi S B and Sharif A H R 2016 Fabrication and investigation on field-dependent properties of natural rubber based magneto-rheological elastomer isolator *Smart Mater. Struct.* 25 1–11
- [26] Hegde S, Poojary U R and Gangadharan K V 2014 Experimental Investigation of Effect of Ingredient Particle Size on Dynamic Damping of RTV Silicone Base Magnetorheological Elastomers *Procedia Mater. Sci.* 5 2301–9
- [27] Rajpal R, Lijesh K P, Kant M and Gangadharan K V. 2018 Experimental study on the dynamic properties of magneto-rheological materials *IOP Conf. Ser. Mater. Sci. Eng.* 402
- [28] Pire M, Norvez S, Iliopoulos I, Le Rossignol B and Leibler L 2011 Imidazole-promoted acceleration of crosslinking in epoxidized natural rubber/dicarboxylic acid blends *Polymer (Guildf)*. 52 5243–9
- [29] Dan Liu Y and Jin Choi H 2014 Fabrication of anisotropic snowman-like magnetic particles and their magnetorheological response *J. Appl. Phys.* 115 2012–5
- [30] Ismail H, Salleh S Z and Ahmad Z 2013 Fatigue and hysteresis behavior of halloysite nanotubes-filled natural rubber (SMR L and ENR 50) nanocomposites *J. Appl. Polym. Sci.* 127 3047–52
- [31] Diani J and Gall K 2006 Finite Strain 3D Thermoviscoelastic Constitutive Model *Society* 1–10

- [32] Surya I, Maulina S and Ismail H 2018 Effects of alkanolamide and epoxidation in natural rubber and epoxidized natural rubbers compounds IOP Conf. Ser. Mater. Sci. Eng. 299
- [33] Xu Y, Zhang D, Cai J, Yuan L and Zhang W 2012 Effects of Multi-walled Carbon Nanotubes on the Electromagnetic Absorbing Characteristics of Composites Filled with Carbonyl Iron Particles J. Mater. Sci. Technol. 28 34–40
- [34] Notice P 13 . EPOXY , POLYURETHANE , ACRYLIC , AND CYAIMOACRYLATE ADHESIVES
- [35] Harun F, Chan C H, Sim L H, Winie T and Zainal N F A 2015 Effect of epoxidation level on thermal properties and ionic conductivity of epoxidized natural rubber solid polymer nanocomposite electrolytes AIP Conf. Proc. 1674
- [36] Ka Wei K, Leng T P, Keat Y C, Osman H and Ying L B 2019 Enhancing compatibility in epoxy/vulcanized natural rubber (VNR)/Graphene nanoplatelets (GNP) system using epoxidized natural rubber (ENR-50) Compos. Part B Eng. 174 107058
- [37] Wang Y, Hu Y, Chen L, Gong X, Jiang W, Zhang P and Chen Z 2006 Effects of rubber/magnetic particle interactions on the performance of magnetorheological elastomers Polym. Test. 25 262–7
- [38] Zhang X, Tang Z, Guo B and Zhang L 2016 Enabling design of advanced elastomer with bioinspired metal-oxygen coordination ACS Appl. Mater. Interfaces 8 32520–7
- [39] Gong Q, Wu J, Gong X, Fan Y and Xia H 2013 Smart polyurethane foam with magnetic field controlled modulus and anisotropic compression property RSC Adv. 3 3241–8
- [40] Pichaiyut S, Wisunthorn S, Thongpet C and Nakason C 2016 Novel ternary blends of natural rubber/linear low-density polyethylene/thermoplastic starch: influence of epoxide level of epoxidized natural rubber on blend properties Iran. Polym. J. (English Ed. 25 711–23
- [41] Luo M C, An R, Gao X X, Zeng J and Huang G S 2016 Role of epoxidation on

- segmental motion of polyisoprene as studied by broadband dielectric spectroscopy *J. Appl. Polym. Sci.* 133 1–8
- [42] Information S 2019 Sodium , 40 wt . % dispersion in oil *Protocols & Articles Peer-Reviewed Papers* 350–1
- [43] Zhang J, Chen X P and Xu J yu 2019 Rheological characteristics of unstable heavy crude oil-water dispersed mixtures *J. Pet. Sci. Eng.* 182 106299
- [44] Stimoniaris A, Skoura E, Gournis D, Karakassides M A and Delides C 2019 Structure and Properties of Epoxy/Fly Ash System: Influence of Filler Content and Surface Modification *J. Mater. Eng. Perform.* 28 4620–9
- [45] Ou C Y and Li S D 2012 Study on the thermal degradation of chitosan-Cu/Ni/Mn complexes *E-Polymers* 2207–11
- [46] Hamzah.R 2015 Structural study of epoxidized natural rubber (enr-50) and its derivatives synthesized 1–47
- [47] Zhang G, Wang H and Wang J 2019 Magnetic stimuli-response properties of polyurethane-based magnetorheological soluble gel *Mater. Res. Express* 6
- [48] Yangthong H, Pichaiyut S, Jumrat S, Wisunthorn S and Nakason C 2019 Mechanical, thermal, morphological, and curing properties of geopolymer filled natural rubber composites *J. Appl. Polym. Sci.* 136 1–17
- [49] Chokanandsombat Y, Sae-Oui P and Sirisinha C 2013 Influence of aromatic content in rubber processing oils on viscoelastic behaviour and mechanical properties of styrene-butadiene-rubber (SBR) for tyre tread applications *Adv. Mater. Res.* 747 471–4
- [50] Kramarenko E Y, Chertovich A V., Stepanov G V., Semisalova A S, Makarova L A, Perov N S and Khokhlov A R 2015 Magnetic and viscoelastic response of elastomers with hard magnetic filler *Smart Mater. Struct.* 24 35002
- [51] Anon Mendeley-Desktop-1
- [52] Information S 2019 Naphthenic acid *Protocols & Articles Peer-Reviewed Papers* 3–5
- [53] Barkoula N M, Alcock B, Cabrera N O and Peijs T 2008 Flame-Retardancy

- Properties of Intumescent Ammonium Poly(Phosphate) and Mineral Filler Magnesium Hydroxide in Combination with Graphene Polym. Polym. Compos. 16 101–13
- [54] Zhang G, Zhou X, Liang K, Guo B, Li X, Wang Z and Zhang L 2019 Mechanically Robust and Recyclable EPDM Rubber Composites by a Green Cross-Linking Strategy ACS Sustain. Chem. Eng. 7 11712–20
- [55] Bose H 2007 Vol. 21, Nos. 28 & 29 (2007) 21 4790–7
- [56] Li Y, Li J and Li W 2013 Design and experimental testing of an adaptive magneto-rheological elastomer base isolator 2013 IEEE/ASME Int. Conf. Adv. Intell. Mechatronics Mechatronics Hum. Wellbeing, AIM 2013 381–6
- [57] Naimzad A, Hojjat Y and Ghodsi M 2014 Comparative Study on Mechanical and Magnetic Properties of Porous and Nonporous Film-shaped Magnetorheological Nanocomposites Based on Silicone Rubber Int. J. Innov. Sci. Mod. Eng. 2 11–20
- [58] Li R and Sun L Z 2013 Viscoelastic responses of silicone-rubber-based magnetorheological elastomers under compressive and shear loadings J. Eng. Mater. Technol. Trans. ASME 135 1–7
- [59] Vega M F, Fernández A M, Díaz-Faes E, Casal M D and Barriocanal C 2017 The effect of bituminous additives on the carbonization of oxidized coals Fuel Process. Technol. 156 19–26
- [60] Ubaidillah, Sutrisno J, Purwanto A and Mazlan S A 2015 Recent progress on magnetorheological solids: Materials, fabrication, testing, and applications Adv. Eng. Mater. 17 563–97
- [61] Aziz S A A, Mazlan S A, Ubaidillah U, Mohamad N, Choi S B, Aziz M A C, Johari M A F and Homma K 2020 Thermal aging rheological behavior of magnetorheological elastomers based on silicone rubber Int. J. Mol. Sci. 21 1–17

- [62] Burhannuddin N L, Nordin N A, Mazlan S A, Aziz S A A, Kuwano N, Jamari S K M and Ubaidillah 2021 Physicochemical characterization and rheological properties of magnetic elastomers containing different shapes of corroded carbonyl iron particles *Sci. Rep.* 11 1–17
- [63] Chai C K, Ratnam C T, Abdullah L C and Yusoff H M 2016 Tensile properties and thermal stability of gamma irradiated epoxidized natural rubber latex with the presence of sensitizer *J. Polym. Mater.* 33 223–32
- [64] Li X, Tan S, Liu G, Hoch M and Zhao S 2016 The effect of paraffinic oil and aromatic oil on the crosslinks and physical properties of Butyl rubber *J. Macromol. Sci. Part B Phys.* 55 494–502
- [65] Ismail H, Galpaya D and Ahmad Z 2009 The compatibilizing effect of epoxy resin (EP) on polypropylene (PP)/recycled acrylonitrile butadiene rubber (NBRr) blends *Polym. Test.* 28 363–70
- [66] Yamamoto Y, Binti Norulhuda S N, Nghia P T and Kawahara S 2018 Thermal degradation of deproteinized natural rubber *Polym. Degrad. Stab.* 156 144–50
- [67] Ubaidillah, Imaduddin F, Li Y, Mazlan S A, Sutrisno J, Koga T, Yahya I and Choi S B 2016 A new class of magnetorheological elastomers based on waste tire rubber and the characterization of their properties *Smart Mater. Struct.* 25 1–15
- [68] Mohamad N, Mazlan S A, Ubaidillah, Choi S B and Nordin M F M 2016 The Field-Dependent Rheological Properties of Magnetorheological Grease Based on Carbonyl-Iron-Particles *Smart Mater. Struct.* 25 1–10
- [69] Ahmad Khairi M H, Mazlan S A, Ubaidillah, Ku Ahmad K Z, Choi S B, Abdul Aziz S A and Yunus N A 2017 The field-dependent complex modulus of magnetorheological elastomers consisting of sucrose acetate isobutyrate ester *J. Intell. Mater. Syst. Struct.* 28 1993–2004
- [70] Yokkhun P, Thongnuanchan B and Nakason C 2014 Influence of epoxide levels in epoxidized natural rubber (ENR) molecules on cure characteristics, dynamic properties and mechanical properties of ENR/montmorillonite clay nanocomposites *Adv. Mater. Res.* 844 247–50

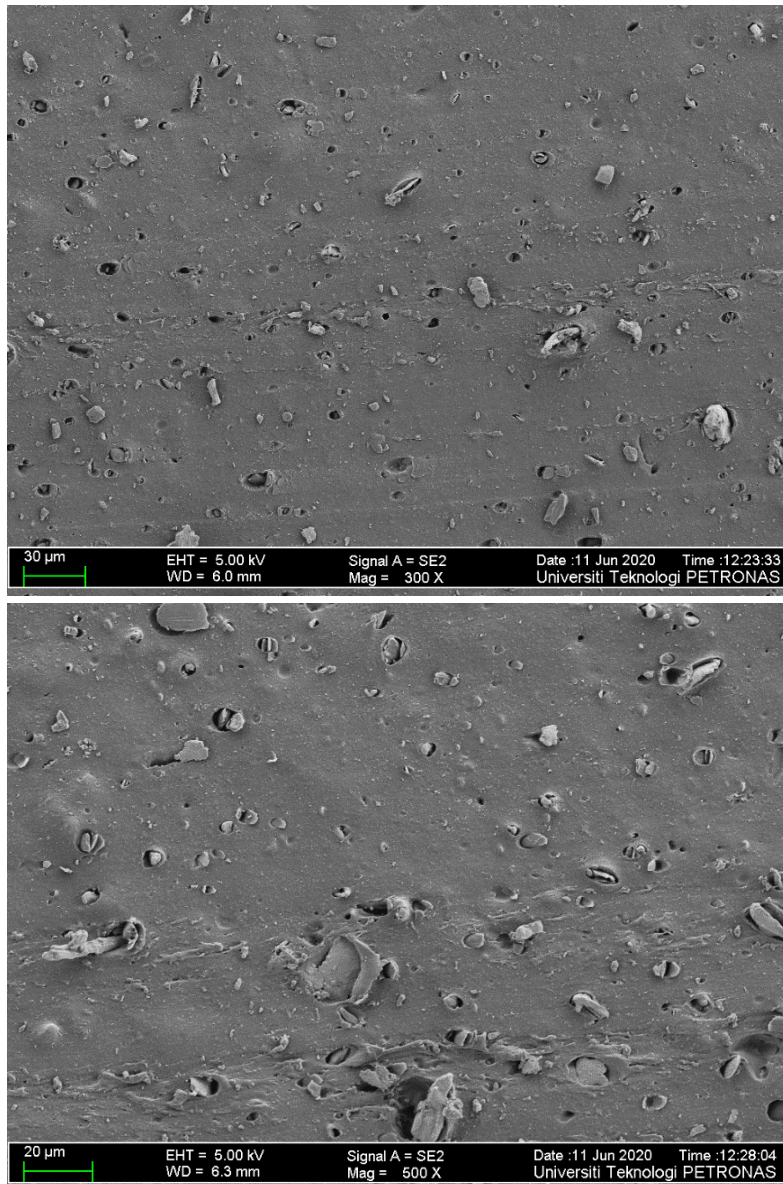
- [71] Sarkawi S S, Aziz A K C, Rahim R A, Ghani R A and Kamaruddin A N 2016 Properties of epoxidized natural rubber tread compound: The hybrid reinforcing effect of silica and silane system *Polym. Polym. Compos.* 24 775–82
- [72] Hoon T C 2006 Epoxidized natural rubber (enr-50) stabilized gold and platinum organosols teoh cheng hoon
- [73] Nie J, Mou W, Ding J and Chen Y 2019 Bio-based epoxidized natural rubber/chitin nanocrystals composites: Self-healing and enhanced mechanical properties *Compos. Part B Eng.* 172 152–60
- [74] Khimi S R and Pickering K L 2014 A new method to predict optimum cure time of rubber compound using dynamic mechanical analysis *J. Appl. Polym. Sci.* 131 1–6
- [75] Fan Y, Gong X, Xuan S, Qin L and Li X 2013 Effect of cross-link density of the matrix on the damping properties of magnetorheological elastomers *Ind. Eng. Chem. Res.* 52 771–8
- [76] Cibulková Z, Polovková J, Lukeš V and Klein E 2006 DSC and FTIR study of the gamma radiation effect on cis-1,4-polyisoprene *J. Therm. Anal. Calorim.* 84 709–13
- [77] Vivirito R, Park F, Application F, Data P, Cain P E and Joseph J 1996 United States Patent (19)
- [78] Lu X, Qiao X, Watanabe H, Gong X, Yang T, Li W, Sun K, Li M, Yang K, Xie H, Yin Q, Wang D and Chen X 2012 Mechanical and structural investigation of isotropic and anisotropic thermoplastic magnetorheological elastomer composites based on poly(styrene-*b*-ethylene-co-butylene-*b*-styrene) (SEBS) *Rheol. Acta* 51 37–50
- [79] Hajalilou A, Mazlan S A and Shila S T 2016 Magnetic carbonyl iron suspension with Ni-Zn ferrite additive and its magnetorheological properties *Mater. Lett.* 181 196–9
- [80] Ubaidillah, Choi H J, Mazlan S A, Imaduddin F and Harjana 2016 Fabrication

and viscoelastic characteristics of waste tire rubber based magnetorheological elastomer *Smart Mater. Struct.* 25 1–14

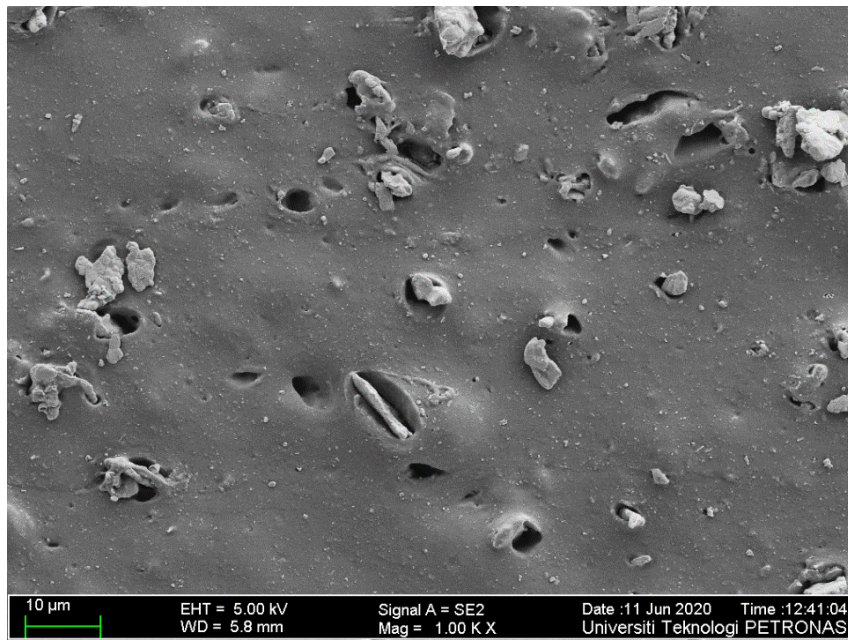
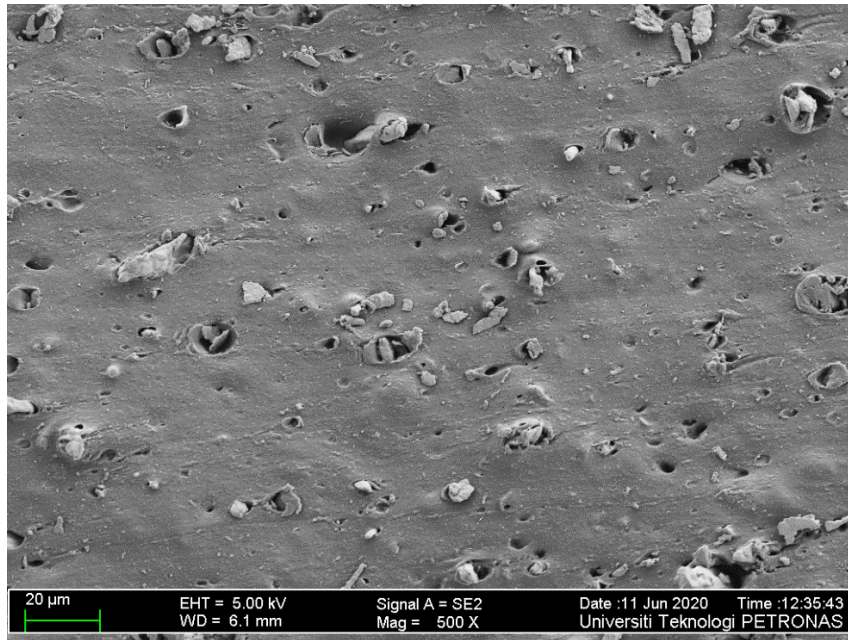
- [81] Gong X L, Zhang X Z and Zhang P Q 2005 Fabrication and characterization of isotropic magnetorheological elastomers *Polym. Test.* 24 669–76
- [82] Lee C J, Kwon S H, Choi H J, Chung K H and Jung J H 2018 Enhanced magnetorheological performance of carbonyl iron/natural rubber composite elastomer with gamma-ferrite additive *Colloid Polym. Sci.* 296 1609–13
- [83] Rohadi A A, Rahmat A R and Kamal M M 2014 Effect of epoxidation level in silica filled epoxidized natural rubber compound on cure, rheological, mechanical and dynamic properties *Appl. Mech. Mater.* 554 71–5
- [84] Agirre-Olabide I, Berasategui J, Elejabarrieta M J and Bou-Ali M M 2014 Characterization of the linear viscoelastic region of magnetorheological elastomers *J. Intell. Mater. Syst. Struct.* 25 2074–81
- [85] Mohamad N, Ubaidillah, Mazlan S A, Imaduddin F, Choi S B and Yazid I I M 2018 A comparative work on the magnetic field-dependent properties of plate-like and spherical iron particle-based magnetorheological grease *PLoS One* 13 1–16
- [86] Yunus N A, Mazlan S A, Ubaidillah, Abdul Aziz S A, Shilan S T and Abdul Wahab N A 2019 Thermal stability and rheological properties of epoxidized natural rubber-based magnetorheological elastomer *Int. J. Mol. Sci.* 20 1–19
- [87] Yunus N A, Mazlan S A, Ubaidillah, Choi S B, Imaduddin F, Abdul Aziz S A and Ahmad Khairi M H 2016 Rheological properties of isotropic magnetorheological elastomers featuring an epoxidized natural rubber *Smart Mater. Struct.* 25 1–11
- [88] Wu J, Gong X, Fan Y and Xia H 2010 Anisotropic polyurethane magnetorheological elastomer prepared through in situ polycondensation under a magnetic field *Smart Mater. Struct.* 19
- [89] Lu X and Li X 2014 Broad temperature and frequency range damping materials based on epoxidized natural rubber *J. Elastomers Plast.* 46 84–95

- [90] Zhang X, Niu K, Song W, Yan S, Zhao X, Lu Y and Zhang L 2019 The Effect of Epoxidation on Strain-Induced Crystallization of Epoxidized Natural Rubber *Macromol. Rapid Commun.* 40 1–5
- [91] Ryu G, Kim D, Song S, Hwang K, Ahn B and Kim W 2021 Effect of epoxide content on the vulcanizate structure of silica-filled epoxidized natural rubber (Enr) compounds *Polymers (Basel)*. 13
- [92] Singh M and Mohd Rasdi F R 2019 Colloidal properties of epoxidized natural rubber latex prepared via membrane separation technology *J. Rubber Res.* 22 153–67
- [93] Phiri M M, Sibeko M A, Phiri M J and Hlangothi S P 2019 Effect of free foaming and pre-curing on the thermal, morphological and physical properties of reclaimed tyre rubber foam composites *J. Clean. Prod.* 218 665–72
- [94] Chaikumpollert O, Sae-Heng K, Wakisaka O, Mase A, Yamamoto Y and Kawahara S 2011 Low temperature degradation and characterization of natural rubber *Polym. Degrad. Stab.* 96 1989–95
- [95] Sarkawi S S, Kifli A, Aziz C, Rahim R A, Ghani R A and Kamaruddin A N 2016 Properties of Epoxidized Natural Rubber Tread Compound : The Hybrid Reinforcing Effect of Silica and Silane System 24 775–82
- [96] Baker C L, Gelling I R, Rubber M and Razak T A Epoxidized natural rubber 87–8

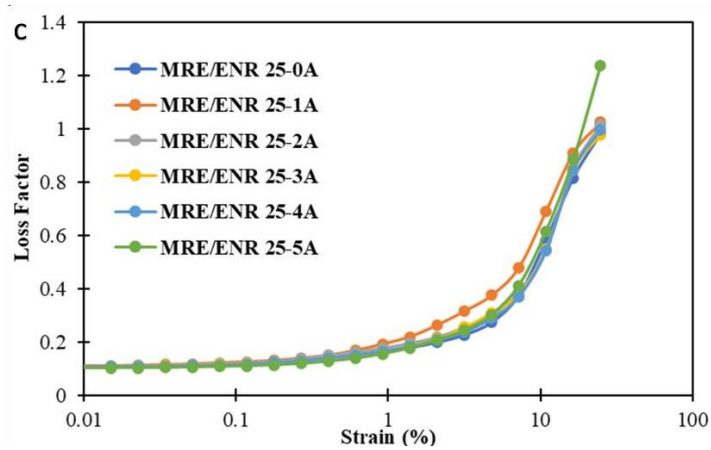
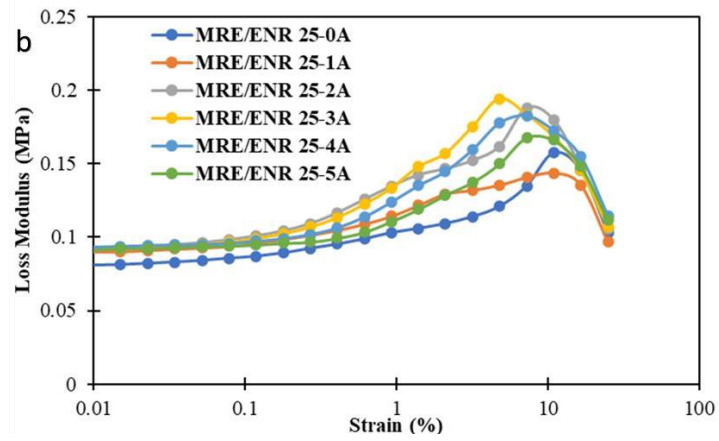
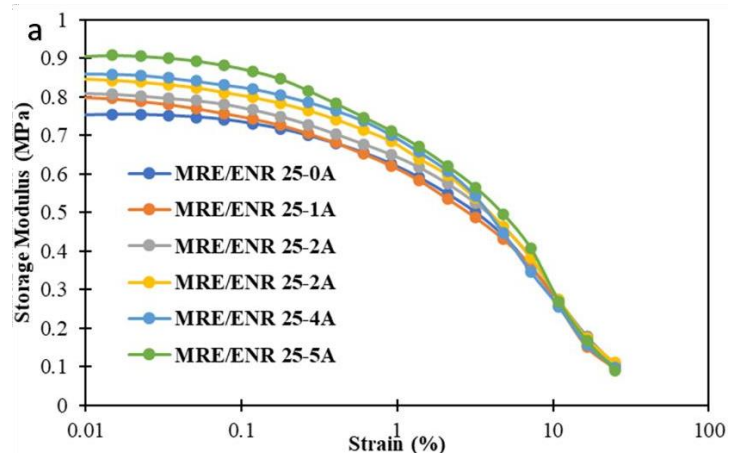
APPENDICES



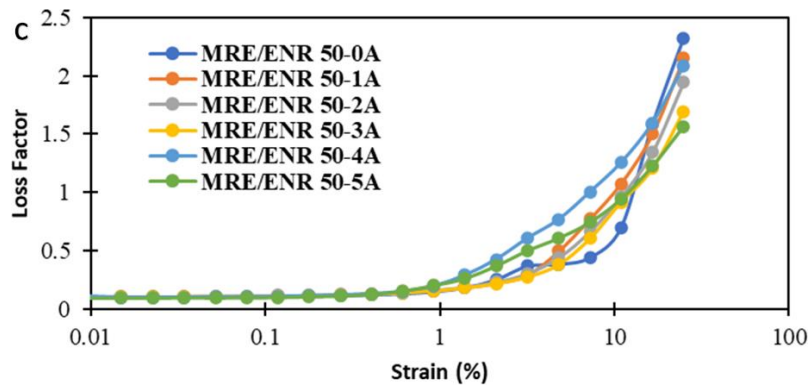
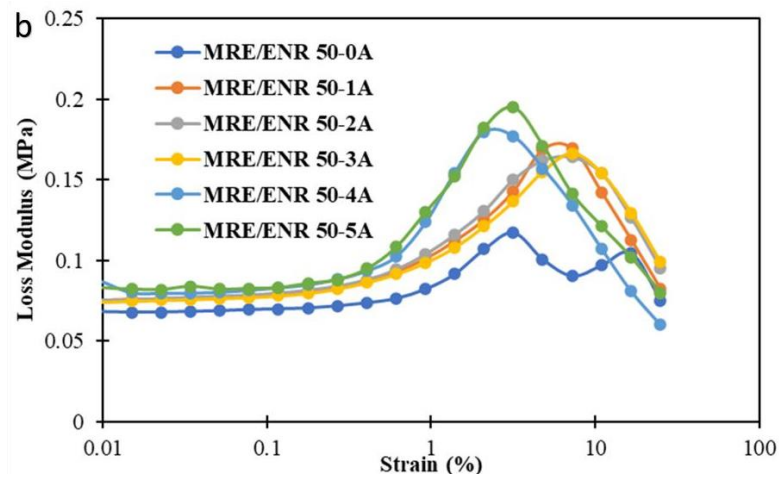
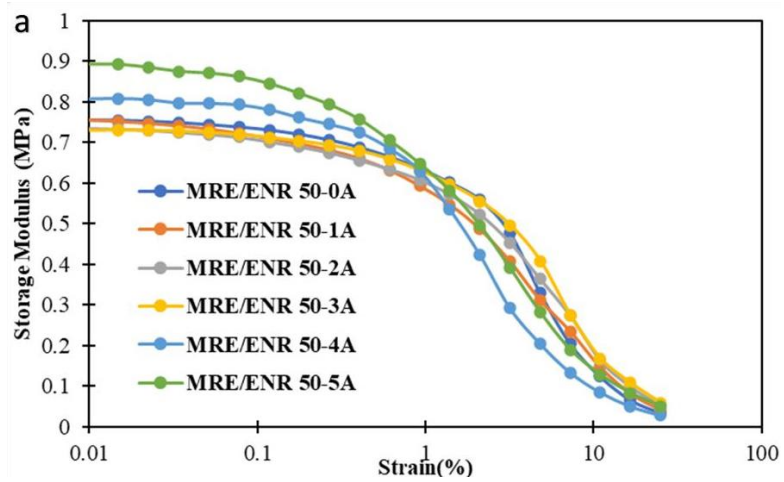
Microstructure ENR 25 based MRE at different scale and magnification



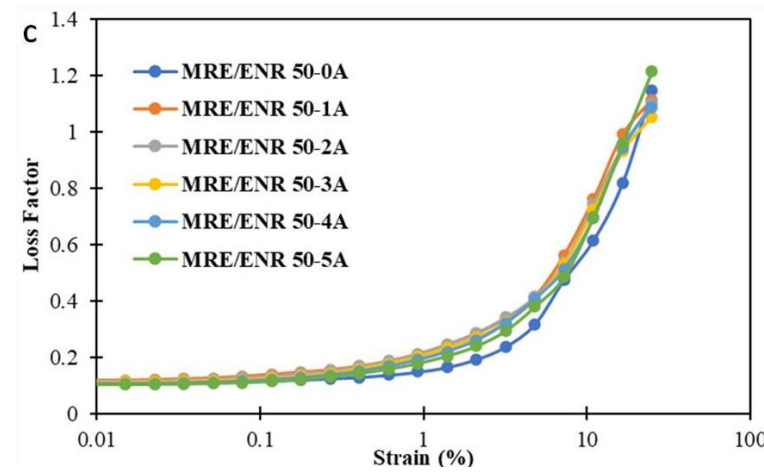
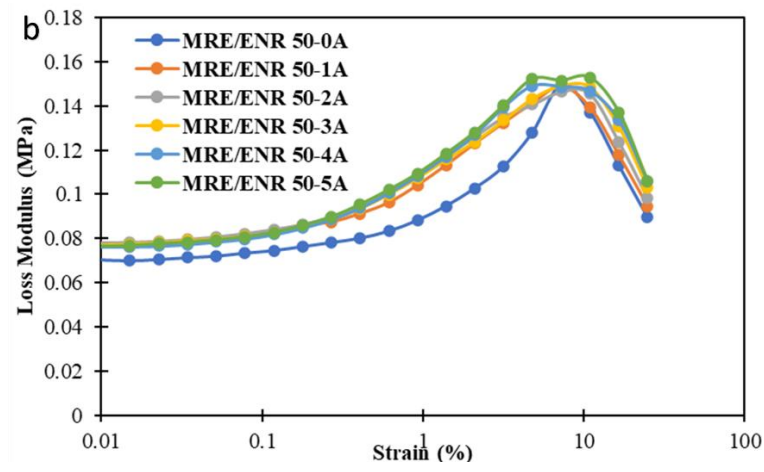
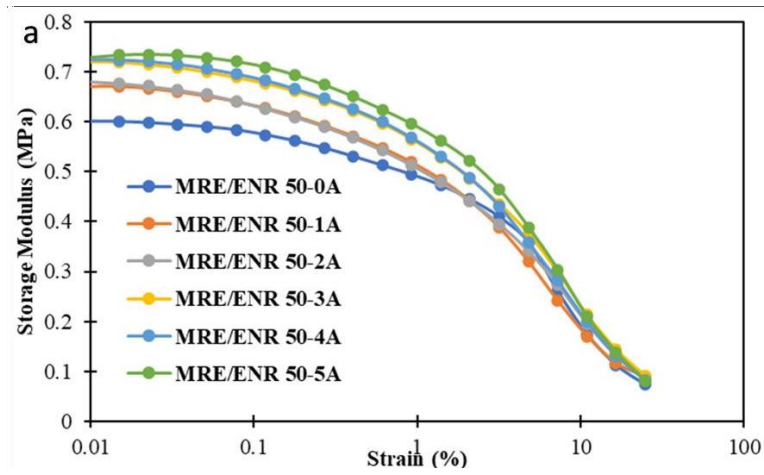
Microstructure of ENR 50 based MRE at different scale and magnification



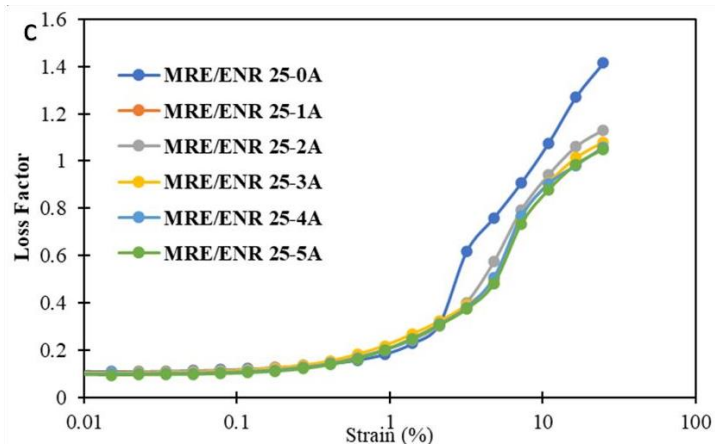
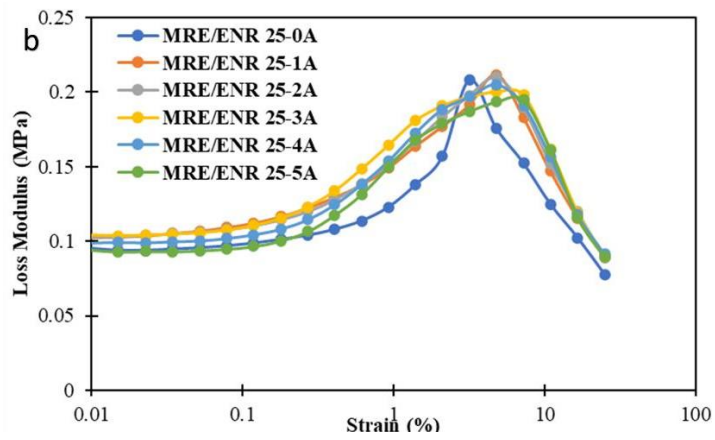
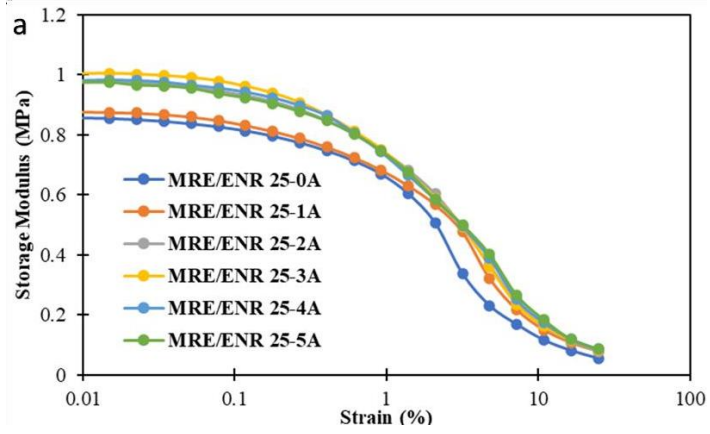
The (a) storage modulus (b) loss modulus (c) loss factor for ENR 25 based MRE (0wt%) at different current supply



The (a) storage modulus (b) loss modulus (c) loss factor for ENR 50 based MRE (0wt%) at different current supply



The (a) storage modulus (b) loss modulus (c) loss factor for ENR 50 based MRE (10wt%) at different current supply



The (a) storage modulus (b) loss modulus (c) loss factor for ENR 25 based MRE (30wt%) at different current suppl